Study on Enhancement of Antibacterial Property by Fluorescent Complex of Hydroxyapatite with Amino Acids Fabricated by Cold Isostatic Pressing

(冷間等方圧加圧法で合成した水酸アパタイト-アミノ酸錯体による抗菌性増強に関する研究)

令和元年10月21日

長岡技術科学大学大学院工学研究科

情報・制御工学専攻

学籍番号　13500684

SARITA MORAKUL

指導教員　大塚　雄市　准教授

Abstract

Titanium alloys is well known to be widely used as the implant materials in the medical, orthopedic surgery and dental fields. Because of its high specific mechanical strength, corrosive resistance and superior biocompatibility comparing to other metallic implant materials. To improve the biocompatibility of titanium alloys, hydroxyapaptite (HAp) is introduced as a coating. HAp coating is ceramic material that has advantage in osteo-conductivity. It improves cell adhesion strength and increases cell proliferation. However, bacterial cell also easily adhere on the surface of HAp coating. After long period of used, there are reports that the patients suffered from the infection problem and revision of surgery is required sequentially. The infection problem is serious issues that causing the sickness and pain in patients. To suppress bacterial infection problem, I study aims at to develop the fluorescent complex of composited photocatalyst gray titania/HAp coating with amino acid. Firstly, I investigated the fabrication of fluorescent complex HAp–amino acid coating based on the mechanical compressive force affected mechanochemical behavior of cold isostatic pressing (CIP) effected on the orientation of ligands. This part of study is focusing on revealing the effects of pressures during CIP process on microstructure of HAp fluorescent complexes and its optical property. It has been reported in previous study from our research group that microstructural dependent property of fluorescent complex improves antibacterial property of photocatalyst coating. However, behind the mechanism of changing in fluorescent property of highly-compressed HAp complex has not been investigated and clarified. The results demonstrated that CIP process successfully fabricated the HAp–amino acid fluorescent complexes. Their fluorescent properties are dependent on pressurization. The higher pressurization, the stronger fluorescent intensity was observed by optical fluorescent

microscope. It is found that the higher pressure also make saturated thickness of complexes and increased the concentration of amino acid proportionally. It is suggested that the packed structure of ligands in fluorescent complexes of HAp–amino acid are formed. To observe the packed orientation, polarized raman spectroscopy measurement was conducted. The results demonstrated that normally arraigned ligands to HAp layer in highly pressurized condition can provide packed ligand structure of HAp–amino acid complex. Highly packed ligands structure of HAp–amino acid complexes emit stronger fluorescence. Our results demonstrated that newly found pressure dependency in optical property of fluorescent HAp–amino acid complex is beneficial to develop biocompatible fluorescent materials or enhancement of antibacterial layers. Secondly, mechanism of enhancement of antibacterial properties of composited gray titania and plasma - sprayed HAp–amino acid fluorescent complex under visible light irradiation was investigated and discussed. Recently, antibacterial coating with visible light sensitive photocatalyst has been widely studied for dental application. Based on the idea of bioinspired by deep sea fluorescent coral reefs, the HAp– amino acid fluorescent complexes are combined with visible light sensitive photocatalyst as the bacterial catcher as well as light concentrator. According to CIP fabrication, HAp–amino acid fluorescent complexes were successfully fabricated by three types of amino acid ligand; Phenylalanine (Phe), Tryptophan (Trp) and Tyrosine (Tyr) respectively. Biocompatible test was conducted by cytotoxicity assay of murine osteoblast like cells. The results showed that the fluorescent complexes of HAp–amino acid ligands are identical similar to HAp coating itself. The bacterial testing was conducted against to the Escherichia coli (E.coli). Antibacterial assays revealed that three type of HAp–amino acid fluorescent complexes and irradiation with three type of light emitting diodes; blue, green and red respectively are significantly decreasing

number of colony forming units (CFU). The mechanism of phenomenon results were explained by Kelvin force microscopy (KFM) that measured surface potential simultaneous visible light irradiation. Comparing of surface potential between HAp and HAp–amino acid fluorescent complexes, it revealed that HAp–amino acid fluorescent complexes preserved the surface potential even after the visible light irradiation. On the other hand, surface potential of HAp coating was significantly decreased by light irradiation. The preservative effect on the HAp–amino acid fluorescent complexes maintained the bacterial adhesion as same as HAp performance. The consequence is antibacterial action of gray titania becomes superior. Finally, our achievement demonstrated that the antibacterial performance is enhanced by the sensitive-photocatalyst fluorescent complexes of HAp–amino acid. The fabrication of fluorescent complexes HAp–amino acid is successfully made by CIP process. The antibacterial property is enhanced during visiblelight irradiation on the the sensitive photocatalyst fluorescent complexes of HAp–amino acid becuase of its potential surface behaves similar to HAp itself during the irradiation. Cell seeding and proliferation were not interrupted and it is compatible for using as dental implants.

Table of Contents

List of Figures

List of Tables

Chapter 1 Introduction

Abstract

In this chapter, I provide a brief overview of the typical biomaterials used in orthopedic and dental implants for clinical application, and highlight the current challenges that need to be overcome. Infection and loss of cell adherence on the surface are among the main problems of current dental implants. In particular, bacterial infections cause can severe illness in patients, therefore requiring revision surgery. To overcome these problems, it is important to consider both biochemistry phenomena as well as underlying mechanics, requiring an interdisciplinary approach.

In this introductory chapter, I propose a new perspective to explain the relationship between the mechanics of a material and the biomechanical behavior of cells, with the ultimate goal of enhancing cell adhesion behavior while conferring the material with an effective antibacterial property. In particular, I suggest a new method of biomaterial preparation using a sensitive photocatalyst with light irradiation to achieve antibacterial enhancement, which is discussed in light of an extensive review of the literature on antibacterial properties of biomaterials. Finally, the objective of this study will be proposed.

1.1 Background

Recently, there has been extensive progress made in understanding the biomechanics of materials, which has led to the development and application of new biomaterials for applications in surgery, such as artificial cardiac tubes for heart disease, artificial hip joints, and dental implants. However, to improve and ensure the quality of life of patients receiving these materials, it is necessary to deeply consider issues of safety and to develop materials that will incur the least amount of economic burden to the medical industry. Several researchers are now focusing on developing and exploiting new technologies to address these issues. Because thousands of surgeries are required to revise or repair tissues that have failed or become damaged owing to disease or trauma, the majority of this research has aimed toward effectively regenerating the damaged tissues using biomaterials that are integrated with living cells, such as metallic or ceramic-based materials, which have been widely applied in the fields of tissue, medical, biomaterial, and mechanical engineering. Specifically, biomaterial engineering is a relatively new field of study for tissue regeneration or replacement. When incorporating a new material into a new immune system or directly in the human body, it is essential to consider the safety of the material and procedure, including anatomical limitations or the risk of infection.

There are many factors to consider according to the intrinsic limitations of biological systems. First, with regard to in vitro culture prior to cell implantation, it is important to consider the effects of the cell culture conditions on the new host environment. For example, the behavior and seeding ability of cells on the surface of an implant material largely depends on the bioreactor device used, and the different types of mechanical and chemical reactions occurring therein.[1] Cells prepared for implantation require expansion, which requires a suitable environment for increasing cell density to promote

cell growth. However, it is also important to consider the cell distribution along the surface of biomaterial. In this regard, the mechanics of the material play an important role so as to support the surface property of the biomaterial such as the wettability or surface energy that will best promote cell adhesion. Another important consideration of an implanted biomaterial is the possibility of infection. Therefore, conferring materials with antibacterial properties has been a major focus of research in biomaterial engineering, which can also help to promote cell adhesion to the surface.

Thus, the aim of the present work was to develop a titanium-based dental implant biomaterial with enhanced antibacterial property.

Fig. 1.1 shows a scheme of the main factors considered for realizing antibacterial enhancement of a biomaterial, including consideration of mechanical and photocatalyst properties for triggering.

1.2 Biocompatibility of a biomaterial

Regardless of whether a tissue has failed because of trauma or another cause, one of the first and most important considerations in the development and design of a suitable biomaterial for medical application is to understand the type of material that can be replaced and to ensure that the material conforms with safety regulations for use in the human body . Overall, the material must be compatible for cells to adhere to the surface and proliferate normally to carry out their required function. After an implant surgery, it is also important to prevent inflammation as much as possible during the healing response to avoid rejection of the material from the body. [2] Currently, metallic-based materials are considered to be the most attractive materials for biomedical applications, particularly for implant

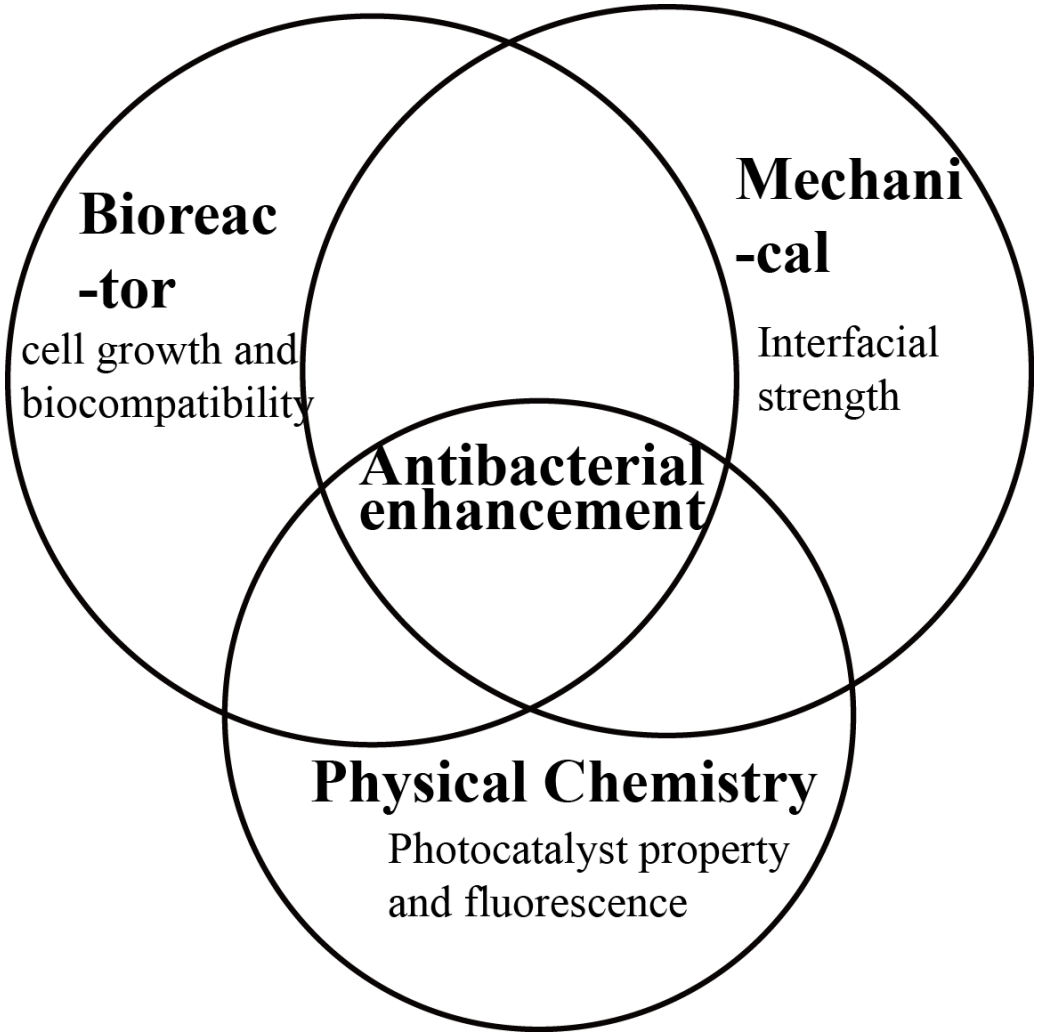

Fig. 1.1 Antibacterial enhancement of cell adhesion from a bioreactor combined with interfacial strength of a cell on a biomaterial with mechanical and photocatalyst properties.

surgery. In particular, titanium alloys are widely used for artificial hip joints and dental implants, which show superior performance with respect to non- sensitive chemical reactions, high mechanical strength, and biocompatibility.

Although the titanium alloys Ti–6Al–4V are the most popular types used in implant materials and for medical orthopedic surgery, these alloys could also induce toxicity compared to more non-toxic elements such as β type alloys. The greater biocompatibility of Ti–6Al–4V titanium allows is attributed to the lower moduli compared to other type of alloys, such as $\alpha + \beta$ alloys [3]. Moreover, the Ti–6Al–4V titanium alloys show higher strength and toughness than $\alpha + \beta$ type alloys. It is also necessary to

consider the actual mechanical loading that could damage the implants during service in the human body. Fig. 1.2 demonstrates cyclic loading through simulating of a walking load and the resulting damage that may occur while using titanium alloys with a biocompatible hydroxyapatite coating. Niinomi et al. [3] investigated the mechanical properties of three types of biomedical titanium alloys to improve the mechanical strength of biomedical materials: commercial pure titanium, Ti–6Al–4V, and Ti–6Al–4V elite. In particular, they focused on the effect of changing the microstructure of the material, and its characteristics on treating a fracture, which is a common and serious clinical challenge. Tensile and fatigue testing were conducted to determine the fracture behavior, i.e., fracture toughness, and fatigue characteristic, respectively, according to the mechanical properties conferred by the different microstructures of the various biomaterials derived from the three titanium alloys. Overall, they found that the moduli of elasticity of the low-modulus β type of titanium alloys degraded after exposure to simulated body fluid while simultaneously applying mechanical fatigue loading. By contrast, the Ti–6Al–4V $\alpha + \beta$ alloy types significantly retained their toughness after being implanted in vivo. Therefore, mechanical properties of the biomaterial must be considered for improving the cell adhesive strength.

Several researchers have addressed the challenge of increasing cell proliferation to realize stronger bonding between the cell and host biomaterial for enhancing bone growth in the last few decades. One of the methods proposed involves the use of a plasma-sprayed hydroxyapatite (HAp) coating on a metallic substrate such as Ti–6Al–4V alloys, which has garnered substantial controversy in the field. The HAp coating was introduced to ensure the bonding between bone and titanium alloys implants as a biocompatible coating, which also has excellent osteoconductivity. Limin et al. (2001)

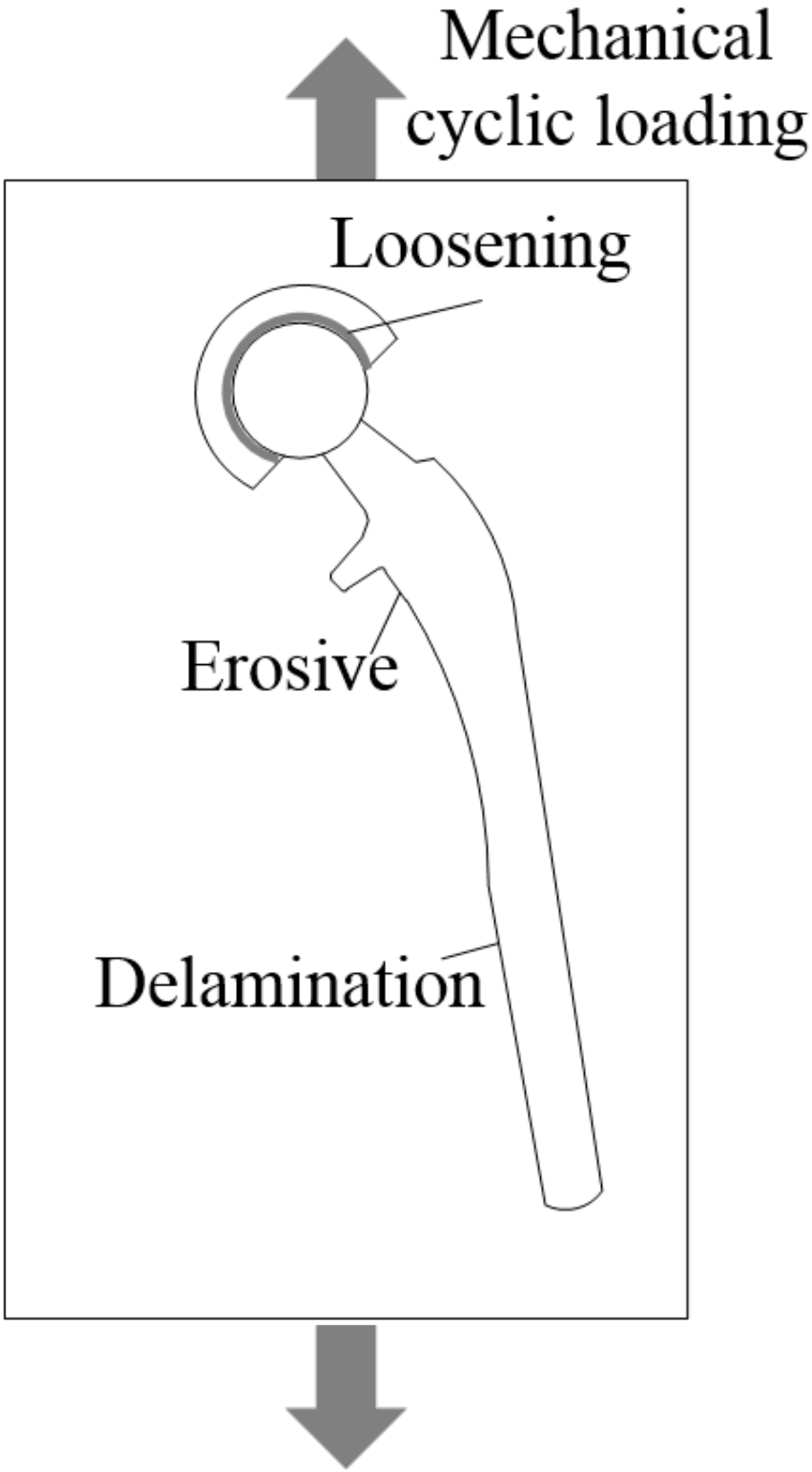

Fig. 1.2 Mechanical loading and its damage to an artificial hip joint implants

[4] and Palm et al. (2002) [5] both investigated the performance of plasma-sprayed HAp coating for practical application to the femoral bone. The results demonstrated that the HAp coating significantly promoted cell growth after implantation and the fixation lasted longer than that not cemented by the HAp coating. Reikeras et al. [6] evaluated the long-term use (1988 to 1993) of a HAp coating as a cement for clinical femoral bone implants, and they found that the HAp coating was successfully deposited on the acetabular component in the patients. Moreover, there was no infection observed in any patient, although wear and osteolysis was clearly observed to prove the bonding of bone to the titanium alloys implant. The authors concluded that the HAp coating provides a suitable fixation material to promote the interaction of bone with the biomaterial, and further helps to resist the mechanical loading, thereby consequently preventing damage from wear.

Moreover, Robert B. Heimann's [7] demonstrated the enhancement of the growth of bone cells using the osteoconductive HAp coating that was deposited onto metallic artificial hip joint and knee joint replacements. The HAp coating process was developed and discussed based on a high-temperature plasma jet, which causes the degradation of hydroxylation and decomposition of the initial deposited substance. The influence of the chemical formation and mechanical characteristic of porous calcium phosphate on cell activity in vitro and in vivo was evaluated based on the characteristic of plasma-sprayed HAp coatings. X-ray diffraction (XRD) and vibrational spectroscopic methods such as Fourier-transform infrared (FTIR) spectroscopy were conducted to determine the distribution of plasma-sprayed HAp coatings, which was found to be homogeneous. Moreover, Raman spectroscopy revealed a stretching band at wavelengths of 949, 962, and 971 cm-$^{-1}$ corresponding to P–O bonds. The crystallinity increased and the thermal decomposition decreased. In addition, residual stress at

the interface between HAp and the Ti–6Al–4V substrate was induced due to thermal expansion of the plasma sprayed. Moreover, to improve the bioconductivity of the HAp coating, it is necessary to consider its mechanical, chemical, and biological performance $Ca_{10}(PO_4)_6(OH)_2$ on titanium alloy implants. Mainly, they investigated adhesion to the implants surface, along with the microstructure and crystalinity of the HAp coating to improve the osteoconductivity and biocompatibility of the biomaterial. The HAp coating was successfully deposited via a plasma spray onto the metallic biomaterial substrate such as titanium alloys. The plasma-sprayed coating did not affect the crystalinity of $Ca_{10}(PO_4)_6(OH)_2$ the HAp coating by changing its oseteoconductivity. Overall, these developments show the importance of consideration of the mechanical, chemical, and biological properties of biomaterials for improving the quality of life of the aging society and orthopedic patients.

1.3 Infection derived from implant biomaterials

The long-term use of an implant biomaterial generally requires several revision surgeries and replacements. This is largely due to the development of a bacterial infection, resulting in serious illness to the patient, which is a particular problem for dental implants. Since complete inhibition of biofilm formation on bone cells and the implant surface is unavoidable, integration of an antibiotic property to the biomaterial substrate on the surface has become indispensable for the prevention of bacterial infection. Development of effective antimicrobial materials will require understanding the mechanism of inhibition of the interaction between the host tissue and bacterial colonization, which has not yet been studied.

In this regard, the study of failures in oral implants has garnered much interest to many researchers.

In particular, the research group of Professor B.R. Charcanovic has been focusing on revealing the failure of oral implants [8], with the ultimate goal of suppressing the bacterial infection problem in biomaterial implants. Moreover, Gupta et al. [9] and Quirynen et al. [10] have examined the risk factors associated with implant failures. There are many criteria used for evaluating the failure of biomaterial implants, such as the mechanical technique of low-insertion torque that considered as the primary loaded component, implants insertion in boneless patients, or the surgical technique of inserting implants. These factors may relate to the failure of implants as well as to bacterial infection colonized on the biofilm surface.

In particular, in orthopedic surgery, joint arthroplasty has been required for revisions owing to the short-term lifespan of the implant.[11] The main reason for the revision is loosening of the joint in implants, which may be related to bacteria forming a biofilm that would interfere between the bone tissue and biomaterial implant at the joint. Bauer et al. [11] examined the loosening failure behavior of a biomaterial implant from a mechanical point of view by examining the mechanism of the failures in arthroplasty surgery. The combination of mechanism failure and infection was addressed based on the wear debris failure in aseptic loosening due to inflammation. Formation of a bacterial biofilm can be considered as the additional particles that cause the linear and erosion of bone osteolysis. Moreover, biomaterial implants are always subjected to mechanical loading that generates a driving force of stress on the component, which is usually localized on bone density so that an interfacial force between the bone and implants is generated. The combination of bone density loss and interference from the bacterial biofilm has a severe influence on aseptic loosening behavior. The authors [11] further investigated the extent of wear debris, and found that the debris particles of

osteolysis appropriately enhanced the fixation of bone with the implants. Although general debris is considered to contribute to loosening of the implants, the debris of osteolysis actually enhanced osteoclast cell proliferation. Therefore, the fatigue failure of wear debris and the creation of a bacterial biofilm at the interface between the bone tissue and implants should be considered in any discussion of the failure of an infected biomaterial implant. Drake et al. [12] focused on the long-term safety of a biomaterial implant by examining adhesion of the bacterium *Streptococcus sanguinis* on a titanium implant surface. The titanium surface profile exhibited a strong degree of roughness, which was considered to be due to the hydrophobic nature of the surface, and low wettability. Given the status of the host tissue and colonization of the bacteria on the implant, formation of a bacterial biofilm on the implants surface was promoted. Moreover, the titanium biomaterial implant was damaged from bacterial colonization over long-term use.

Indeed, this challenge of bacterial infection of implants has been a long-standing task to overcome, with a long history of research spanning over several decades, from 1966 to 2007. Dental implants are particularly prone to bacterial infection, as they are more likely to suffer from biofilm formation. Subramani et al. [13] proposed that the surface roughness is related to the ability for biofilm formation and bacterial adhesion. They suggested that the surface modification of dental implants with a titanium alloy substrate might prevent biofilm formation by changing the properties of the biomaterial, such as the surface free energy and its potential surface chemistry. The main challenge is that the attachment of a target cell must be promoted by supporting osteogenic proliferation, whereas bacteria proliferation and biofilm formation must be simultaneously prevented.

Bruellhoff et al. [14] proposed one of the first strategies to suppress bacterial infection of dental im-

plants through preventing biofilm formation through surface modification to enhance the antibacterial property of the material.

This specific configuration allowed cells to adhere or not depending on the interaction of peptide-binding molecules. The antibacterial effect of a selective adhesion base on peptides and adhesive ligands was further emphasized by Fiedler et al. [15], who used multipotent mesenchymal stromal cells (MSCs) such as bone marrow-derived MSCs to enhance cell proliferation and osteogeneration. At 30 days after seeding the cells on the implants, the cell adhesion behavior showed normal spreading on the implants. Moreover, RT-PCR analysis and a viability test with the MTT assay were performed to identify and quantify the osteoblastic cells. The MSCs and SaOS-2 cells showed different adhesion responses to the protein peptide, which demonstrated that cell proliferation could be improved with an adhesion peptide via specific protein absorption on the surface. Besides dental implants, bacterial infection remains a serious clinical challenge in orthopedic surgery such as the use of knee hip joint or periprosthetic joint implants. Hansen et al. [16] comprehensively studied infection in periprosthetic joints, and proposed a treatment aiming to suppress such infection by focusing on the molecular mechanisms of the cell reaction. Specifically, by applying advanced diagnostics and the development of new molecular techniques, they successfully achieved modified biomaterial implants with anti-biofilm and antimicrobial properties.

However, these techniques are still not suitable to completely suppress the bacterial infection efficiently. To achieve this goal, it is essential to continue to study the mechanisms of bacterial infection and proliferation of bone cell tissues from the persepctive of the biological and mechanical processes of cell adhesion.

1.4 Antibacterial modification of biomaterial implants

1.4.1 Antibiotic effects and sustainability

To effectively suppress the bacterial infection that causes severe problems such as the mechanical failure and degradation of biomaterials used in orthopedic surgery, especially dental implants, many researchers have proposed new methods for surface modification of the biomaterial substrate with titanium alloys. The use of chemical elements such as silver ion-doping on the surface of titanium alloys has been broadly demonstrated to be the most effective method for enhancing the antibacterial property of a biomaterial. Recently, the nanotube surface of titanium alloys has attracted attention as another strategy to suppress bacterial infection by focusing on the cell adhesion mechanism. As discussed in the section above, bacterial infections often occur rapidly after application of a dental implant. Chen et al. [17] proposed that a modified surface with silver doping of a HAp coating would confer an antibacterial property and cytotoxic effect to a biomaterial. They evaluated these effects in vitro against two type of bacteria, *S. epidermidis* and *S. aureus*, which have different cell wall characteristics. After co-sputtered Ag–HAp was deposited onto the biomaterial titanium alloy substrate, the contact angle, surface roughness, and XRD data were obtained to evaluate the characteristics of the coating. XRD analysis confirmed that Ag–HAp was successfully deposited on the biomaterial titanium alloy substrate. The wettability for cell adhesion was evaluated and the contact angle of the deposited Ag–HAp coating was significantly lower than that of the titanium alloy itself. Moreover, a reduction of colony numbers was observed for both bacteria in the Ag–HAp-coated group. Although the bioactivity of bone cells was not interrupted, the cytotoxicity was increased in the group treated

with the Ag–HAp coating.

Similarly, Fielding et al. [18] examined the antibacterial characteristics of doping with a composite of silver and strontium along with a plasma-sprayed HAp coating to improve the interaction between bone cells and the implant material. The addition of strontium as a binary dopant was expected to reduce the cytotoxicity of the coating by strongly releasing metal ions from the silver doping. Strontium acts as a replacement element for Ca^{2+} ions in osteoblasts during calcium-mediated processes, and further behaves as a sensing receptor for bone cell formation. Although strontium showed excellent enhancement of osteoblast proliferation, its addition did not effectively suppress the cytotoxicity induced from the silver doping. Cell proliferation and activity were observed by measurement of the optical density, an MTT assay, and fluorescent microscope observations. Moreover, field emission-scanning electron microscopy observation was used to examine the cell morphology and adherence on the treated surface after 3 days of cultivation for the cell seeding process on the coated surface, and the cumulative release of silver ions was evaluated.

Although silver ion doping provides excellent antibacterial enhancement to a biomaterial, this effect is not sufficiently sustainable for long-term application [19]. Trujillo et al. [20] attempted to decrease the silver doping concentration to reduce the cytotoxicity, and evaluated the antibacterial effect with a silver-doped HAp thin film sputtered on a titanium substrate with different amounts of silver: 0.5 wt% and 1.5 wt%. *Staphylococcus epidermidis* and *Pseudomonas aeruginosa* were seeded on the surface of the prepared implant and cell adhesive behavior was observed.

However, they did not mention whether differences in the cell wall of bacteria would influence the resistance to the exposure of released metal ions.

Lim et al. [21] also evaluated the effect of the concentration of silver-doped HAp for enhancing the bioactive and antibacterial properties of a biomaterial. X-ray photoelectron spectroscopy indicated that initiation of ions releasing in deionized water had a similar releasing rate. The combination of chitosan and silver ion films was added to the HAp coating before being deposited on the Ti–6Al–4V substrate of the biomaterial implant by thermal substrate methods. [22] XRD analysis and scanning electron microscopy observation was conducted to characterize the modified surface, and the amount of silver ions was evaluated by atomic absorption spectroscopy. They found that adhesion of *Escherichia coli* cells significantly decreased by 14% comparing to a sample without silver ions. However, this experiment only showed the release of silver ions over the short term. Owing to the poor sustainability of silver-doped particles, release of the metal ion was only efficient at the initiation stage [19, 23]. Therefore, despite the excellent antibacterial property of silver ions, its performance is not sustainable for long-term use in implant surgery. In general, studies aiming toward antibacterial enhancement of a biomaterial have mainly focused on strategies in which an antibiotic is applied to detach the bacterial cell off of the implant surface. In this case, both the bacterial and bone cells are exposed to the same antibiotic treatment, resulting in cytotoxicity in vivo rather than the desired effect of preventing bacterial infection. The use of conventional antibiotic agents is cytotoxic to bone cells because of its high concentration ions releasing from silver and it scarcely controllable. In summary, to reduce bacterial colonization, antiseptic surface coating has been applied to prevent biofilm formation; however, it is also necessary to consider the effects of this coating for promoting the activity of osteoblasts. Thus, the next challenge toward improving the antibacterial property of implants requires reconsideration of design by aiming to reduce bacterial growth while simultaneously preserv-

ing the proliferation of bone cells and effectively fixing the implant to the bone tissue. Importantly, the remaining problem to be overcome is to reduce the cytotoxcity against bone cells induced from silver-doping the surface and prolonging its efficient stability.

1.4.2 Effect of antimicrobial enhancement of a biomaterial on bacteria and bone cells

As highlighted above, the surface energy and cell adhesion behavior are important factors to consider for improving the antibacterial property of an implant material and along with increasing cell proliferation. Gottenbos et al. [24] provided evidence that cell adhesive behavior depends on the surface charge of implants through examining the antimicrobial effects of positively and negatively charged biomaterials implanting in vivo. Gram-negative bacilli were cultivated on a positively charged biomaterial surface and the infection level was evaluated. A glass sample surface was conferred with a different charge by modification of a polymethacrylate group for seeding *E. coli* and *P. aeruginosa*, respectively. At 48 hours after seeding, 50% of the positively charged surfaces had non-adhered *E. coli*, whereas the negatively charged surfaces were seeded by both bacteria.

Therefore, a biomaterial with a highly positive charge reduces the risk of infection more than a negatively charged surface.

However, increasing the dose of the antibiotic has been shown to reduce the effectiveness of the antibacterial property or degrade the drug efficiency. [25] The bacterial cell wall has a complex layer, and the mechanism contributing to the potential energy cannot be predicted. Therefore, the antibacterial protein and peptide molecular structure should be targeted with consideration of both the cell

adhesion behavior and cell surface potential energy.

Lim et al. [26] provided insight into the mechanism of the use of an antibiotic to eliminate bacteria by silver ions (Ag^+) destroying the cell wall and penetrating the bacterium to kill the bacterial cell. The antibacterial property of Ag,Si–HAp was observed and compared to that of HAp alone after seeding the bacteria on the substrate for 168 hours. They found that cell proliferation was enhanced by Si–HAp, while Ag^+ metal ions were strongly released to destroy the cell wall. Transmission electron microscopy and plasma spectroscopy demonstrated that the crystal structure of silver ion diffusion was distributed evenly across the Ag,Si–HAp surface. The crystal structure of the silver ion interfered with *S. aureus* adhesion, demonstrating that leakage of the destroyed cell wall allows for silver ions to enter the nucleus of the bacterial cell.

Harris et al. [27] also attempted to enhance the antibacterial property of a titanium oxide surface by adding peptides/proteins to suppress *S. aureus* adhesion. The extracellular matrix (ECM) may react undesirably on a polypeptide; for example, poly(L-lysine)-grafted poly(ethylene glycol) (PLL–g–PEG) resulted in a notable decrease of fibroblast and osteoblast cell adhesion. This was attributed to the lack of a specific peptide-integrin acceptor restored on the surface, so that the ECM proteins were not able to be absorb, resulting in decreased activity. SEM and fluorescent microscopy were conducted to evaluate the viability of bacterial cells that adhered on the treated surface between PLL–g– PEG and PLL–g–REG/PEG–RGD. The modified surface of PLL–g–REG/PEG–RGD showed excellent attachment of fibroblasts and osteoblasts while also reducing *S. aureus* adhesion. It was expected that a higher density of bacterial cells would be observed on rougher surfaces. However, the roughness of the sample surface did not have a significant effect on bacterial adhesion or

viability. Although other aspects of the surface topography beyond roughness, such as the size of the surface and surface wettability likely would also affect adhesion behavior, there are few studies on the relationship between the enhancement of antibacterial properties and cell adhesive behavior. Zhang et al. [28] examined the effects of the topography of a modified surface with antibiotic properties on enhancing osteoblast proliferation and detachment of bacterial cells. They aimed to develop an implant that could increase bone cell activity and reduce the risk of bacterial infection for materials used in orthopedic surgery such as knee or hip implants. They applied atom transfer radical polymerization (ATRP) with a trichlorosilane agent, which was confined to an oxidized titanium surface, and focused on the release of methacrylic acid sodium salt (MAAS), while silk sericin was immobilized on the poly(MAA) surface. The characteristics of the modified surface were investigated by X-ray photoelectron spectroscopy, XPS measurements, and water contact angle measurement. The results demonstrated that oxide titanium was successfully immobilized by P(MAA) based on XPS measurement, and the water contact angle was significantly lower than that of the titanium surface. The P(MAA)-immobilized titanium showed clear hydrophilic properties, which enabled bacterial cell adherence. However, the hydrophilic property may not be the only factor to consider for improving of cell adhesion. In addition, the potential transfer between protein peptides and cell behavior should be considered toward achieving cell adhesion enhancement. Khadali et al. [29] observed the interaction of the cell surface between hydrogen bonds forming multi-layers with non-toxic effects to osteoblasts from P(MAA) or P(AA). However, mammalian fibroblasts were detached because of the carboxylate and sulfonate groups. Zhang et al. [28] indicated that the good adhesion and proliferation of osteoblasts from modified Ti–g–P(MAA-silk), owing to the addition of silk sericin protein, which is

caught by silk fibers and differentiated. Importantly, silk siricin had different effects on osteoblast and bacterial cell adhesion. Chen et al. [30] examined the binding activity of an antimicrobial peptide to a biomaterial surface. Atomic force microscopy indicated that the surface topography plays an important role in controlling bacterial adhesion. The orientation of the antimicrobial peptide immobilized on the biomaterial surface was also shown to have a great effect on the cell adhesion property. Thus, both the interaction between the hydrogen bond of the peptide and ECM and the surface topography are important considerations for improving cell adhesion to an implant surface.

Fig. 1.3 illustrates the changes in cell proliferation over time on implant surfaces coated with hydroxyapatite alone and with hydroxyapatite and an antibiotic. The hydroxyapatite surface without the antibiotic allowed bone cells to grow gradually over time and cell adhesion increased, thereby demonstrating enhanced biocompatibility. By contrast, the hydroxyapatite surface with antibiotic largely suppressed cell proliferation by destroying the peptide layer and its cell wall so that the cell could no longer reside on the surface and died once the nucleus was exposed to the antibiotic. Therefore, although the antibacterial property was enhanced, this property could not be effectively controlled, resulting in cytotoxicity. Overall, this review of the literature on efforts to improve the antibacterial property of artificial bone implants or dental implants for orthopedic surgery demonstrates that the most important parameters to consider are not only the bioreactive interactions between the peptides of cell and the biomaterial surface but also the complex potential energy that influences cell adhesion behavior. Moreover, from a mechanical point of view, the surface topography such as the roughness, orientated morphology, or surface energy has important effects on cell adhesion behavior.

Therefore, it is necessary to reconsider a new strategy for reviewing the mechanism of antibacterial

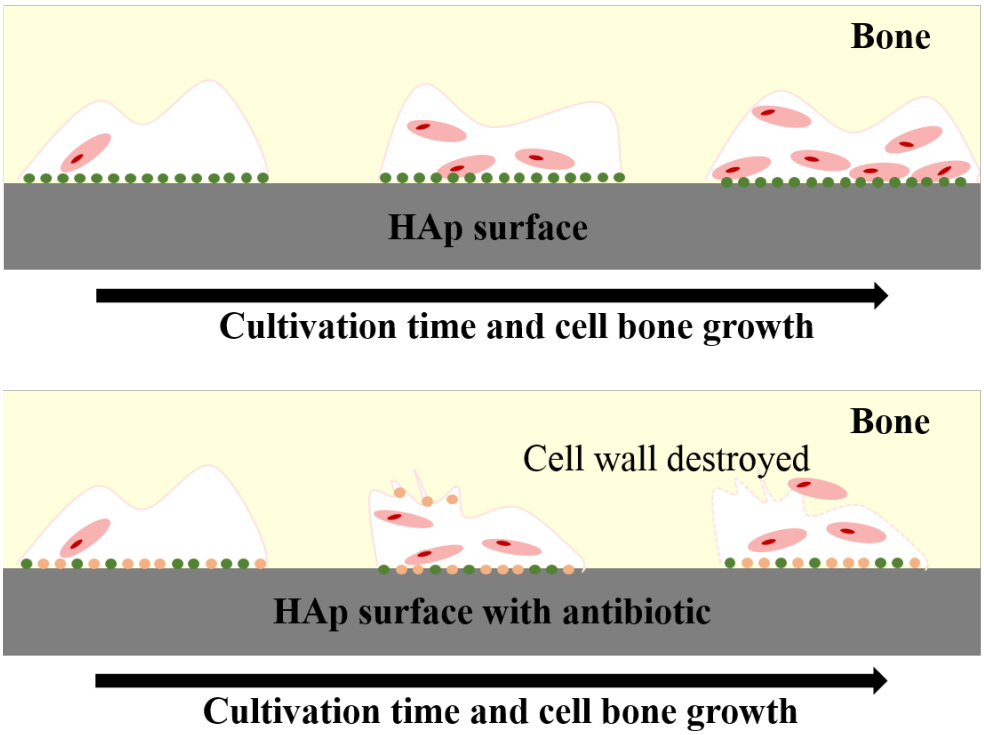

Fig. 1.3 Cell proliferation and adhesion on a HAp-coating and HAp–antibiotic-coated implant surface.

enhancement in orthopedics surgery and dental implants. Importantly, materials should be developed that show an effective antibacterial property with both biocompatibility and sustainability.

1.4.3 Developing nanostructure implants with antibacterial properties

The previous section presented the scope of concepts for developing new biomaterials with enhanced antibacterial property by modifying the surface or immobilizing antibacterial agents on the surface. Although the modified layer may be effective to reduce the number of bacteria adhering to the implant material, the controllability and sustainability remain major limitations to the application of this concept, which is largely due to a lack of understanding of the mechanism on the enhancement of cell adhesion in relation to antibacterial agents. A passive coating is expected to prevent

bacterial adhesion on an implanted surface by controlling the surface topography, wettability, surface energy charge, or even crystal structure. Although surface roughness was intensively investigated in vivo by Rimondini et al. [31] with the aim of reducing the colonization of bacterial cells, laser profilometer measurments and SEM observations revealed the surface characteristics with no significant reduction in cell colony formation. Moreover, Puckett [32] investigated the relationship between the nanostructure of a titanium surface and bacterial adhesion behavior.

According to the bioreactive effect of protein absorption between each cell type onto protein peptide agents on cell adhesion, three type of bacteria, *S. aureus*, *S. epidermidis*, and *P. aeruginosa*, were chosen to immobilize on the conventional titanium rough surface and on the nanostructure surface, respectively. The nanorough titanium surface formed a TiO_2 crystal structure, which showed an excellent ability at preventing bacterial attachment comparing to the amorphous nanotubular and nanotextured titanium surface, which has a superior property of surface energy, surface roughness, and fibronectin absorption. Based on the hydrophilic property enhanced from the smooth surface, cell adhesion was expected to be outstanding. However, these results contradict with the theory of wettability. They suggested that fluoride was present in the nanotubular and nanostructure, whereas there was no sign of fluoride formation in the nanorough surface of titanium. The crystalline structure showed differences between the anodized, nanorough, and conventional titanium surface.

Anatase and rutile of the crystalline TiO_2 photocatalyst were observed, while the nanostructure and nanotubular were amorphous of TiO_2. Thus, the surface chemistry of the anodized surface plays an important role in detachment of bacterial cells.

Podporska et al. [33] developed an anodization method of conventional titanium, and demonstrated

the formation of crystalline TiO_2 photocatalyst to enhance the antibacterial property of the biomaterial. XRD and Raman spectroscopy were conducted to characterize the crystalline amorphous titanium nanostructure modified with a hydroxyl group, and *E. coli* and *S. aureus* were used to evaluate the antibacterial property. The titanium nanotube surface showed a significant effect on detachment of bacterial adhesion under UV light irradiation. A conduction band electron of e^-_{CB}, which takes the oxygen in the atmosphere to generate superoxides known as oxygen radicals ($\cdot O_2^-$), from the valence band of h^+_{VB} was activated by UV irradiation. This photocatalyst property was a significant factor contributing to the biological activity of TiO_2. Thus, the surface hydroxyl group, physico-chemical properties of the modified surface, and interfacial strength of the mechanical property all effectively play important roles in control the antibacterial property of a biomaterial. However, these previous results [[32], [33]] also revealed that the cell adhesion behavior is independent from the roughness property of an implant surface. Moreover, the wettability or surface charged hydrophobicity and hydrophilicity do not appear to be important factors to consider for improving cell adhesion behavior and realizing antibacterial enhancement. These suggestions strongly indicate that the antibacterial property will not be derived from the surface chemistry alone but also requires activation of an agent to effectively control the antibacterial effects, which can be achieved with a photocatalyst that is sensitive to light irradiation.

1.5 Photocatalyst for improving the antibacterial property of an implant biomaterial

The biological inspiration for the light-inducible effect of fluorescence came from the discovery of mesophotic reefs in the deep seawater up to 50–60 meters of depth.[34] To survive in such environments, the photosynthesis efficiency needs to be enhanced, which requires fluorescence to be excited; thus, synthetic fluorescent pigments have been designed to control the potential of animals kept in the darkness. Investigation of the light-independent accumulation of fluorescent pigments identified that a photoconversion wavelength shift from green to red light was obviously induced in the absence of UV light. These findings indicate that fluorescence can play a role as a trigger from light irradiation and pull out photocatalyst properties such as oxygen radicals inducing bacterial death.

Recently, fluorescent complexes of HAp coating on Ti–6Al–4V titanium alloys were proposed by Matsuya et al. [35] to develop agents with a controllable antibacterial property induced by a photocatalyst. First, they successfully fabricated a stacked luminexcent complex of 8 hydroxyquinoline (8Hq) molecules on a HAp coating by a cold isostatic pressing (CIP) process. Calcium ions in HAp ($Ca_{10}(PO_4)_6(OH)_2$) and 8Hq (C_9H_7NO) were formed by mechanical loading and chemical reaction simultaneously. 8Hq–HAp complex showed the greenish fluorescence while UV light irradiation was applied. An organic material readily shifts the fluorescent wavelength by shearing force or pressurization. [36] In the solid condition of particles, a mechano-chemical reaction is induced between the impurity of molecule structure and oxide on the surface. Preliminary results obtained by fluorescent microscope observations showed that a fluorescence red-shift from the CIP-treated HAp–8Hq com-

plex. There was no interfering precipitation with the HAp coating itself as demonstrated by XRD analysis. Raman spectroscopy further revealed a longer shifted wavelength with an on increase of pressurization. The stacked aromatic ring of the benzene structure of 8Hq in the complex was determined to be the causes of the shifting in its photoluminescence.

Despite the successful fabrication of the ligands complex of 8Hq molecules with HAp through the CIP process, immersion testing in simulated body fluid (SBF) demonstrated that the fluorescent 8Hq–HAp layer did not dissolve. In addition, four-point bending of fatigue testing was conducted with the HAp/gray titania–8Hq complex with a rectangular dimension of $50 \times 10 \times 3$ mm^3, in order to confirm that the mechanical loading would not degrade the fluorescent property of the sample in practical application. The remaining fluorescence was observed by a fluorescent microscope. Therefore, this material is expected to be biocompatible and show a sustainable antibacterial property for the design of a dental implant. Several studies have since investigated the 8Hq–HAp fluorescent complex for enhancing antibacterial property by applying visible light irradiation. Matsuya et al. [37] performed antibacterial testing with a HAp/gray titania/8Hq fluorescent complex for coating with sensitive visible light irradiation in vitro against to *E. coli*. The Ti–6Al–4V substrate was deposited by a plasma-sprayed HAp/gray titania coating, and then CIP was performed with 8Hq fluorescent ligands at 800 MPa. The plasma spray had a thermal effect on the Ti_2O_3 powder, thereby changing its phase into TiO_2 with a rutile crystalline structure, as observed by FTIR and XRD spectroscopy. The suspension of *E. coli* with a controlled initial density was used as the reference group and comparing with that exposed to LED light; blue, green, and red light irradiation was applied for 1 hour, respectively.

The optical density at 600 nm was then evaluated to determine the growth rate of *E. coli*, and

then the colonies were cultivated. First, a significant difference was detected between the HAp/gray titania without complex coating and HAp/gray titnia with 8Hq complex coating. The latter group showed a gradual decrease in bacterial growth the growing rate of E. coli is gradually decreasing in irradiated group comparing to the non-irradiated group. A significant reduction of colony numbers was observed in the fluorescent complex 8H8/HAp/gray titania coating group, specifically under red light irradiation, which resulted in free radical generation.

It was concluded that the HAp–8Hq with gray titania coating could effectively prevent bacterial adhesion from the implant surface while applying light irradiation. This suggested that antibacterial enhancement could be achieved by increasing the LED light intensity or photosensitizing induced by 8Hq from the photocatalyst. Consequently, the conventional abutment of titanium alloys was successfully applied using this biomaterial fabrication method. As mentioned above, the antibacterial property of a biomaterial should be biocompatible, reduce the risk of infection, and decrease the chance of damaging of implants. However, the mechanism by which light irradiation enhances the antibacterial property and bacterial attachment have not yet been clarified. The effect of light intensity on enhancing the production of free radicals does not appear to have significance for its antibacterial effects [37]. Therefore, further work is needed to consider the potential contributions of the thermal effect, power intensity, and electrostatic potential on the surface for effectively controlling bacterial cell adhesion behavior.

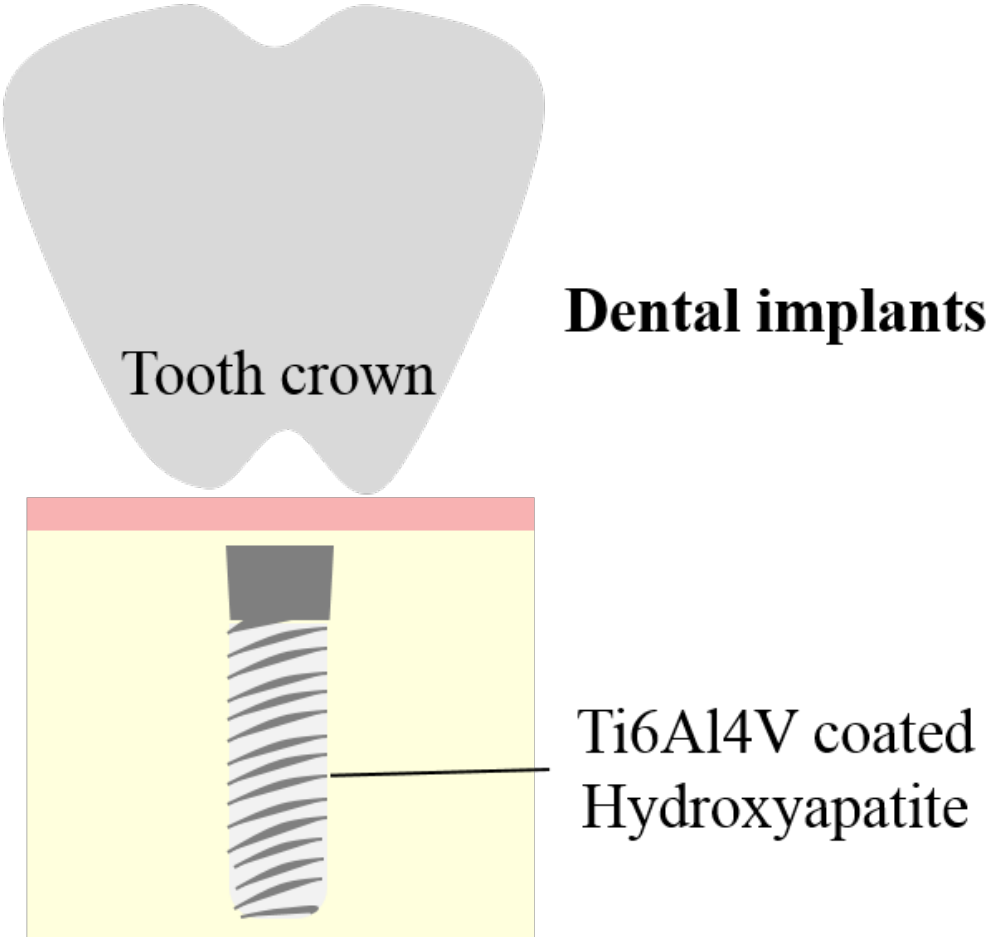

Fig. 1.4 Hydroxyapatite coating on Ti–6Al–4V for use in dental implants

1.6 Motivation and purpose of present study

1.6.1 Motivation

Based on the background above, the aim of the present work was to evaluate the sensitivity of light intensity and the biocompatibility of this specific antibacterial property of 8Hq/HAp with gray titania coating for preparation of a new dental implant material.

The titanium alloy Ti–6Al–4V has been widely used as a biomaterial for orthopedic surgery for decades, especially in dental implants (Fig. 1.4), and many researchers have focused on its long-term durability and biocompatibility. Despite extensive research to overcome the problem of infection in

dental implants, a new modified implant surface with enhanced antibacterial property is necessary. This material must overcome the current problems highlighted in the sections above, including the non-sustainable surface of the antibacterial agent-doped surface, uncontrollable antibacterial property leading to cytotoxicity of bone cells, and effective cell adhesion behavior.

Despite the good antibacterial property induced by the photosensitive fluorescent complex 8Hq/HAp via light [37], the antibacterial enhancement and metal ion release of 8Hq ligands are still limited for effective clinical application, and showed toxicity to bone cells. Therefore, the aim of the present work was to develop ligands for the design of a new fluorescent complex that enhances the antibacterial property and is not toxic to human cells. In addition, previous studies did not examine the effects of the light intensity of visible irradiation, such as increasing free radicals, photosynthesis activity, or energy surface changes, on cell adhesion behavior. Importantly, the mechanism of enhancement of the antibacterial property by light irradiation has not yet been clarified.

During the fabrication of fluorescent 8Hq/HAp complex by CIP, the applied mechanical loading on solid particles was discussed; however, the potential of loading dependency for increasing the fluorescent property has not yet been revealed. Although the CIP process can be effectively applied to a complex shape such as the abutment of a dental implant, the fluorescent complex was distributed on the abutment sample by UV light irradiation. [35] Moreover, the effect of mechanical loading such as residual stress or compacted orientation of complexity was not discussed in-depth, which could play an important role for improving the fluorescent intensity, which would in turn enhance the antibacterial property. These remaining questions and unknown mechanisms served as the specific motivations for continuing this line of investigation with the present work.

1.6.2 Objective of the present study

The main objective of the present study was to develop a new plasma-sprayed HAp-coated conventional Ti–6Al–4V biomaterial with optimized antibacterial property for use as a dental implant by applying light irradiation with a sensitive photocatalyst. First, we aimed at improving the fabrication methods of the fluorescent complex of HAp–amino acid ligands. We optimized the fluorescent intensity by examining the pressure dependency during the CIP process, which plays an important role on increasing the antibacterial efficiency. Second, the surface characteristics of the fluorescent complex HAp—amino acid were determined to clarify the cell adhesion behavior while applying light irradiation on the antibacterial coating on the implant surface. Finally, we aimed to develop strategies for potential further optimization of this antibacterial application for further study.

1.6.3 Scope of the present study

This work therefore expands upon previous studies conducted in our research group as highlighted in the sections above by focusing on the development of the antibacterial property of a fluorescent complex of a HAp coating with aromatic organic ligands and determining its photocatalyst property under light irradiation. To further suppress the cytotoxicity and achieve control over the antibacterial property of a dental implant, a novel method of antibacterial enhancement of a HAp/fluorescent ligands complex with gray titania coating on a Ti–6Al–4V biomaterial is introduced, as outlined in Fig. 1.5. In Chapter 1, all of the relevant evidence of previous research investigating biocompatible biomaterials for use as orthopedic implants is summarized, and the remaining challenges are highlighted. Accordingly, the novel concept of this study is presented by enhancing the antibacterial property of a

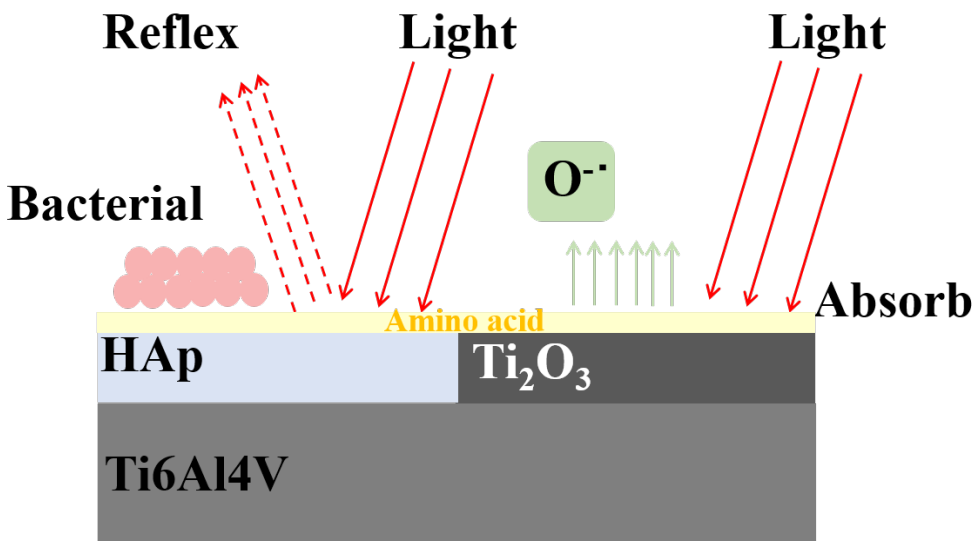

Fig. 1.5 Enhancement of the antibacterial property of a dental implant from visible light irradiation on a fluorescent HAp–amino acid complex with gray titania coating.

biomaterial such as a sensitive photocatayst via light irradiation and its free radical property. Conventional titanium alloys were developed for use as an implant material because of their high corrosive resistance and biocompatibility in the human body.

In Chapter 2, the fabrication method for the antibacterial coating on the plasma-sprayed HAp coating on conventional the Ti–6Al–4V biomaterial is described. This chapter aims at revealing the effects of the pressure applied during the CIP process on the microstructure of HAp fluorescent complexes and their optical properties. Although the microstuructural-dependent properties of HAp fluorescent complexes in improvin the antibacterial property of a photocatalyst-coating layer has been reported, the underlying mechanism driving these changes in the fluorescence property of highly compressed HAp complexes has not yet been unveiled. The CIP process was used to successfully fabricate the HAp–amino acid fluorescent complexes, and their fluorescence intensity was increased by increasing the pressure during fabrication. Although the thickness of the amino acid layer was saturated under higher pressure, the concentration of the amino acids proportionally increased with higher pressure,

suggesting the packed structure of ligands in the HAp–amino acid complexes. Polarized Raman spectroscopy measurement clearly detected the normally arranged ligands on the HAp layer in highly pressurized conditions, which can provide the highly packed ligand structure in HAp–amino acid complexes. This structure could in turn emit stronger fluorescence by increasing the density of the complexes. This newly found pressure dependency in the optical property of HAp–amino acid complexes will be beneficial to develop biocompatible fluorescent materials or enhancement agents of antibacterial coating layers.

Chapter 3 was performed to reveal the mechanism of the enhancement of antibacterial properties of gray titania by plasma-sprayed HAp–amino acid fluorescent complexes under irradiation with visible light. Antibacterial coatings with visible light-sensitive photocatalysts have been widely studied for application to dental implants. Although these photocatalysts have been safely applied to the oral cavity, their efficacy is not high because of the low energy of irradiating light. Consequently, in this study, HAp–amino acid fluorescent complexes were combined with visible light-sensitive photocatalysts to act as bacteria catchers as well as light concentrators, based on an idea inspired by the mechanisms of deep-sea fluorescent coral reefs. HAp–amino acid fluorescent complexes were successfully fabricated from three types of amino acid ligands using a CIP process. A cytotoxicity assay on murine osteoblast-like cells revealed that the biocompatibility of the HAp–amino acid fluorescent complexes was identical with that of HAp. Moreover, antibacterial assays using *E. coli* showed that the three types of HAp–amino acid fluorescent complexes and irradiation with three types of light-emitting diodes (blue, green, and red) significantly decreased the numbers of colony-forming units. Furthermore, the surface potentials of HAp or HAp–amino acid fluorescent complexes were mea-

sured by Kelvin probe force microscopy with simultaneous visible-light irradiation, which revealed that the HAp–amino acid fluorescent complexes preserved the surface potentials even after irradiation with visible light, whereas those of HAp were significantly decreased by the irradiation. Such a preservative effect of the HAp–amino acid fluorescent complexes maintained the bacterial adhesion performance of HAp and consequently enhanced the antibacterial action of gray titania.

Finally, Chapter 4 provides an overall conclusion of this successful investigation of the effective antibacterial property of the fluorescent HAp–amino acid complex with gray titania coating on a conventional Ti–6Al–4V substrate by applying visible light irradiation. The CIP process was used to successfully fabricate the fluorescent complex of HAp–amino acid ligands. The exploitation of pressure dependency could improve the fluorescent property. The conventional light irradiation with a sensitive photocatalyst enhanced the antibacterial property. Moreover, standardization of this fabrication method was achieved to ensure its reliability for application as implants or other biomaterials for use in the medical industry. Therefore, through this work, it is now possible to fabricate biomaterial implants that are biocompatible, with controllable and reliable antibacterial property using a plasma-sprayed HAp coating conventional titanium alloy.

Chapter 2 Fabrication of HAp–Amino Acids Complexes using CIP and their Optical Properties

Abstract

This study aims to reveal the effects of pressure during cold isostatic pressing (CIP) on the microstructure and optical properties of fluorescent HAp complexes. Although the microsturucture-dependent properties of fluorescent HAp complexes have been reported to improve the antibacterial properties of photocatalyst coating layers, the mechanism behind the changes in the fluorescence properties of highly compressed HAp complexes has not yet been unveiled. CIP was successfully used to fabricate fluorescent HAp–amino acid complexes, and their fluorescence intensities increased with increasing fabrication pressure. Peak wavelength of fluorescence emitted by the HAp–amino acid complexes exhibited yellow to red shift. Although the thickness of the amino acid layer was saturated in higher pressure cases, the concentration of amino acids increased proportionally with pressure, which suggests changes in the packing structures of the ligands in the HAp–amino acid complexes. Polarized Raman spectroscopy measurements clearly detected ligands normally arranged to the HAp layer under high pressure fabrication conditions, which can provide the tightly packed ligand structure in the HAp–amino acid complexes. These tightly packed ligand structure in the HAp–amino acid complexes could emit stronger fluorescence owing to the increased density of complexations. This

newly found pressure dependency in the optical properties of HAp–amino acid complexes is beneficial for developing biocompatible fluorescence materials or enhancement agents for antibacterial coating layers.

2.1 Introduction

Titanium alloys are widely used for artificial hip joints and dental implants because of their high mechanical strength and corrosion resistance[3, 4]. In order to bond titanium alloys implants to bone, hydroxyapatite (HAp) coating layers are normally applied as the biocompatible coating owing to its excellent osteoconductivity [4, 5, 6]. HAp coating layers have successfully been deposited by plasma-spraying on the surface of Ti-6A-l4V alloys for dental implants[7]. However, after long-term use, the need for implant revision increases owing to bacterial infection [12, 8, 9, 10]. Especially for dental implants, inhibiting the attachment of biofilms on the surfaces of the dental implants is indispensable for preventing bacterial infection[12, 13, 14, 16]. Researchers have tried depositing silver ions or TiO_2 nanotubes on the surfaces of implants in order to suppress bacterial infections[17, 18, 20, 38, 21, 39, 40, 22, 23, 41]. Unfortunately, such conventional antibacterial agents also suffer human cells because of difficulty in controlling the concentration of the antibacterial agents. Therefore, the development of antibacterial and biocompatible coating layers is important for suppressing infection in dental implants[42, 43, 44]. Researchers have proposed several methods for modifying surface charges by chemical treatments [24, 26] or adding peptides/protein [27, 28, 30] to fabricate such the multifuctional coating layers. Although these coating layers inhibit bacterial attachment on the surfaces of implants, their antibacterial properties are hard to control because of

the absence of antibacterial agents.

Fluorescent complexes of HAp combined with photocatalysts have recently been proposed as enhancement agents for the controllability of antibacterial properties [35, 37, 45]. This technology was biologically inspired by the light-condensing effect of fluorescence in mesophotic reefs at the depth of 50–60 m in seawater, which increases the efficiency of photosynthesis [34]. In the case of a fluorescent complex of HAp with 8-hydroxyquinoline (8Hq), differing amounts of pressure during the fabrication process could provide changes in fluorescence intensity and peak wavelength [35]. Furthermore, the surface charges on the surface of HAp coating layers were stably changed by ligands in the HAp complexes, which affected their antibacterial performance[45]. Although the microsturucture-dependent properties of HAp fluorescent complexes improved the antibacterial property of a photocatalyst coating layer [37, 45], the mechanism behind the changes in the fluorescence of highly compressed HAp complexes has not yet been unveiled.

This study aims to reveal the effects of pressure during cold isostatic pressing (CIP) on the microstructure of fluorescent HAp complexes and their optical properties. Firstly, the fluorescence wavelengths of different types of HAp complexes were observed by photoluminescence (PL). Raman spectroscopy was conducted for both pure powder and fluorescent complexes of HAp with amino acids in order to discuss the concentration of ligands. Raman spectra can reveal residual stress [46], the formation of hydrogen bonding[47, 48], or dimers and phase changes[49]. An effect of mechanical loading on the peaks shift in the Raman spectra of amino acid ligands has been observed by in situ Raman spectroscopy as well as four-points bending(4PB)[46]. Polarized Raman spectroscopy was also conducted to discuss the orientation of the fluorescent complexes of HAp with amino acid

coating layers. The relationships between changes in the microstructure of the HAp complexes and their optical properties were discussed.

2.2 Experimental procedure

2.2.1 Preparation of specimens

Three types of amino acids pure powder; Phenylalanine, Tryptophan, and Tyrosine (Kishida Chemical Co. Ltd., Osaka, Japan), were used. The pure powders of the amino acids were filled in silicone molds of a rectangular shape (KE-17, Shin-Etsu Chemical Co. Ltd. Tokyo, Japan). The silicone molds were wrapped tightly using a plastic wrap and put into a vacuum incubator for 1 hour . The molds were finally sealed in plastic bags using a vacuum sealer machine (AS-V-01, Kyutarou, Asahi Industry Co. Ltd., Japan). The molds were pressurized using a Cold Isostatic Pressing machine (Model P-500, Kobe Steel, Ltd, Japan) with the conditions of 200, 400, 600, 800 MPa and holding time of 20 minutes, respectively (Fig. 2.1). Those pressurizing conditions were referred by previous studies [35, 45].

Fluorescent complexes between HAp with the three types of amino acids were fabricated by the CIP process. HAp powders and amino acids powders were mixed in a ball mill at the weight ratio of 1:1. The mixed powders were then dried in a vacuum chamber for 1 hour, and sealed in plastic bags using a vacuum sealer machine. The sealed plastic bags were subsequently placed in the vacuum chamber again for 24 hours. The sealed plastic bags were pressurized using the CIP machine with the same pressurized conditions.

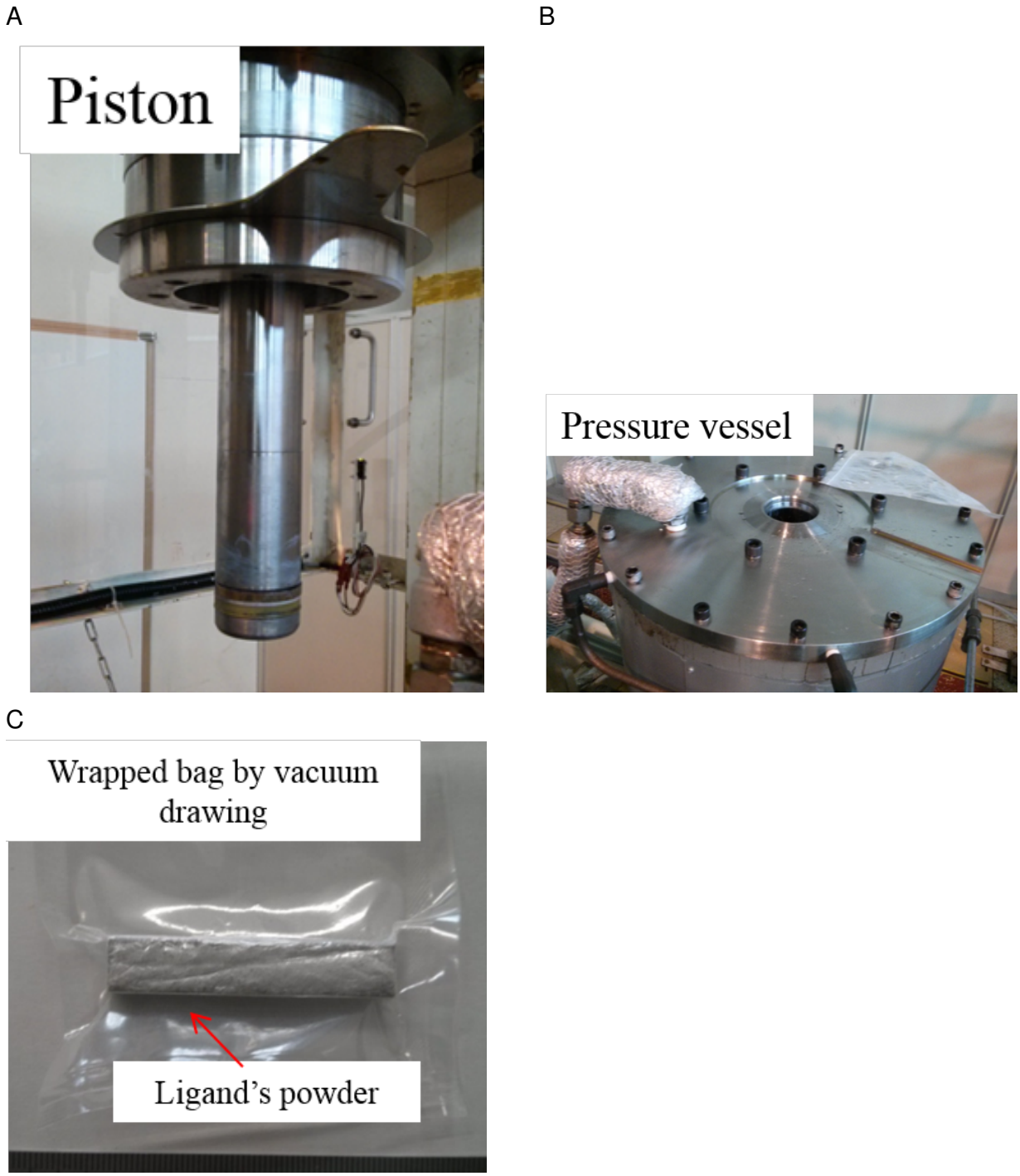

Fig. 2.1 Cold Isostatic Pressing (CIP) machine for fabricating HAp–amino acid complexes. (A)Piston. (B) Pressure vessel which was filled with water. (C) Wrapping samples using a vacuum sealing machine.

The same CIP procedure was applied to sealed amino acid powders on plasma-sprayed HAp Titania coating layers on Ti-6Al-4V substrates with the dimensions of $50 \times 10 \times 3$ mm^3. For 4-point bending in raman spectroscopy, amino acid powders were adhered on a surface of Ti-6AL-4V substrates with

the dimensions of $35 \times 5 \times 3$ mm^3. The adhesive used was cyanoacrylate base cement (CC-33A, Kyowa, Japan). The side surface of the amino acids layers were polished using # 1200 emery paper. A strain gage (KFG-2-120-C1-11L1M2R, Kyowa, Japan) was adhered on the compression side of the substrates.

2.2.2 Optical property measurements

Fluorescence from HAp–amino acid complexes was observed by fluorescent microscope (BZ-8100, Keyence Co., Ltd.). The excitation source were 360±20 nm, 470±20 nm and 540±12.5 nm respectively with exposure time for 0.5 s. The filtering diffraction of light was DF and MF40. The luminescent results were observed in blue(460±20 nm), green(535± 25 nm) and red (605±27.5 nm) fluorescence. Photoluminescence(PL) spectra was also observed using Fluorescence Spectrophotometer (F-7000, Hitachi High Technology, Japan). Photoluminescence excitation (PLE) and PL spectra were measured from 200nm to 800 nm using the sampling interval of 10nm, scanning rate of 30000 nm/min, excitation slit of 5nm, emission slit of 20nm and photomultiplier voltage of 400 V, respectively. UV - filter was inserted at the emission side in order to cut the fluorescence emitted by amino acids whose maximum wavelength was in the UV range (290nm(Phe),305nm(Tyr),and 350nm(Trp), respectively)[50]. Though the HAp powders reflected the excitation light, the PL intensity was calculated using the background subtraction of the intensity of HAp powders from the one of HAp–amino acid complexes. PL spectra were fitted into Gaussian function ($a \exp(-\frac{(x-b)^2}{2c^2})$;indeterminate coefficients;a, b, c) using a non-linear least-squares method solved by Gauss - Newton method in R 3.4.2 package. Quantum yields of fluorescence by HAp–amino acid complexes were also mea-

sured using absolute PL quantum yields measurement system (Quantaurus-QY, Hamamatsu Photonics, Japan).

2.2.3 Surface morphology measured by Scanning Probe Microscope(SPM)

In order to evaluate a thickness of ligands layers of HAp–amino acid complexes, SPM measurement were conducted. Micro vickers hardness tests were firstly applied on the surface of the HAp–amino acid fluorescent complex layers to expose HAp coating layers at the edges of Vickers markers. Contact modes measurements using a cantilever of Micro cantilever, OMCL-TR800PSA-1, Olympus with the conditions of laser operating point at 0.2 volt, P-gain 0.001 and I-gain of 700.0 (SPM-9700, Shimadzu Co. ltd.). The thickness of the ligands layers was then measured by steps in surface profiles by SPM measurements.

2.2.4 Raman spectroscopy measurements

Raman spectroscopy measurements were conducted to identify structural changes in fluorescent complexes between HAp with amino acid powders. Laser source was 532 nm (25mW) ,grating #2400, magnification lens $\times$100, exposure time of 4 seconds and accumulation of 20 times were used in the measurements (LABRAM HR 800, Horiba Jobin Yvon). In order to suppress fluorescnce during the raman spectroscopy measurement, 785nm laser source wer also used (NRS-7200, Jasco).

For mechanical loading tests, a four-point bending jig [46] was placed under the CCD camera of the raman spectroscopy instrument(LABRAM HR 800, Horiba Jobin Yvon). Load step was 10 N and and raman spectra at a maximum bending stress point was observed by every 10 N until the specimen was

broken. The applied load was converted into bending stress σ using the elastic formula of 4-points bending.

2.2.5 Polarized Raman spectroscopy measurements

Polarized raman spectroscopy measurements were conducted to observe anisotropy of spectra intensity of HAp fluorescent complexes. Each of three types of polarization lenses; SPF-30C-32, WPQ-5320-2M, or Z-Polarizer(Z-Polarizer-532-QzM-4), (OptoSigma, California, USA) were inserted in an input path or an output path of laser line in the raman spectroscopy machine. (LABRAM HR 800, Horiba Jobin Yvon). Measurement conditions were the same as in the cases of raman spectroscopy without using the polarizers. In the case of Z -direction polarization measurements, it was impossible to insert the Z-Polarizer in the output path of laser due to its polarization mechanism. Therefore, the Z-polarizer was inserted only in the input pathway.

In order to analyze alignment angles of the ligands in HAp/amino acid complex, Raman tensor analyses for orientation angles of molecules in a single crystal [51] were applied to analyze the polarized Raman measurement results. The relation of raman tensors between $\boldsymbol{\alpha}^{lab}$ in the laboratory axis system XYZ with $\boldsymbol{\alpha}^{mol}$ in the molecule axis system xyz is shown in the following equation,

$$\boldsymbol{\alpha}^{lab} = \boldsymbol{R}^T \boldsymbol{\alpha}^{mol} \boldsymbol{R} \cdots\cdots (2.1)$$

where $\boldsymbol{R}$ is the orthogonal rotation matrix using angles ϕ, θ, ψ. A peak of 997 cm^{-1} in phenylalanine was selected for the calculation because it was the strongest peak and an in-plane vibration mode[52]. Raman tensors $\boldsymbol{\alpha}$ are defined by the next equation[51, 53],

$$\boldsymbol{\alpha} = \alpha_3 \begin{bmatrix} r_1 & & \\ & r_2 & \\ & & 1 \end{bmatrix} \cdots\cdots (2.2)$$

In the case of in-plane bending mode [52], $r_1 = r_2$ in equation (2.2). The relationship between polarized raman intensity$\boldsymbol{I}_{ij}$ with the raman tensor is then expressed as the following equation,

$$\boldsymbol{I}_{ij} = K|e_i^T \boldsymbol{R}^T \boldsymbol{\alpha}^{mol} \boldsymbol{R} e_j|^2 \qquad \text{(i,j=X,Y,Z)} \cdots\cdots (2.3)$$

where e_i is the unit vector of the exciting radiation. The equation (2.3) has five unknowns, $r_1 = r_2$, ϕ, θ, ψ and K. Polarized raman measurement results for five pairs are then necessary. Using Z-polarizer enabled us to complete the five measurements. Five non-linear simultaneous equations using the equation (2.3) were numerically solved using R 3.4.2 package. Though the second order of the equation (2.3) could not provide an unique solution, we obtained several pairs of angles. The pair which had maximum values in the angles were selected as an orientation angle.

2.3 Results

2.3.1 Pressure dependency of fluorescence property of HAp–amino acid complexes

Fluorescent microscopy observations revealed that all three types of HAp–amino acid complexes emitted fluorescence, and those maximum values in wavelength were highly dependent on the pressure used during fabrication (Fig. 2.2). Fluorescence emitted by amino acid was in the UV range

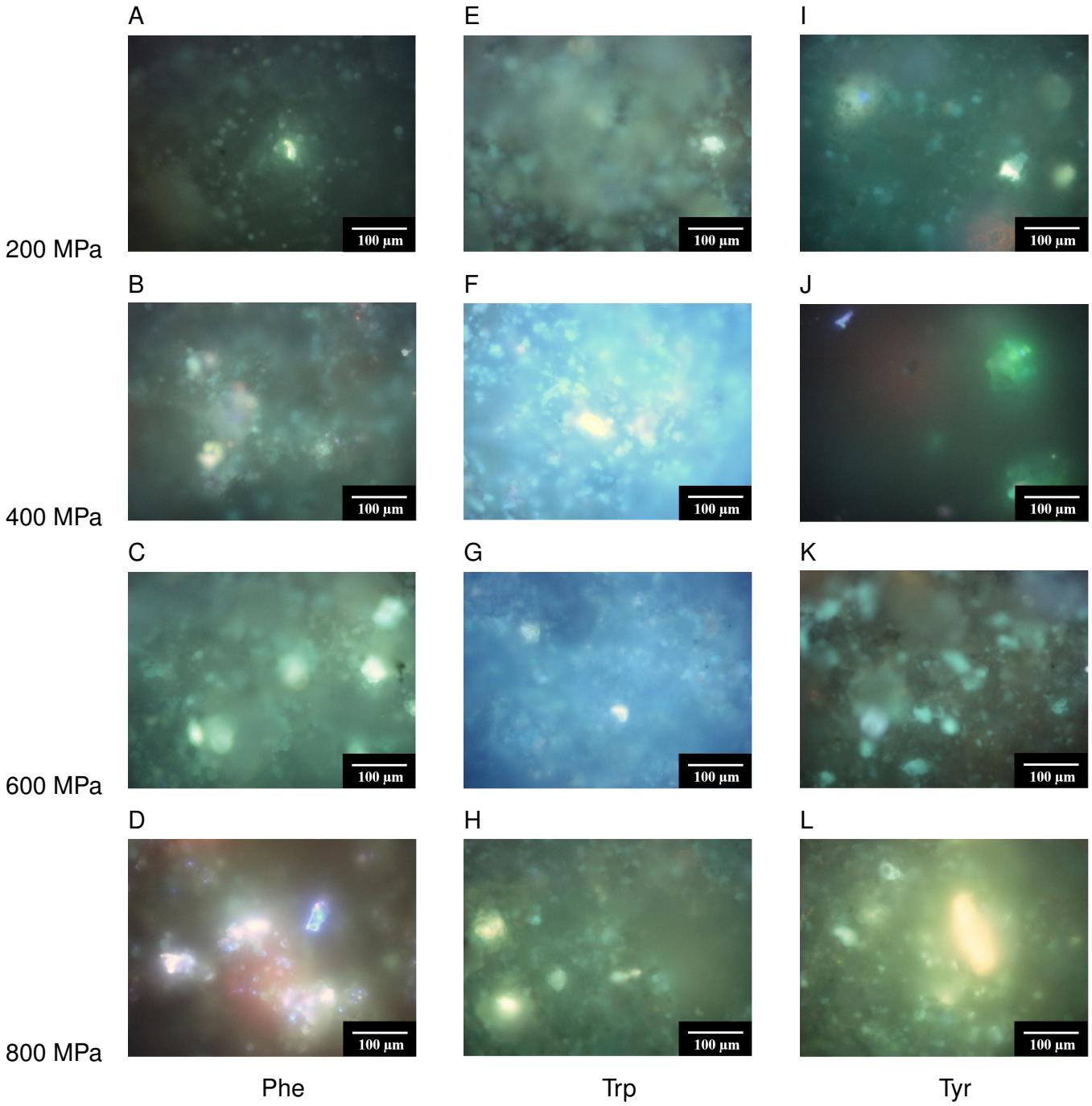

Fig. 2.2 Pressure dependency on fluorescence intensity emitted by HAp–amino acid complexes. (A–D) HAp-phenylalanine (Phe) complex. (E–H) HAp-tryptophan (Trp) complex. (I–L) HAp-Tyrosine (Tyr) complex. All pictures are merged images of of red, green, and blue fluorescent images. Exposure time in all images was 0.5 s.

(290nm(Phe),305nm(Tyr),and 350nm(Trp), respectively [50]), and the HAp complexes emitted green to yellow fluorescence by Metal-Ligands Charge Transfer (MLCT) [35]. Though the complex layer was covered by unreacted amino acids, the diffraction or UV fluorescence by amino acid surface,

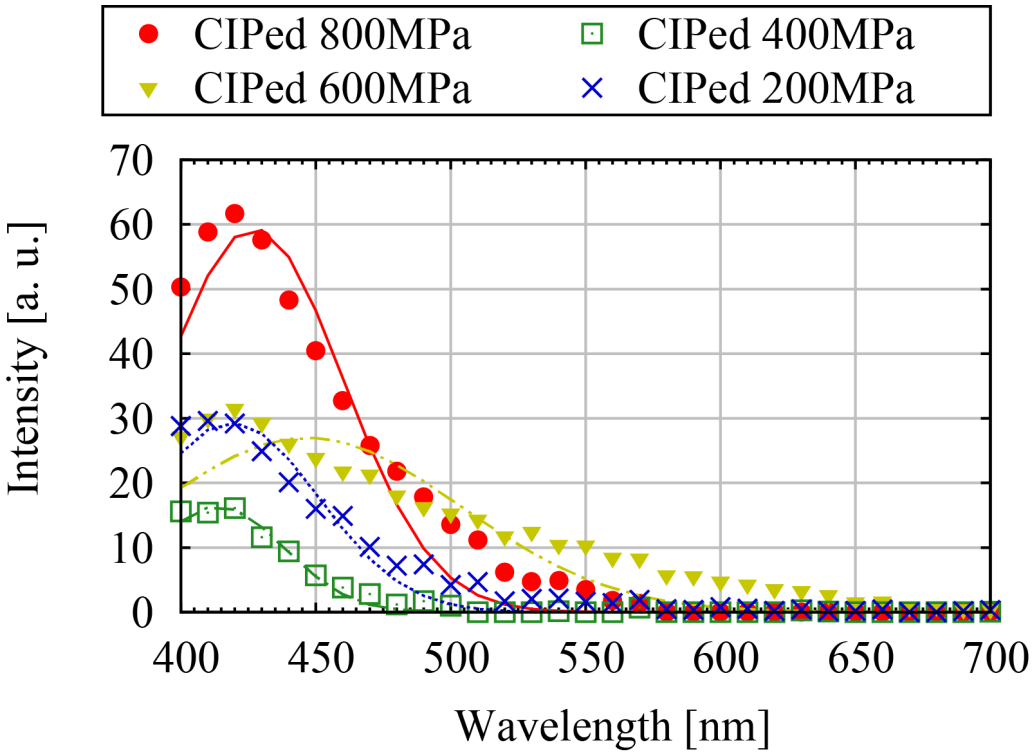

Fig. 2.3 Pressure dependency on photoluminescence spectra emitted by the powders of HAp-phenylalanine (Phe) complex (Excited by 330nm).

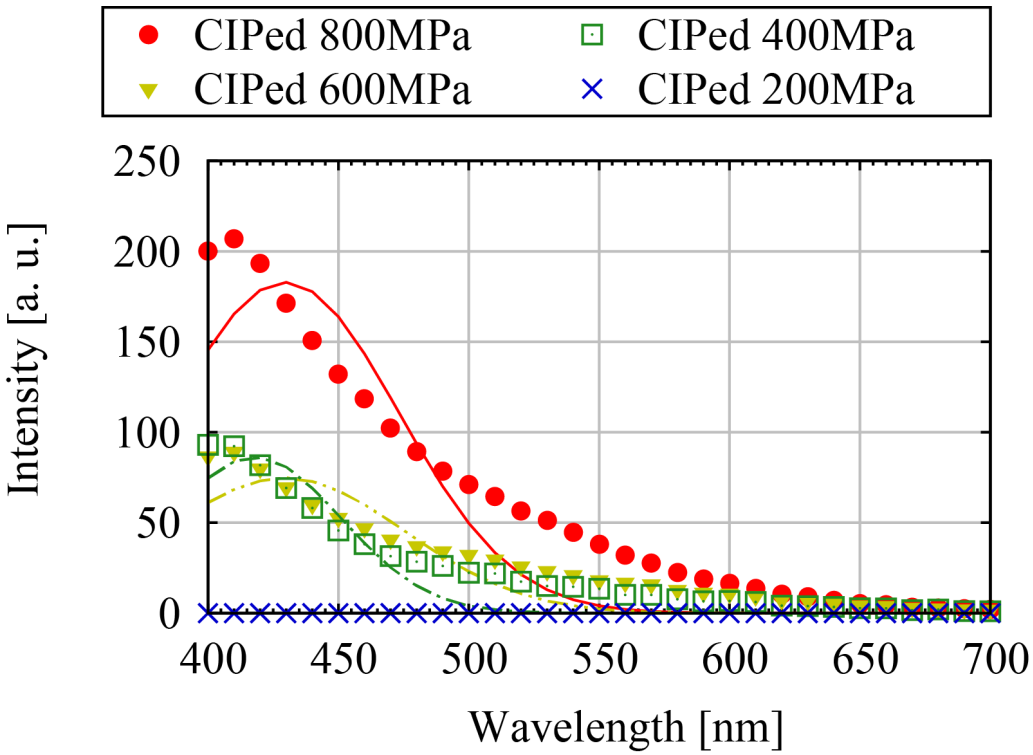

Fig. 2.4 Pressure dependency on photoluminescence spectra emitted by the powders of HAp-Tyrosine (Tyr) complex (Excited by 330nm).

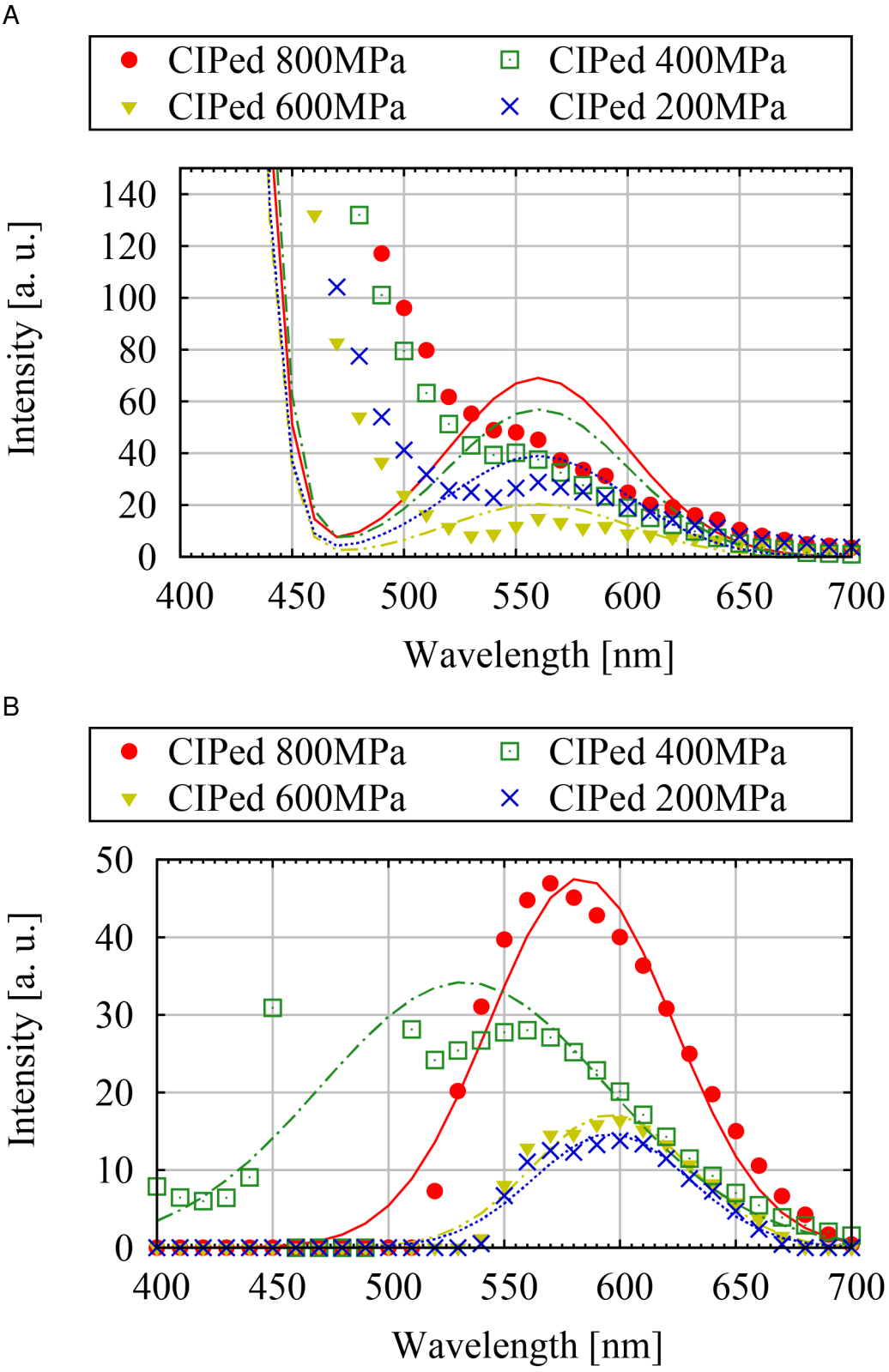

Fig. 2.5 Pressure dependency on photoluminescence spectra emitted by the powders of HAp–amino acid complexes. (A) HAp-tryptophan (Trp) complex (Excited by 280nm). (B) HAp-Trp complex (Excited by 480nm)

which could not be perfectly suppressed by UV filter, was observed. Observed fluorescence was then blue to green in the low pressure cases (Fig.2.2(a-c,d,-g,i-k)). On the other hand, high pressure could decrease thickness of unreacted layer and increase concentration of the HAp–amino acid complex, which led to dominant composition of fluorescence emitted by the complexes (Fig. 2.2(d,h,l)). Especially in the case of highly compacted case, intermolecular interaction among benzene rings in the amino acid molecule increased ($\pi - \pi$ stacking [54]), which can promote red-shifted fluorescence. We have observed fluorescence of HAp-Phe complex after water immersion, and fluorescence color was changed from blue-green, yellow to red[45] . These results can be explained by the removal of unreacted amino acid layer and exposure of HAp–amino acid complex layer which was stacked on the surface of HAp. Consequently, the change in fluorescence color in Fig.2.2 can be attributed to decreased fluorescence by amino acid themselves as well as increased concentration of HAp–amino acid complex.

The PL spectra also showed increased yellow to red fluorescence in the case of 800MPa (Figs. 2.3,2.4,2.5). In the case of HAp-Phe complex, it was the most excited by 330nm though the maximum absorption wavelength in Phe itself was 257 nm[50], which simply certified the complexation. Higher compression provided broadened peak to yellow light region (the 600 MPa in Fig.2.2 (c) and Fig. 2.3), and stronger fluorescence from blue to red light region (the 800 MPa in Fig.2.2 (d) and Fig. 2.3). HAp-Tyr complex was also excited mostly by 330nm though the maximum absorption wavelength in Tyr itself was 275 nm [50]. Green fluorescence was firstly increased in the cases of 400 MPa and 600 MPa cases (Fig.2.2 (j,k) and Fig. 2.4), and finally yellow light region subsequently increased in the 800 MPa case, which led to stronger as well as broadened peak (Fig 2.2 (j,k) and Fig. 2.4).

Fluorescence of the HAp-Trp complex excited by 280 nm (maximum absorption wavelength of Trp [50]) showed strong blue fluorescence probably due to the leaked bottom edge of UV fluorescence by Trp itself. However, the existence of a peak at 560-580 nm (yellow) was significantly detected and its intensity was increased at highly compressed cases (Fig. 2.2 (e,f,g) and Fig. 2.5). PL spectra of the HAp-Trp complex excited by 480 nm (newly formed maximum absorption peak in PLE spectra) showed that yellow fluorescence was increased especially at the 800 MPa case (Fig. 2.5(B)) , and the peak was matched with the fluorescence microscope observation (Fig.2.2 (h)). A higher peak at the 400 MPa of HAp-Trp complex was not due to HAp-Trp complex but to an increased concentration of Trp because it showed blue fluorescence emitted by Trp itself (Fig.2.2(f) and blue-shifted peak inFig. 2.5(B)). The highest pressure cases commonly demonstrated increased intensity as well as yellow to red shifted fluorescence (Fig.2.2(D,H,L) and Figs. 2.3,2.4,2.5), which revealed the pressure dependency of fluorescence.

In the case of 800MPa, quantum yields of HAp-Phe and HAp-Trp complexes were gradually increased (Figs.2.6,2.7). probably due to increased concentration of the complexes. Those of the HAp-Tyr complex were not increased regardless of the pressure conditions (Fig.2.8). In the 200 MPa case in the HAp-Phe complex,the values were widely fluctuated due to diffraction or reflection light by HAp particles because the case did not exhibit strong fluorescence (Fig.2.2(a)). These values of quantum yields were identical to those of the solid state fluorescent complexes [55].

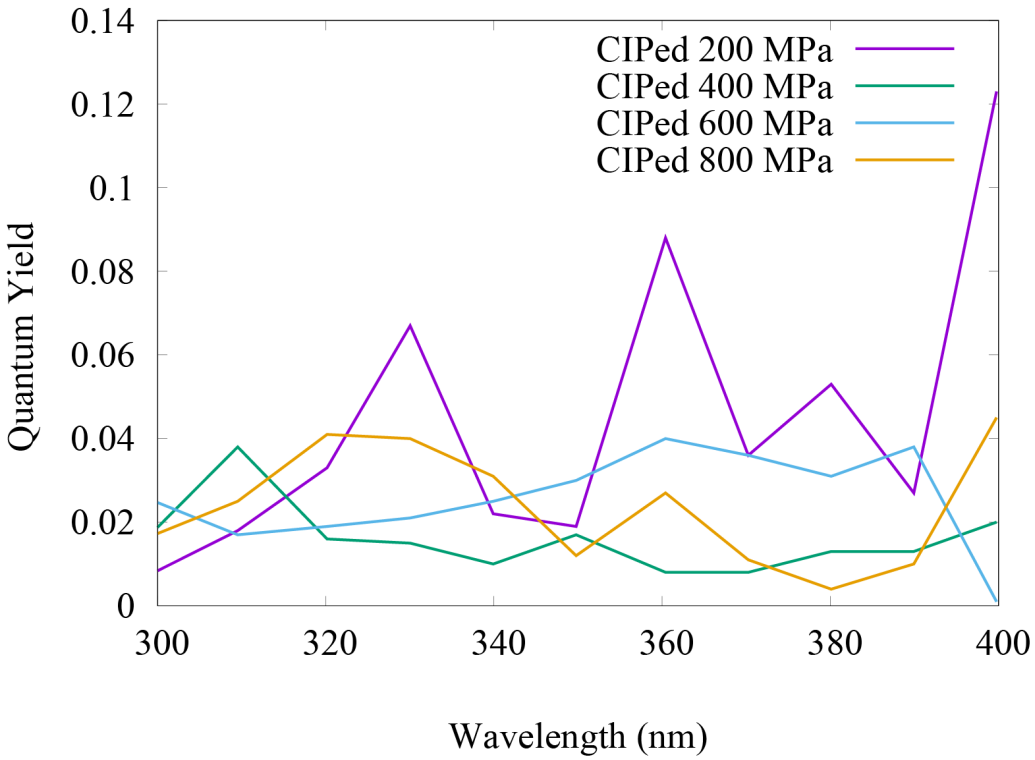

Fig. 2.6 Pressure dependency on absolute quantum yields of fluorescence emitted by the powders of HAp-phenylalanine (Phe) complex.

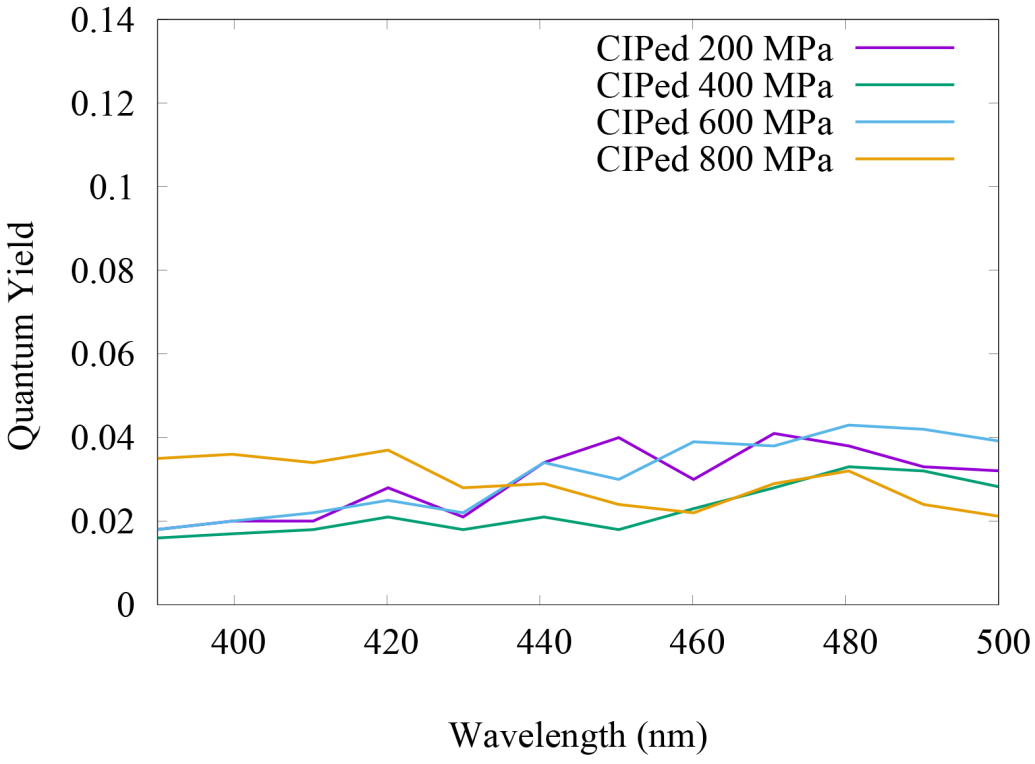

Fig. 2.7 Pressure dependency on absolute quantum yields of fluorescence emitted by the powders of HAp-tryptophan (Trp) complex.

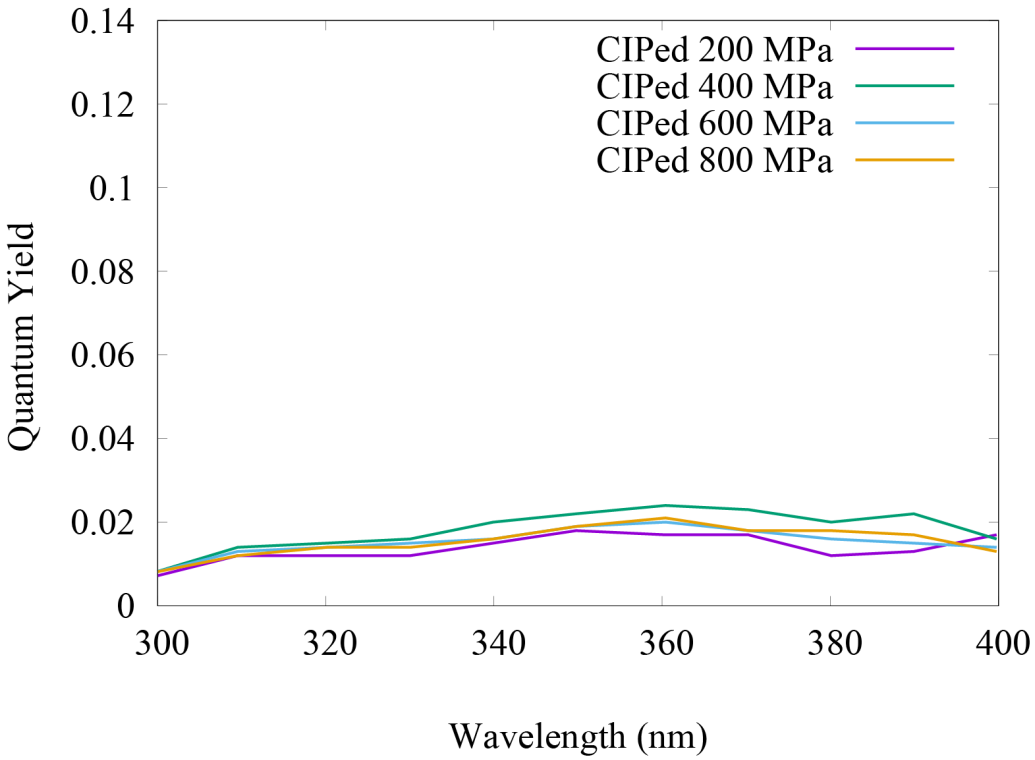

Fig. 2.8 Pressure dependency on absolute quantum yields of fluorescence emitted by the powders of HAp-Tyrosine (Tyr) complex

2.3.2 Thickness of amino acids ligands on HAp coating

SPM measurement revealed increased thickness of ligands of HAp-Phe complex which was fabricated by higher pressure(Fig. 2.9A,B). Surface morphology was changed from flat to shallow terraced fields as indicated by red dashed lines (Fig. 2.9(a-d)), which specified the amino acid layer at the indentation edges. We retrieved cross-sectional surface profile and removed inclinations in the surfaces using a baseline correction, and then the thickness of the ligand layer was finally measured by maximum height in the amino acid area. Measured thickness of amino acids were increased with increasing fabricating pressure(Fig. 2.10). Such the saturated thickness was commonly observed regardless the types of amino acids (Fig. 2.10). HAp-Try complex had a thinner thickness probably due to its repulsive force by polarized charge at its surface.

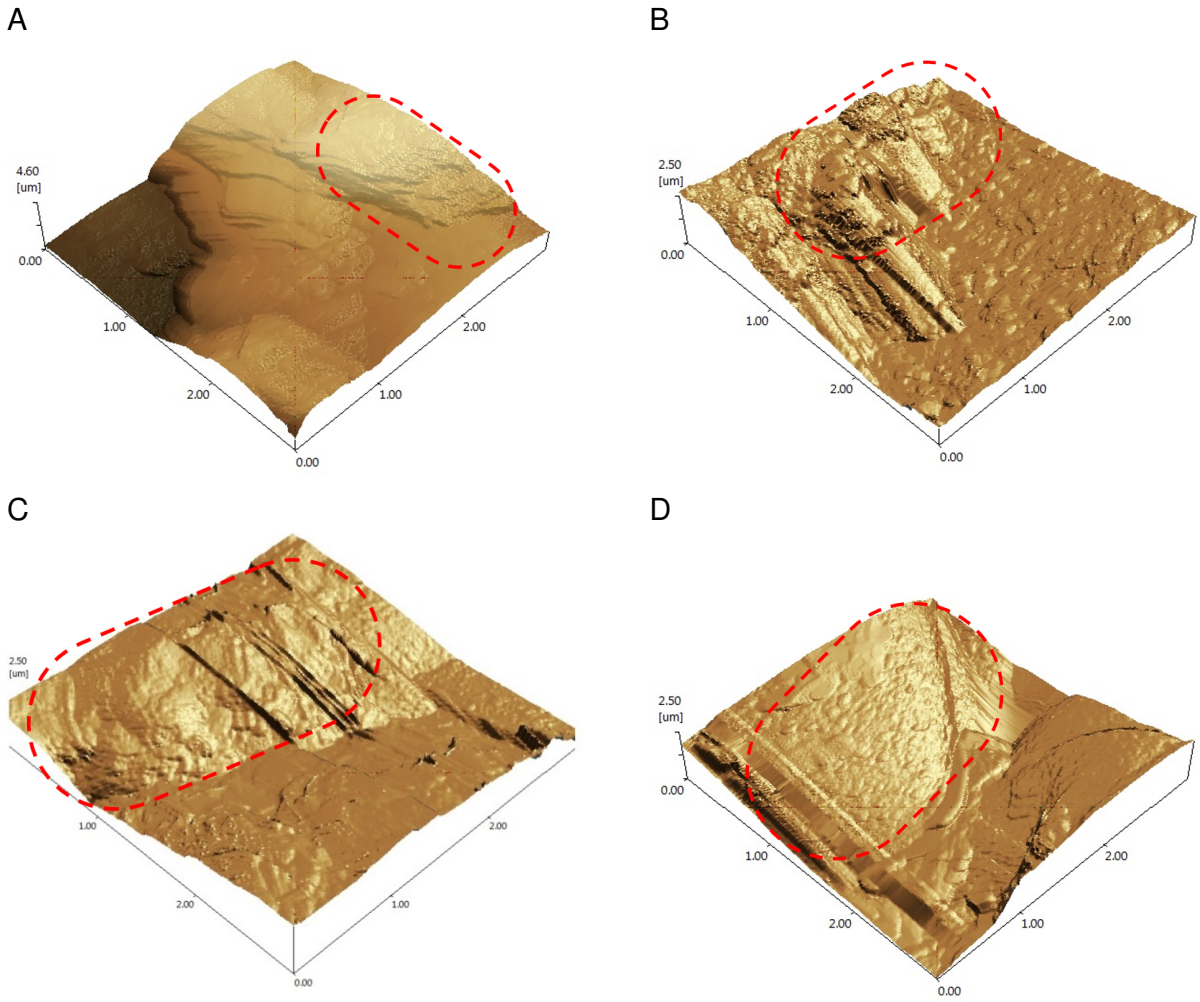

Fig. 2.9 Scanning Probe Microscopy(SPM) image for HAp–amino acid complexes at the indentation edges made by micro Vickers hardness indenter. (A) HAp-Phe complex CIPed 200 MPa. (B) HAp-Phe complex CIPed 400 MPa (C) HAp-Phe complex CIPed 600 MPa. (D) HAp-Phe complex CIPed 800 MPa Red dash lines indicate the area of amino acid layers at the indentation edges.

2.3.3 Pressure dependency of raman spectra of HAp–amino acid complexes

Raman spectroscopy measurement was conducted to observe the molecular structure of amino acid molecules in HAp–amino acid fluorescent complexes. The pressure itself did not affect significantly the Raman shift of the strongest peak δ in of Phe (Fig. 2.11(a)) though the peak intensity was proportionally increased due to increased concentration by compaction. The formation of the HAp-Phe complex shifted the δ peak by approximately 10 cm^{-1}, regardless of the fabrication pressure (Fig. 2.11(b)). There are two considerable mechanisms of the peak shift, e.g., residual stress[46] and for-

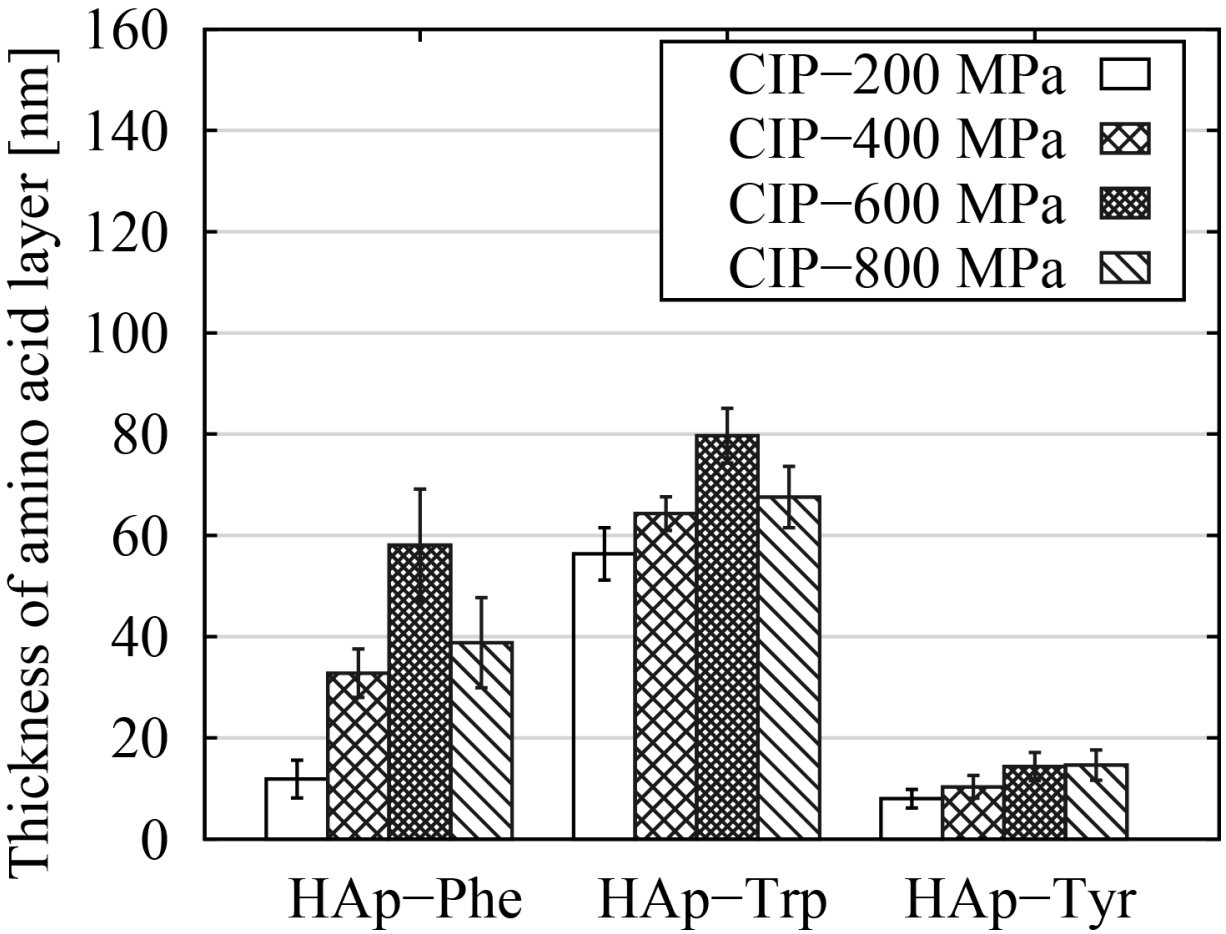

Fig. 2.10 Pressure dependency of thickness of amino acid layer measured by SPM.

mation of chemical bond[47, 48, 49]. 4-Point bending determined that peak shift coefficient of Phe was approximately - 0.5cm^{-1}/ GPa((Fig. 2.12). The obtained values was identical to a reported value (-0.58cm^{-1}/ GPa) by diamond anvil test conducted by da Silva *et. al.*[56]. In phenylalanine case, stress softening by elongation of molecule chain may decrease strain in the phenylalanine and then low peak shift coefficient was obtained. The low value of peak shift coefficient can simply reject a hypothesis that major cause of peak shift was mechanical residual stress (10 cm^{-1} in peak shift corresponds to - 20 GPa of residual stress). Therefore, the peak shift (Fig. 2.11A and B) was due to formation of chemical bonds such as hydrogen bond, dimer of complexations. During the complexation, coordinate bonds between surface Ca^{+2} ions in HAp crystals with the amino group and

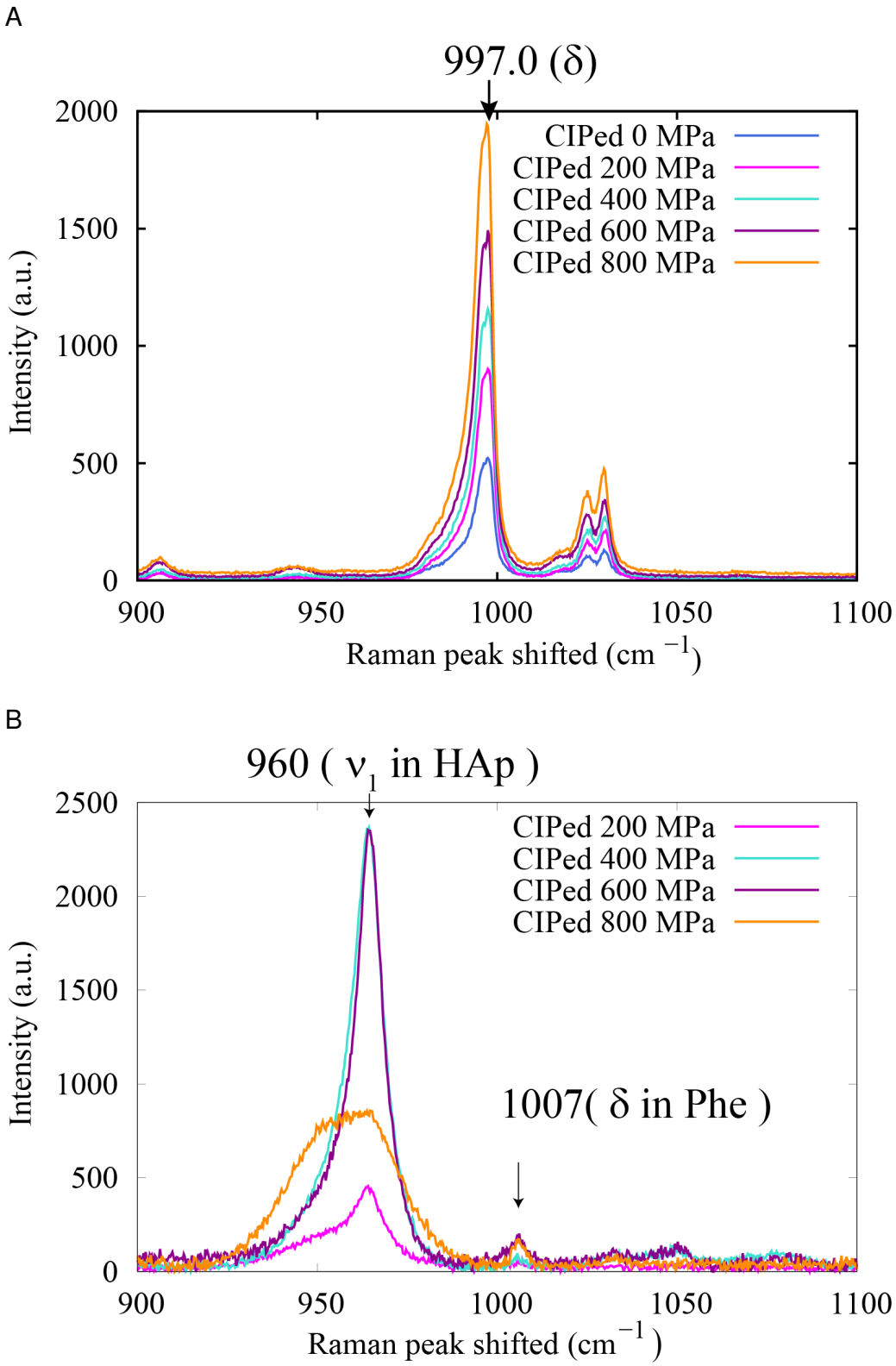

Fig. 2.11 Pressure dependency on raman spectra of HAp-phenylalanine (Phe) complex. (A)Phe powder after CIPed. (B) HAp-Phe complex.

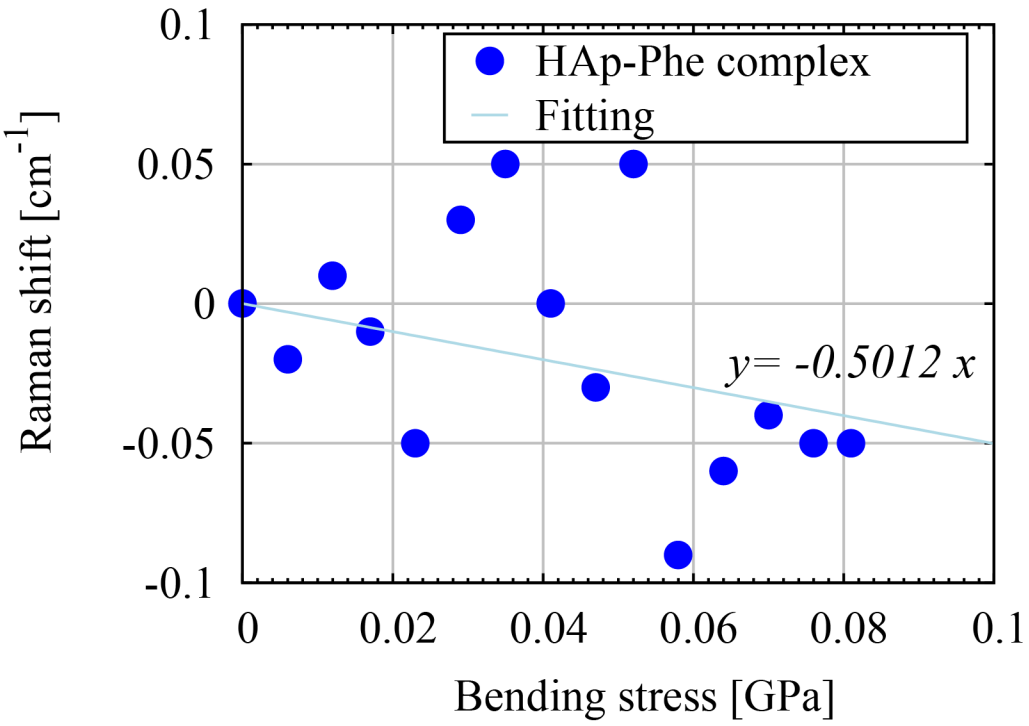

Fig. 2.12 Peak shift at the major peak of Phe subjected to 4-Point bending.

the carboxyl group in amino acid molecules can be formed. The HAp–amino acid complex emits fluorescence by MLCT [35] and $\pi - \pi$ stacking [54]between molecules induced by highly compaction can shift fluorescent wavelength toward red.

Relative concentration of amino acids on the surface of HAp–amino acid complexes was estimated using intensity ratio of raman spectra between the one of HAp with the other of amino acids. he relative concentration was commonly increased by increasing pressure in CIP process (Figs.2.13,2.14,2.15). Though the thickness of amino acid was saturated at higher pressure cases (Fig. 2.10), the observed values of concentration of amino acid were proportionally increased to pressure. Such the result indicated that a packing structure of amino acid was changed in a high pressurized condition.

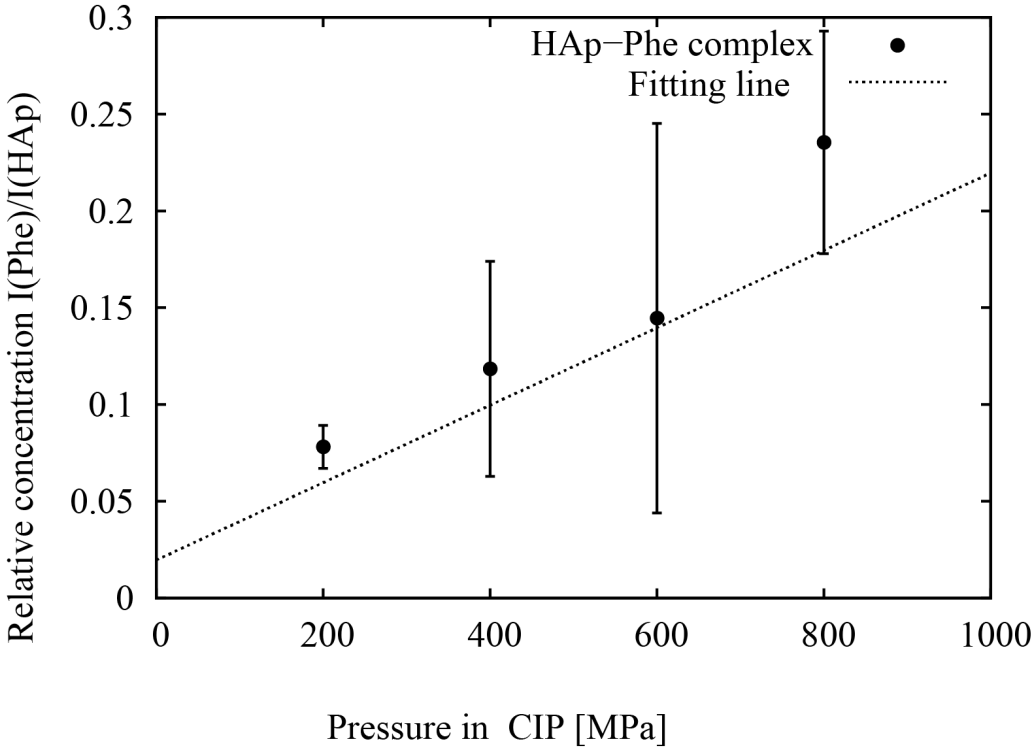

Fig. 2.13 Relative concentration of amino acid ligands in HAp-Phe complex

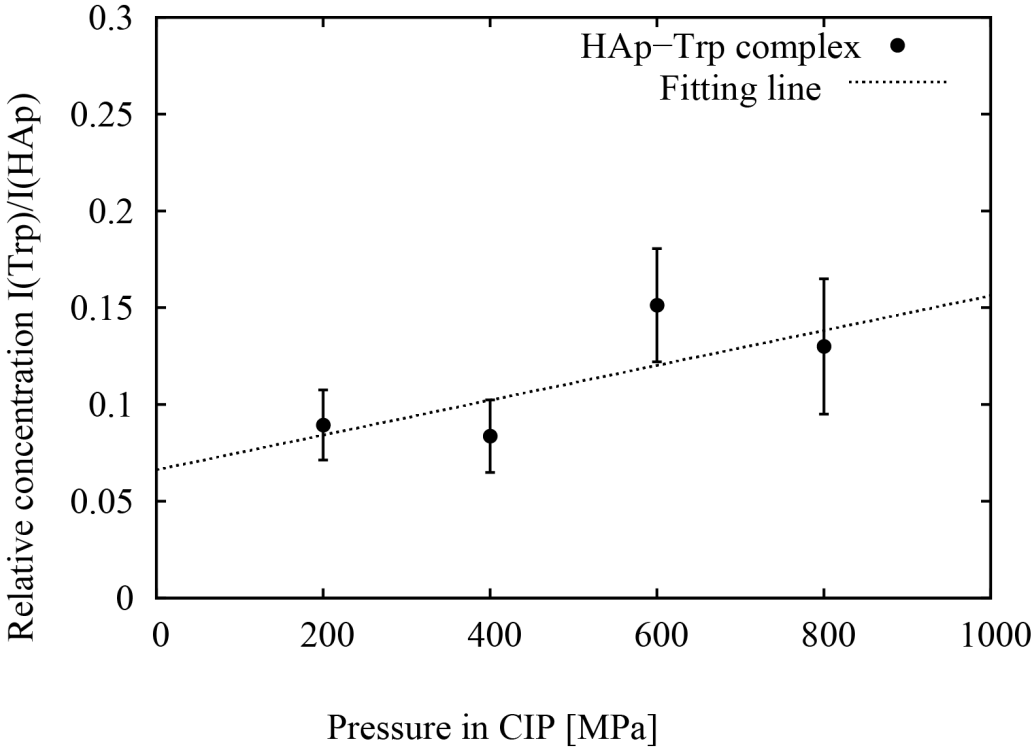

Fig. 2.14 Relative concentration of amino acid ligands in HAp-Trp complex

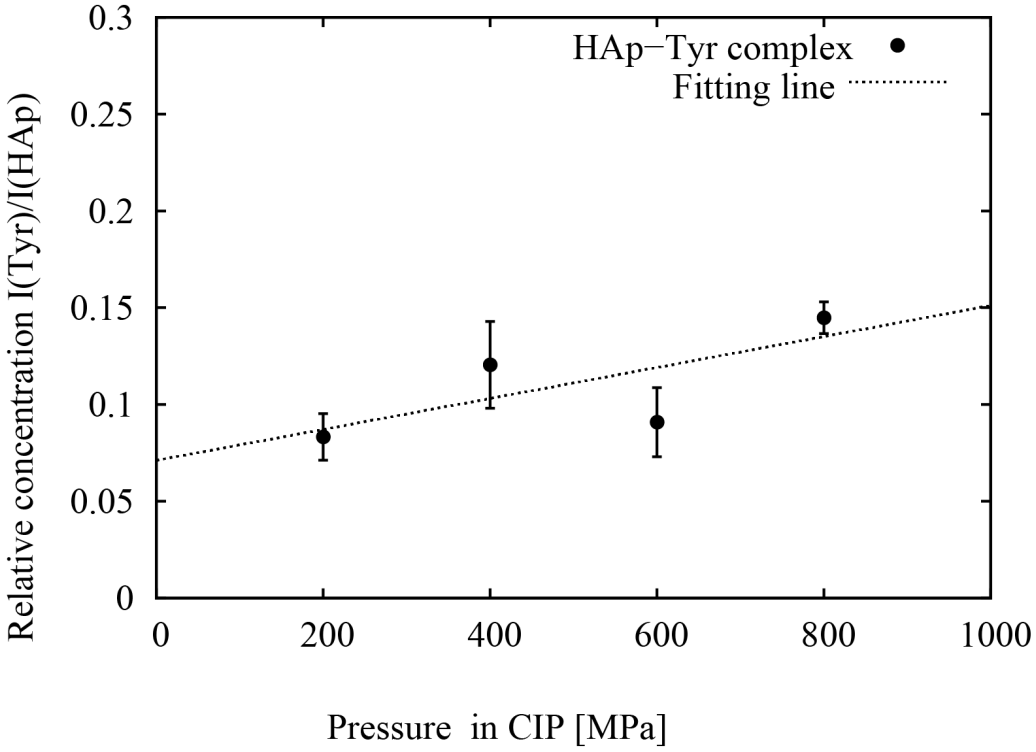

Fig. 2.15 Relative concentration of amino acid ligands in HAp-Tyr complex

2.3.4 Detection of orientation of amino acid ligands by polarized Raman spectroscopy

Polarized raman spectroscopy measurement was then conducted in order to observe orientation behavior of amino acid ligands in HAp–amino acid complex layers. Numerically calculated angles of orientation using the equation (2.3) demonstrated that the Phe ligand in HAp-Phe complex was more normally arraigned to the HAp coating in highly pressurized conditions (Fig.2.16). In the case of 800 MPa, orientation angle was seemed to be saturated and the tendency was corresponded to the saturated thickness of ligands. Such the highly packed structure of ligands in fluorescent complex could affect its chemical, physical and optical properties[35, 48, 51].

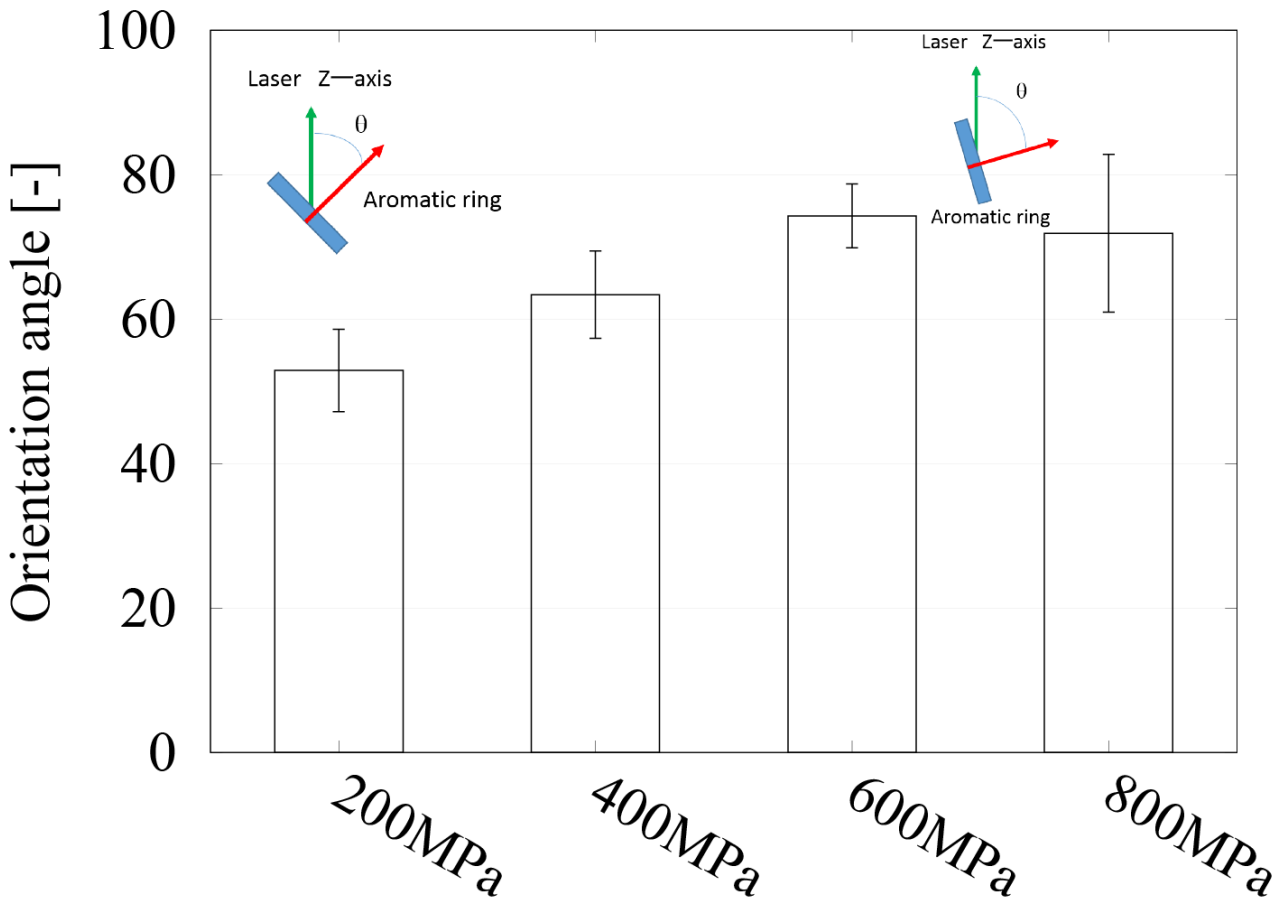

Fig. 2.16 Orientation angles of Phe ligands in a HAp-Phe complex. The angles were calculated using equation (2.3).

2.4 Discussion

The present study observed the effect of pressure on optical property and microstructure of HAp–amino acid complexes. Fluorescent microscopy demonstrated that microscopic fluorescent intensities emitted from the HAp–amino-acid complexes were increased by increasing fabricating pressure(Fig. 2.2), though the peak wavelength in PL spectra and quantum yields were not sensitive to the pressures (Figs. 2.3,2.4,2.5 and Figs. Figs.2.6,2.7,2.8,). SPM measurement detected the saturated values in the thickness of ligands layer in the HAp–amino acid complexes ((Fig. 2.10), though the proportional increase in the concentration of the ligands was commonly observed by raman spectroscopy(Figs.2.13,2.14,2.15). 4-Point bending test with raman spectroscopy measurement denied

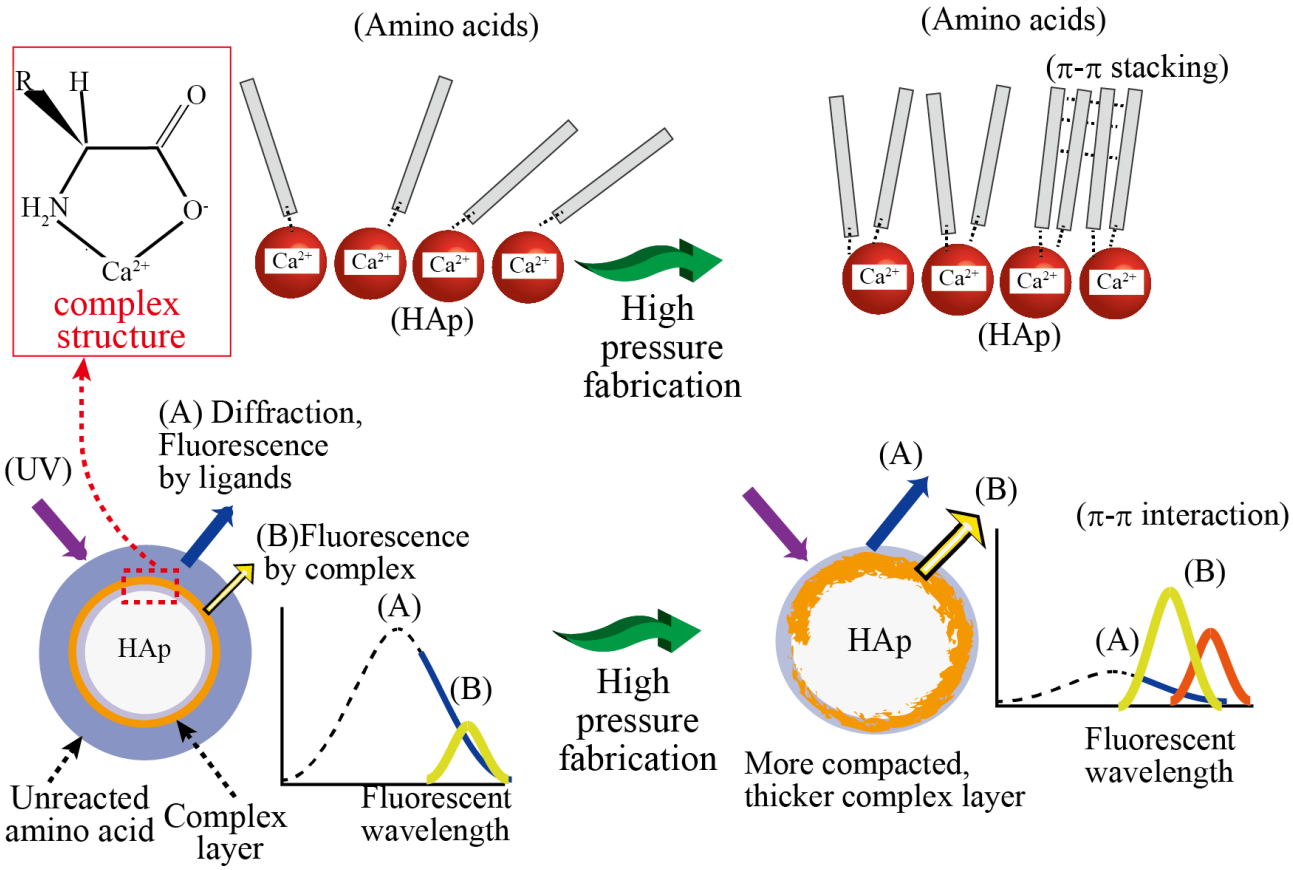

Fig. 2.17 Schematic illustration demonstrated that highly packed structure of ligands could enhance optical property of HAp–amino acid complex fabricated by CIP.

the effect of mechanical strain on the changes in raman spectra((Fig. 2.12), and the peak shift in raman spectra clearly suggested the formation of ligands by complexation ((Fig. 2.11A and B). The result of raman spectra also indicated that molecular interaction condition between HAp with amino acid was not much influenced by fabricating pressure (Fig. 2.11B). Polarized raman spectroscopy measurement clearly detected the normally arraigned ligands to the HAp layer in highly pressurized conditions (Fig.2.16), which can provide highly packed ligand structure in HAp–amino acid complexes.

The schematic illustration on the effect of pressure pressure on optical property and microstructure of HAp–amino acid complexes is then shown in Figure 2.17. Though the amino acid molecules

have a polarized charges at a side chain in the molecule, such the electric charges could be repulsive force to prevent aggregation during compression. Such the repulsion among adjacent molecules on the surface of HAp could reduce a frequency of complexation in the case of lower pressure. In highly compressed cases, though the repulsive force would be worked among molecules, the higher pressure could provide more dense, compacted layer of amino acid layers by normal arraignment of the molecules onto the surface of HAp coating. Consequently, such the compacted layer of amino acid could increase close contacted area at the surface of HAp and subsequent increased frequency of complexation. Therefore, more packed HAp–amino acid complex layer, which emitted brighter fluorescence, could be fabricated. The above interpretation can explain the reason of different thickness of the amino acid layer according to the types of side chains. Phenylalanine(Phe) and Tryptophan (Try) are hydrophobic ones and then the intermolecular repulsive forces between aromatic rings in the neighboring molecules would be small and then the highly compacted layer could be formed. On the contrary in the case of Tyrosine (Tyr), which has a hydroxyl group (-OH) in its side chain, exhibited hydrophilic property and then larger repulsive force was worked to prevent compaction of the ligands. We found the pressure dependency in optical property of HAp–amino acid complexes and such the result is beneficial to develop biocompatible fluorescent materials for bioimaging application etc. Such the HAp fluorescent complexes can enhance antibacterial property of titania as well as adjusting cell adhesion behavior of HAp itself[35, 37, 45].

The peak wavelength of HAp–amino acid complexes was not sensitively shifted by fabricating pressure probably due to the small molar amount of the molecules, which could not be strained by the compression. Nagura *et. al.* reported that tetrathiazolylthiophene molecule showed specific red shift

in its fluorescent wavelength when it was subjected to shear load [36]. Such the mechanocromic behavior is quite beneficial to adjust optical property of the fluorescent materials. In the present study, we used the single molecule of amino acid as the ligands in the complexation. Using polyamino acid may provide more pressure dependent optical property due to its molecular interactions among strained polymers. Such the effects by the molecular structure of the ligands should be further investigated in the future studies. Quantum yield is still low compared with the one in solution because of re-absorption behavior of light in highly dense solid structure. Especially the existence of unreacted layer of amino acid onto the HAp–amino acid complexes might reduce fluorescence intensity. Additional treatment, such as heating or immersion etc, should be tried to optimize fluorescent property of the HAo -amino acid complexes.

2.5 Conclusion

CIP process successfully fabricated the HAp–amino acid fluorescent complexes and their fluorescence intensity was increase by increasing the pressure during fabrication. Though the thickness of amino acid layer was saturated in higher pressure cases, the concentration of amino acid proportionally increased by the higher pressure, which suggest the packed structure of ligands in the HAp–amino acid complexes. Polarized raman spectroscopy measurement clearly detected the normally arraigned ligands to the HAp laryer in highly pressurized conditions, which can provide highly packed ligand structure in HAp–amino acid complexes. Highly packed ligand structure in HAp–amino acid complexes could emit stronger fluorescence by increased density of the complexes. The newly found pressure dependency in optical property of HAp–amino acid complexes is beneficial to develop bio-

compatible fluorescent materials or enhancement agent of antibacterial coating layers.

Chapter 3 Enhancement Effect on Antibacterial Property of Gray Titania Coating by Plasma-Sprayed Hydroxyapatite-Amino Acid Complexes during Irradiation with Visible Light

Abstract

The aim of this study was to reveal the mechanism of enhancement of antibacterial properties of gray titania by plasma-sprayed hydroxyapatite (HAp)–amino acid fluorescent complexes under irradiation with visible light. Although visible-light–sensitive photocatalysts are applied safely to oral cavities, their efficacy is not high because of the low energy of irradiating light. This study proposed a composite coating containing HAp and gray titania. HAp itself functioned as bacteria catchers and gray titania released antibacterial radicals by visible-light irradiation. HAp–amino acid fluorescent complexes were formed on the surface of the composite coating in order to increase light intensity to gray titania by fluorescence, based on an idea bioinspired by deep-sea fluorescent coral reefs. A cytotoxicity assay on murine osteoblastlike cells revealed that biocompatibility of the HAp–amino acid fluorescent complexes was identical with the that of HAp. Antibacterial assays involving *Escherichia coli* showed that the three types of HAp–amino acid fluorescent complexes and irradiation

with three types of light-emitting diodes (blue, green, and red) significantly decreased colony-forming units. Furthermore, kelvin probe force microscopy revealed that the HAp–amino acid fluorescent complexes preserved the surface potentials even after irradiation with visible light, whereas those of HAp were significantly decreased by the irradiation. Such a preservative effect of the HAp–amino acid fluorescent complexes maintained the bacterial-adhesion performance of HAp and consequently enhanced the antibacterial action of gray titania.

3.1 Introduction

A titanium alloy coated with plasma-sprayed hydroxyapatite (HAp) has been widely applied to biomedical components, such as dental implants, artificial hip joints, and knee joints [7]. One of the major causes of revision of such implants is loosening [11]. The HAp coating promotes a stronger bond between surfaces of implants and human bone, thereby resulting in earlier fixation of the implants and their long service life [4, 57, 6, 5]. Nonetheless, another cause of revision procedures—bacterial infection—recently came up as a serious problem [43, 16, 9, 8, 13, 10]. Bacterial infection on the surface of implants forms a biofilm, which causes peri-implantitis and inflammation of the surrounding tissues [10]. Damage by bacterial infection occurs in approximately 5% of cases of revision or reconstruction of orthopedic implants [43]. To prevent a fracture caused by bacterial infection, an antibacterial technology is necessary.

Two types of coating, i.e., passive coating and active coating, have been widely studied as an antibacterial agent on the surface of implants [44, 14, 58]. Passive coating is intended to prevent adhesion of bacteria to the surface of implants by controlling surface morphology, wettability, con-

ductivity, surface charge, or crystal structure of a substrate [24, 58, 59]. Surface morphology, such as roughness or height, greatly affects bacterial adhesion behavior [31, 32, 33]. Although a polished surface can reduce bacterial adhesion, such a reductive effect of the roughness decrease reaches a plateau below a certain level of roughness. Hydrophilicity of the surface also has a major impact on bacterial adhesion [12]; however, the wettability of surfaces cannot last in long-term use. An active coating, which contains mesoporous materials or nanofibers, releases antibacterial agents such as metal ions, an antibiotic, free radicals, or nitrogen monoxide [43, 8, 44, 14, 58, 42, 60, 61, 62, 63, 64, 65, 66, 67]. Placing Ag ions on surfaces is the most widely studied technique as an antibacterial modality [61, 62, 66, 17, 68, 18, 20, 69, 26, 22, 70, 71, 23, 41]. An antibiotic [72], peptide [73, 74, 30], or organic compound like polycaprolactone or chitosan [65, 75, 41] have also been tested as antibacterial agents. Though these released antibacterial agents show adequate performance, controlling or maintaining these concentrations in body fluids is difficult. Unfortunately, the released antibacterial agents suppress osteointegration at the interfaces between implants with surrounding tissues. Antibacterial agents that do not obstruct osteointegration are preferable.

A multifunctional coating that can inhibit bacterial infection as well as maintain osteointegration was recently considered because of the crucial capacity for preventing revision of orthopedic implants [43, 44]. Multifunctional coatings are classified into a) those inhibiting bacterial adhesion via non-toxic compounds [14, 27, 28, 76], b) composites with controlled release of an antibacterial agent with an agent promoting osteoblast adhesion [77, 78, 79, 40], and c) those stimulating the release of an antibacterial agent, e.g., by UV irradiation or a magnetic field [80, 81]. The RGD peptide [14, 27, 28] can reduce bacterial adhesion whereas fibronectin can adhere to the surface covered by the RGD pep-

tide. Nonetheless, the RGD peptide has no antibacterial effect (does not kill bacteria). A controlled release of an antibacterial agent such as Ag ions or gallium may reduce viability of bacteria while the activity of osteoblasts can be preserved [79, 40]. Balancing the release rate with a concentration of the agent is a challenge in long-term use. UV irradiation of a photocatalyst [80] or application of a magnetic field [81] may exert significant antibacterial effects, but they simultaneously affect human-cell viability. Light-activated antibacterial effects of nanofiber or nanofibrous membranes, which were made of organic molecules based on benzophenones or polyphenols, were reported [82, 83, 84]. When considering bonding coating onto the surface of metallic implants, multifunctional coatings based on plasma-spraying technology are beneficial because plasma-sprayed coatings have sufficient interfacial strength with metallic substrates. Matsuya *et. al.* developed a composite coating containing a fluorescent complex of hydroxyapatite with a visible-light–responsive photocatalyst, and this composite coating has an antibacterial effect induced by visible-light irradiation [35, 37]. On the other hand, the ligand of the HAp complex was also cytotoxic. A visible-light–responsive plasma-sprayed coating, which can possess both antibacterial property and cytocompatibility, has not been developed to date.

Here we proposed a new biocompatible composite coating containing a fluorescent complex of HAp with gray titania, as shown in Fig. 3.1. HAp itself functioned as bacteria catchers and gray titania released antibacterial radicals by visible-light irradiation. HAp–amino acid fluorescent complexes were formed on the surface of the composite coating in order to increase light intensity to gray titania by fluorescence. Fabricating a fluorescent complex of HAp from biocompatible ligands such as amino acids can overcome the limitations seen in other studies [35, 37]. Therefore, the aim of this

study is to reveal the enhancement mechanism of antibacterial properties of titania by HAp fluorescent complexes after light irradiation. A cytotoxicity assay involving osteoblasts and an antibacterial assay using *Escherichia coli* were conducted to clarify the performance of the proposed multifunctional coating. Bacteria on the surface of the coating, which are bound by the HAp complex, can be exposed to a higher concentration of radicals produced by a photocatalyst. Intensity of such interactions between bacteria and the surfaces of biomaterials has been investigated by atomic force microscopy (AFM) [85, 86, 87, 88], which has uncovered the effects of wettability, surface roughness, or morphology on the bacterial adhesion behavior. Surface potential is also an important property affecting the adhesion behavior of bacteria on the surface of biomaterials [89, 90], and Kelvin force microscopy (KFM) can detect the changes in surface potential induced by light irradiation [91, 92]. The surface potential on the surface of HAp complexes under light irradiation was measured by KFM to elucidate its light-induced mechanism of enhancement of antibacterial properties.

3.2 Experimental procedures

3.2.1 Fabrication of composite coating of HAp with gray titania

Ti-6Al-4V plates were machined to the dimensions of $50 \times 10 \times 3$ mm. HAp powders (HAP-100, Taihei Chemical Co., Ltd., Japan) were sieved at approximately 90 μm and were crushed by ball milling. The HAp powders were deposited on the Ti-6A-l4V plates by plasma spraying (model 9 MB, Seltzer Meteco under the following conditions: current of 500 A, controlling voltage of 68 V, particle feed rate of 15 g/min, and spraying distance of 140 mm). The average thickness of the HAp

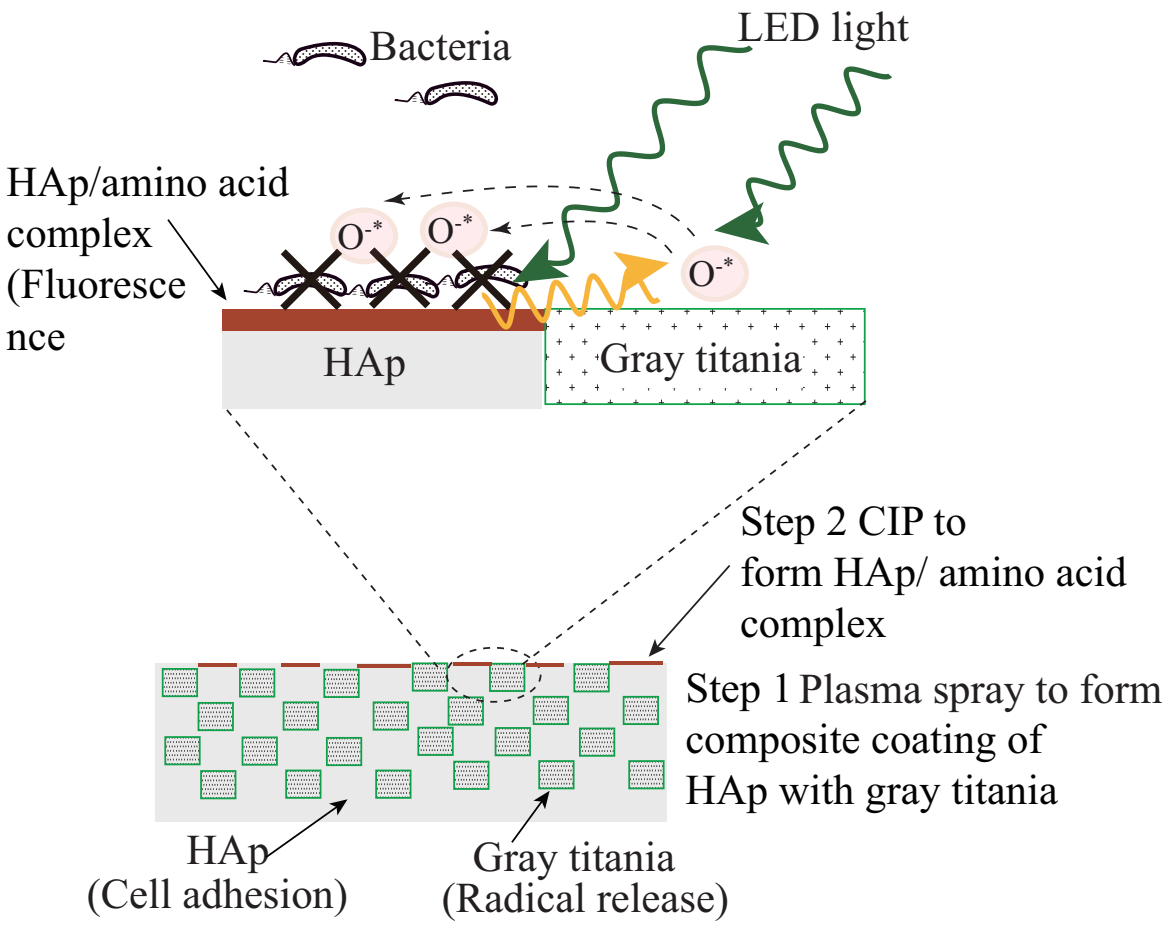

Fig. 3.1 The model of antibacterial properties of a composite photocatalyst with fluorescent HAp–amino acid complex as a coating under light irradiation.

coating was approximately 100 μm. Ti_2O_3 powder (TIE02PB, Kojundo Chemicals,Japan) was sieved through 90μm mash as well. The average particle size of Ti_2O_3 was smaller than 90μm. The powder composed of 80 wt%HAp/20 wt% Ti_2O_3 was mixed in a ball mill for 1 hour. Only photocatalyst coating exhibited insufficient antibacterial property due to the suppression of bacterial adhesion[93], and then we selected the ratio so that the surface of HAp particles can be partly covered by Ti_2O_3 particles. Matsuya *et.al.* reported that plasma-sprayed Ti_2O_3 was transformed into Rutile(TiO_2) with Ti_6O_{11}, which could produce oxygen radicals under visible-light irradiation [37]. They called the plasma-sprayed Ti_2O_3 coating as gray titania coating [37], which is used in the present study.

3.2.2 Fabrication of the HAp complex with an amino acid by cold isostatic pressing (CIP)

Three amino acid ligands—phenylalanine (Phe), tryptophan (Trp), and tyrosine(Tyr) (Kishida Chemical Co., Ltd., Osaka, Japan)—were used for complexation with HAp. The three types of aromatic amino acids were selected due to their strong fluorescent property. Namely, 500 mg of an amino acid powder was placed on the surface of a plasma-sprayed HAp coating, and all the samples were sealed with plastic bags on a vacuum drawing machine. The sealed HAp coating was next dried in an incubator at 40 °C for 24 h. Finally the sealed HAp coating bags were pressurized by CIP (Model P-500, Kobe Steel, Ltd., Japan) at maximum pressure 800 MPa and holding time 20 min [35].

3.2.3 Examination of fluorescence emitted by the HAp complex with amino acids

Fluorescent properties of HAp complexes with one of three amino acids were examined under ultraviolet irradiation with excitation wavelength of 315–400 nm (FPL27BLB, Sankyo Denki Co., Ltd.). The HAp amino acid complex coating was then immersed in distilled water for 7 days and 30 days in order to remove unreacted amino acid on the surface. HAp amino acid complex should be hardly soluble in water and then the remained fluorescence after the immersion can certify the existence of the complex. The wavelength of fluorescence was evaluated by luminescence microscopy (BZ-8100, Keyence Co., Ltd., Japan.), before and after 30-day immersion. Three types of excitation source, 360 ± 20, 470 ± 20, and 540 ± 12.5 nm with exposure time of 0.5 s were employed to observe

blue (460 ± 20 nm), green (535 ± 25 nm), and red fluorescence (605 ± 27.5 nm).

3.2.4 Cytotoxicity assay

Mouse MC3T3-E1 osteoblasts (RIKEN Bioresorce Center, Japan) were used to evaluate cytotoxicity of HAp fluorescent complexes with an amino acid. HAp fluorescent complexes with an amino acid coating were sterilized using an UV light. Plasma-sprayed HAp coating is used for metallic implants to enhance their osteoconductivity [7]. Osteoblast cells are used for observing cytocompatibility of HAp coating containing antibacterial agents in order to observe whether the osteoconductivity of HAp coating would be deteriorated by antibacterial agents[18, 94]. Osteoblasts were cultured in the high-glucose DMEM medium that was supplemented with 10% of fetal bovine serum (FBS), L-glutamine (WAKO, Osaka, Japan), and 1% of a Penicillin-Streptomycin solution (Sigma-Aldrich, Osaka, Japan), at 37 °C in an incubator (SANYO, MCO-18AC, 5% CO_2 with 100% humidity). A Trypsin-EDTA solution (0.05% w/v; WAKO, Osaka, Japan) served for cell detachment during subculturing. The MC3T3-E1 cells at 8 $\times 10^4$/ml were also cultured on the surface of a fluorescent HAp–amino acid complex in 24-well plates for 24 h. The composition of the medium and cell density were determined by referring a previous study [95] for stable incubation. The adherent and proliferating cells were counted with Cell Counting Kit 8 (CCK8, DOTITE, Dojindo Laboratories, Japan) and their optical density was measured using a microplate reader with the filter wavelength of 450 nm. Values of optical density are proportional to the concentration of living cells containing in the medium and the significant decrease in the values of optical density indicates the toxicity of materials.

Table 3.1 Conditions of antibacterial testing. Labels in the columns indicate each condition

LED type	Specimen		Testing method	
	HAp /Titania	HAp complex /Titania	Irradiation time	Bacteria count
Non irradiation	C_-/L_-	C_+/L_-	1 [hour]	OD CFU (Colony Forming Unit)
Blue (425nm)	C_-/L_{B+}	C_+/L_{B+}		
Green (532nm)	C_-/L_{G+}	C_+/L_{G+}		
Red (630nm)	C_-/L_{R+}	C_+/L_{R+}		

3.2.5 Evaluation of antibacterial properties of HAp fluorescent complexes with Gray titania

Antibacterial assays involving *E. coli* K12 were conducted to confirm the enhancing effects of HAp fluorescent complexes on antibacterial properties of gray titania under visible-light irradiation. We previously reported an effectiveness of HAp /8-Hydroxyquinoline complex as an enhancement agent of antibacterial property of gray titania[37]. However, 8-Hydroxyquinoline itself has cytotoxicity. E.Coli was used in the antibacterial test in order to directly compare the enhancement effect by HAp fluorescent complex of the toxic ligand with the ones by the complexes without toxic ligands (amino acids). Several researches[77, 81] also used E.Coli to discuss basic antibacterial property of their developed multifunctional coating. Three laser types of visible light, 425 nm (blue), 532 nm (green), and 630 nm (red), were used for irradiation at controlled irradiance of 50 mW/cm^2. Irradiation conditions are summarized in Table 3.1. Both HAp/Gray titania coating and HAp complex /Gray titania coating were tested against bacterial Escherichia Coli K12 (E.Coli). The Luria–Bertani (LB) medium consisting of bacto tryptone (10 g/L), bacto yeast extract (5 g/L), NaCl (5 g/L), and deionized water, was sterilized in an autoclave at 120 °C, 1.2 ks (TOMY, SX-500). A suspension containing *E. coli* was cultured directly on an HAp coating in the LB medium. Turbidity was measured on a spec-

trophotometer (Hitachi U-1100 at wavelength 600 nm). Because the initial values of OD fluctuated, OD values after specific hours were normalized to the one at 0 hour (immediately after light irradiation) to evaluate growth rate of *E.Coli*[49]. [37]. The *E. coli* suspension, following the incubation, was diluted 10^7-fold. Next, 0.2 mL of the diluted suspension was grown on LB nutrient agar and incubated at 37 ° C for 18 h. Colonies on the LB nutrient agar medium were counted in the pictures of the plates.

3.2.6 KFM analysis of the surface of HAp fluorescent complexes

KFM analyses of the surfaces of HAp or HAp–amino acid complexes were carried out to clarify the effects of ligands on surface potential during light irradiation. HAp plates made by CIP were employed for KFM to reduce the effect of surface roughness on this analysis. A fixed stand of LEDs was set in front of a scanning probe microscope, SPM-9700 (Shimadzu Science Co., Ltd.).

Two types of LED light, 425 nm (blue), and 532 nm (green) served for the irradiation at irradiance 50 mW/cm^2. The measurement was conducted in a dark room at room temperature (25 °C. At first, KFM analyses before light irradiation were conducted in a region of 1000 × 1000 nm. Immediately after completion of the scanning by KFM cantilever, a LED lamp was turned on, and the same scan was repeated in the same region. Surface potential was calculated using the average value of the analyzed region, and the surface potentials before and after LED irradiation were designated as V_{off} and V_{on}, respectively. Changes in surface potential were calculated as $V_{on}-V_{off}$. Analytical conditions of KFM were as follows: laser potential at operating point of 0.2 V, frequency adjustment of 67 kHz, driving gain of 0.5, and I-gain of 700.0. The cantilever used in the KFM analysis was EFM-

20 (Nanoworld Innovate Technology Product Corporation). The KFM analysis was performed in triplicate by moving to different positions for each type of HAp fluorescent complexes.

3.2.7 Statistical analysis

ANOVA and multiple comparison by Holm's method were applied to the results of the cytotoxicity assay, the antibacterial assay, and the KFM analysis. The significance level was set to $p < 0.05$. All statistical analyses were performed in the R3.4.2 software.

3.3 Results

3.3.1 Fluorescence wavelength for different ligands (amino acids)

The CIP process successfully fabricated HAp–amino acid complexes (Fig. 3.2), as in the case of a HAp-8-hydroxyquinoline complex [35]. Tris(8- hydroxyquinoline)aluminum (Alq3) is a typical fluorescent complex [60] and HAp with 8-hydroxyquinoline could form a fluorescent complex fabricated by mechanochemical method[96]. The result exhibited that Ca ion in HAp crystal with molecules of amino acid can also form a complex. Static compression of 800 MPa produced a coordination bond between Ca ions in the HAp crystal and an amino group in hydrophobic amino acids (Phe, Trp) or a hydrophilic amino acid (Tyr). The HAp–Phe and HAp–Tyr complexes manifested variation in wavelength from blue (Fig. 3.2A and C) whereas the HAp–Trp complex showed approximately yellow fluorescence (Fig.3.2B). Changes in fluorescence from HAp–amino acid complexes were observed after water immersion. (Fig.3.2). Fluorescence emitted by HAp–Trp and HAp–Phe complexes

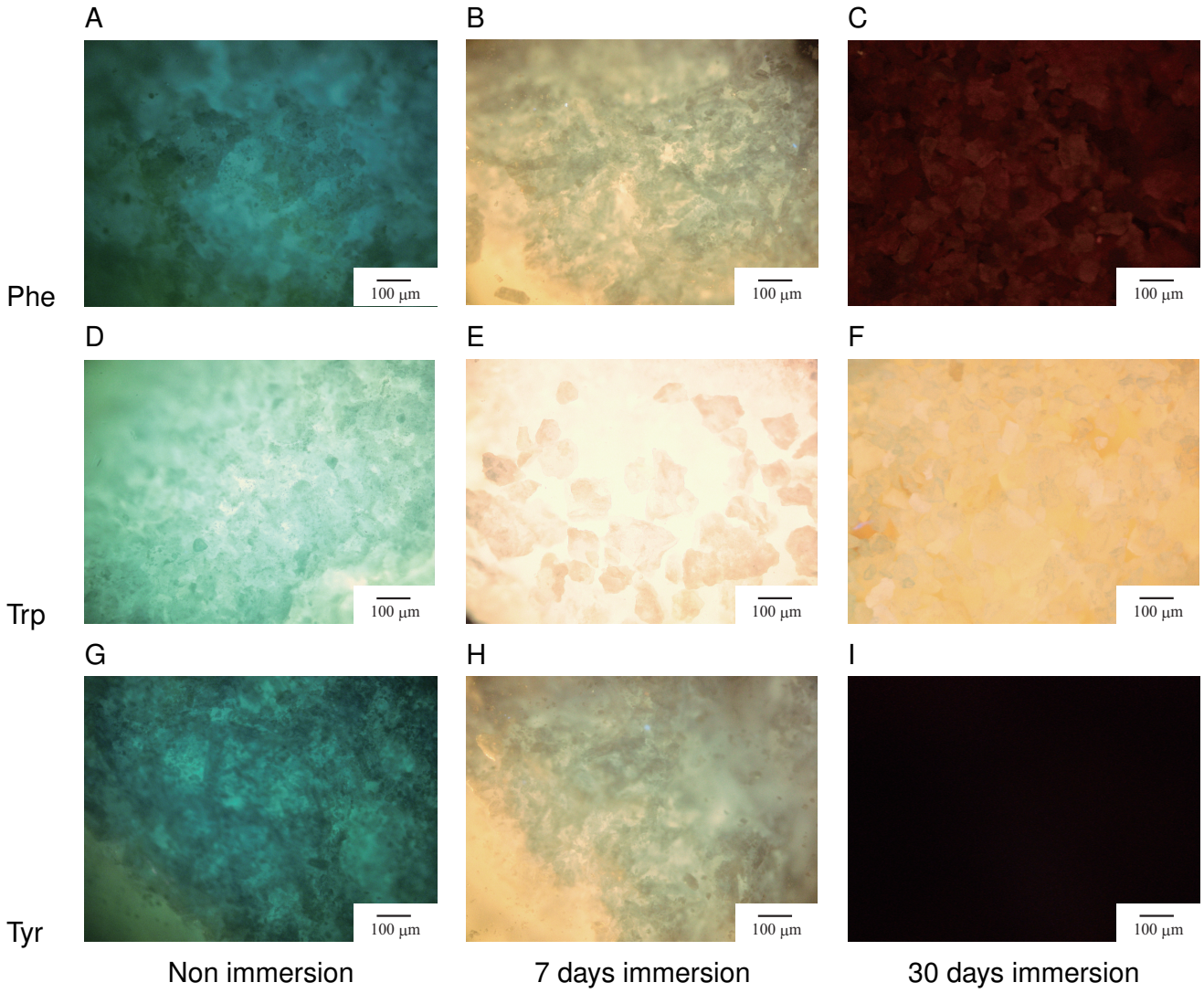

Fig. 3.2 Effects of types of ligand in HAp–amino acid complexes on fluorescence wavelength. (A–C) HAp-phenylalanine (Phe) complex. (D–F) HAp-tryptophan (Trp). (G–I) HAp-tyrosine(Tyr) complex. (A,D,G) Before immersion. (B,E,H) After 7-days immersion. (C,F,I) After 30-days immersion. All pictures are merged images of of red, green, and blue fluorescent images. Exposure time in all images was 0.5 s.

was certainly retained, thus confirming the stability of coordination bonds in the HAp–amino acid complexes in a liquid medium. Fluorescence wavelength was red-shifted in the cases of HAp–Trp and HAp–Phe complexes due to the dissolution of unreacted amino-acids ligands (Fig. 3.2B,C,E,F), which was also reported by previous study[35]. We did not test a simulated body fluid in the assay to prevent precipitation of amorphous calcium phosphate, which blocked excitation light for the surface of HAp–amino acid complexes. A HAp fluorescent complex shows precipitation behavior equivalent

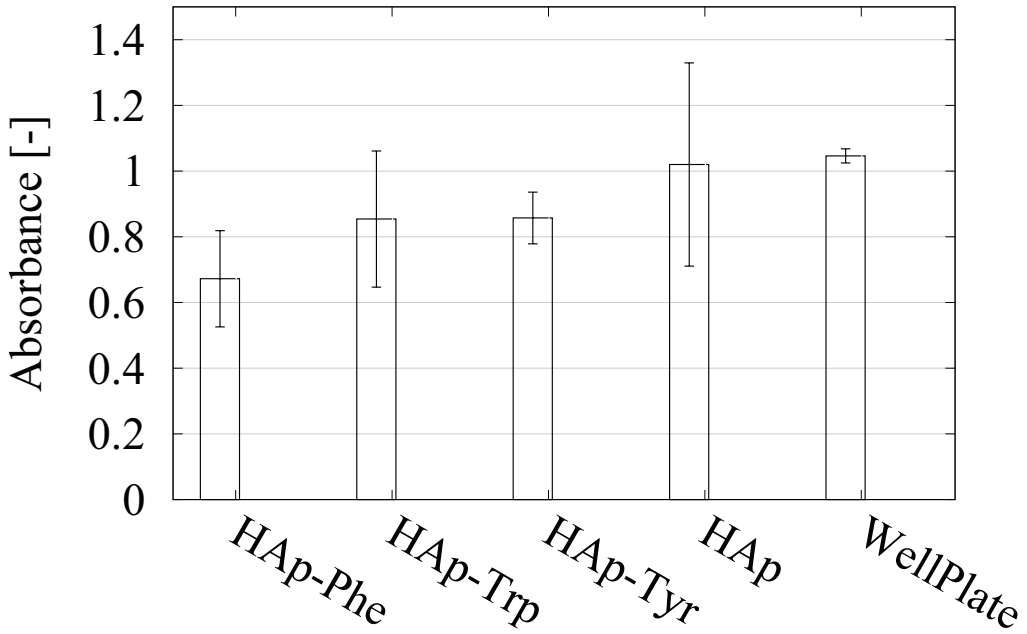

Fig. 3.3 Effects of ligands in HAp–amino acid complexes on toxicity toward MC3T3-E1 osteoblasts. Osteoblasts were directly cultured on the surface of every sample. Data are presented as the mean ± standard deviation of triplicate samples ($*p < 0.05$).

to that of HAp itself [35].

3.3.2 Toxicity of HAp–amino acid complexes toward osteoblasts

Cytotoxicity of HAp–amino acid complexes was evaluated on MC3T3-E1 osteoblasts without light irradiation (Fig. 3.3). Although ANOVA detected a difference (F-value 2.39 [$df = 14$], $p = 0.02$), no significantly different pairs were detected by the multiple-comparison test (Holm's method). This result is due to the small deviation in plate wells and indicated that cytotoxicity of HAp–amino acid complexes is equivalent to that of HAp, which is considered enough to promote osteointegration.

3.3.3 Enhancing effects of HAp–amino acid complexes on antibacterial properties of gray titania

To confirm the enhancing effect of HAp–amino acid complexes on antibacterial properties, OD_{600} values were measured. Note that OD values were normalized to initial values [37]. Without complexes, radical generation by gray titania was not enough to reduce the growth rate (Fig. 3.4B). HAp–amino acid complexes significantly reduced the growth rates according to OD values even in the case without irradiation (L_-), and red LED irradiation (L_{B+}) was the most effective in reducing the growth rates (OD values) regardless of the type of ligand (Fig. 3.4C-E).

CFUs of *E. coli* were also assessed after 18 h cultivation to confirm the effects of both factors: the presence of complexes and types of irradiation. The best pair was a complex with red LED irradiation (C_+/L_{R+}): the percentages of control (C_-/L_{R-}) were 26.9% ± 0.9% (HAp–Phe complex), 37.3% ±5.6% (HAp–Trp complex), 19.0% ± 3.3% (HAp–Tyr complex) (Fig. 3.5A–C). Such percentages of reduction were consistent with the ones reported for other types of multifunctional coating [77, 78, 79, 40, 80, 81], though the antibacterial property was not stronger than the one of conventional Ag ions and other materials[17, 68]. Two-factor ANOVA revealed that the factor of the presence of complexes had a significant effect, regardless of the type of LED irradiation (Fig. 3.5D-F). HAp complex cannot produce any antibacterial agent such as radicals by itself [37]. Therefore, the enhancing effect of HAp–amino acid complexes on antibacterial properties of gray titania was indispensable to achieve sufficiently strong antibacterial properties using a visible-light–sensitive photocatalyst.

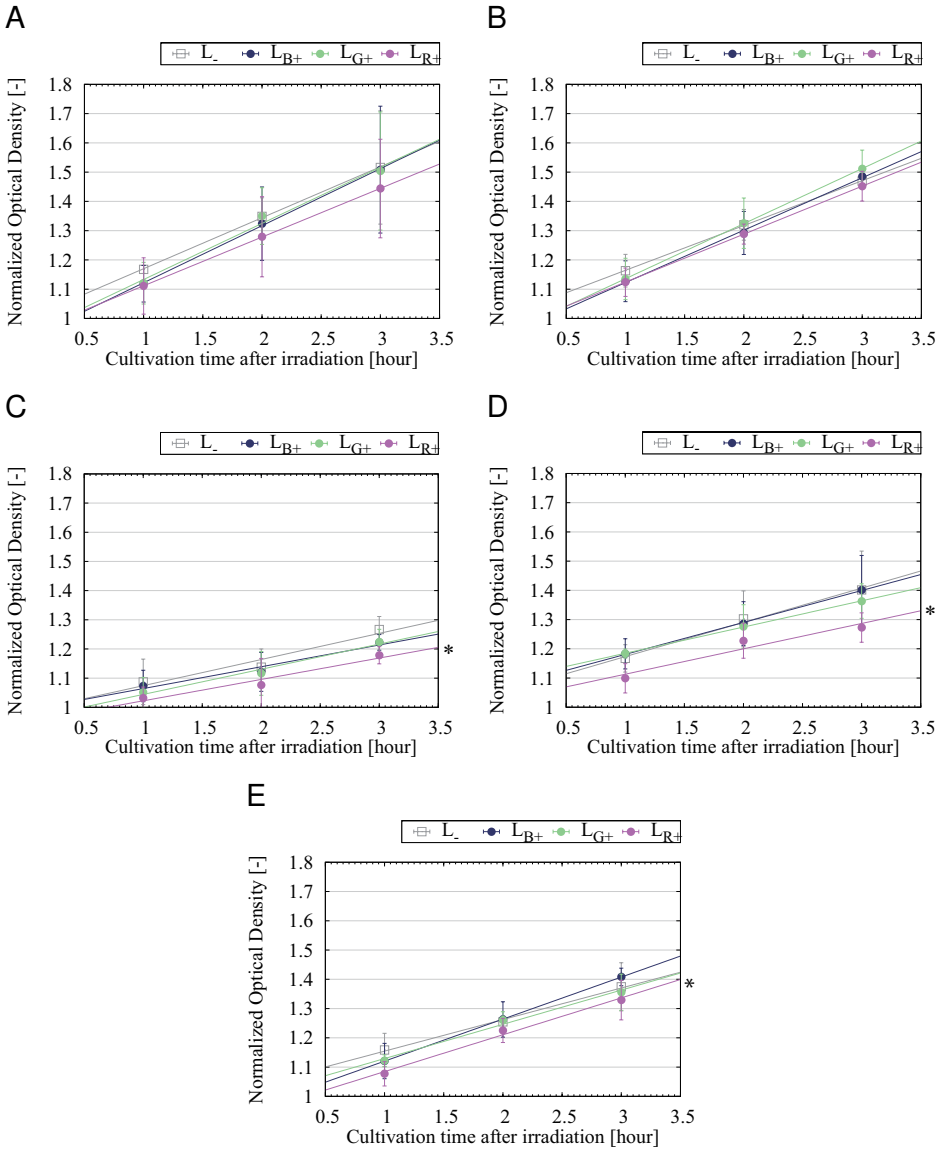

Fig. 3.4 Changes in OD values of an *E. coli* suspension under the influence of irradiation with LEDs. (A) HAp coating. (B) HAp–gray titania coating. (C) HAp–Phe complex/gray titania coating. (D) HAp–Try complex/gray titania coating. (E) HAp–Tyr complex/gray titania coating. The types of LED irradiation $L_-, L_{B+}, L_{G+}, L_{R+}$ are no irradiation, blue LED irradiation, green LED irradiation, and red LED irradiation, respectively. Data are presented as the mean ± standard deviation of triplicate samples ($*p < 0.05$)

3.3.4 The effect of light irradiation on the surface potential of HAp–amino acid complexes

Although only LED irradiation of gray titania produced free radicals as antibacterial agents, in some cases effects of LED (L_+) on antibacterial property were not significant probably due to the reduced

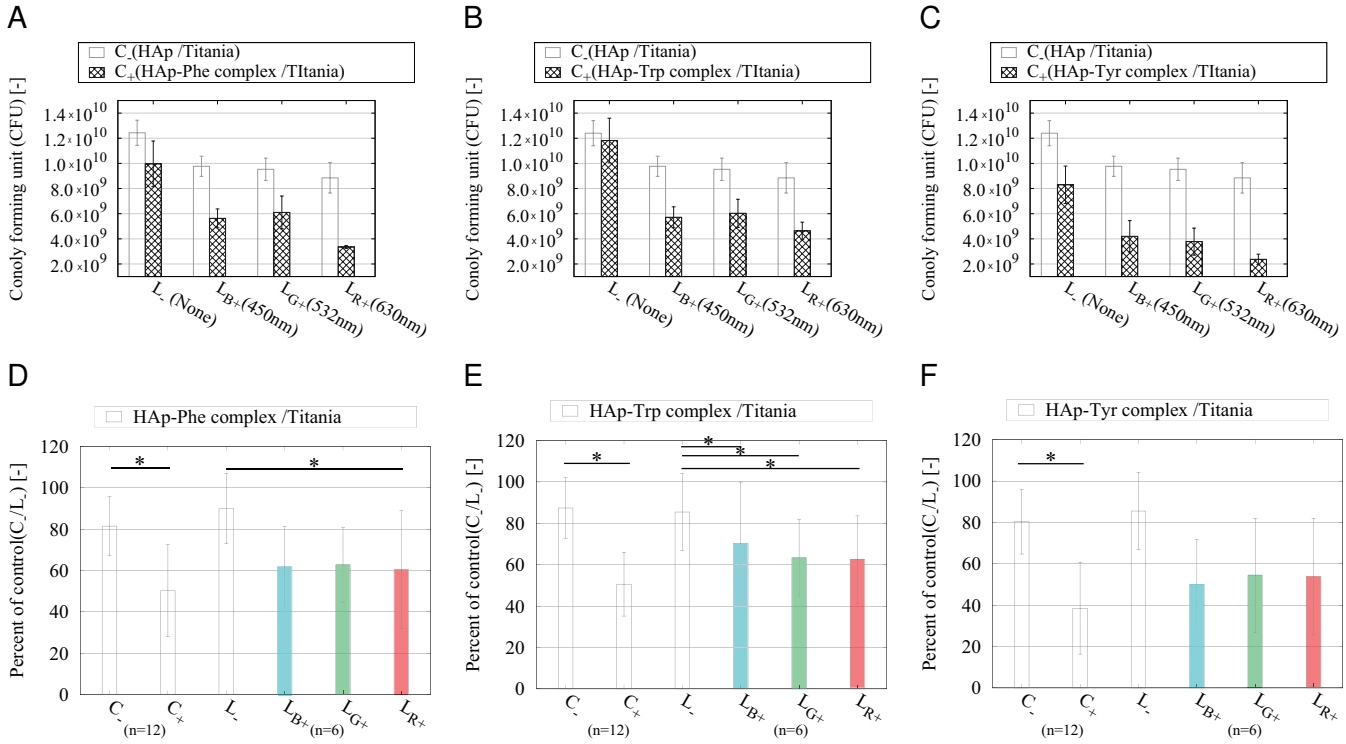

Fig. 3.5 Enhancing effects of HAp–amino acid complexes on antibacterial action of gray titania under irradiation with blue, green, or red LEDs. (A–C) Changes in CFUs. (D–F) Percentage of control (C_-/L_-) for both factors: the presence of a complex and laser irradiation. Data are presented as the mean ± standard deviation of triplicate samples ($*p < 0.05$)

effect of HAp as cell catcher (Fig. 3.4). We then hypothesized that LED irradiation reduces cell adhesion performance of a HAp coating. To test the hypothesis, surface potentials of HAp and HAp–amino acid complexes were examined by KFM. LED irradiation reduced the surface potential of HAp though that of HAp–amino acid complexes was not changed (Fig. 3.6A and B). The surface potentials of HAp–amino acid complexes were dependent on the type of ligand (Fig. 3.6C) and its order of magnitude seemed to negatively correlate with the percentage reduction in CFUs (Fig. 3.4A–C). LED irradiation significantly reduced the surface potential of HAp, and HAp–amino acid complexes inhibited such a reduction (Fig. 3.6D). Red LED was not suitable for the KFM analysis because it disturbed manipulation of the cantilever using the same wavelength. We also measured surface temperature by infrared (IR) thermography during LED irradiation both in the case of CFU evaluation

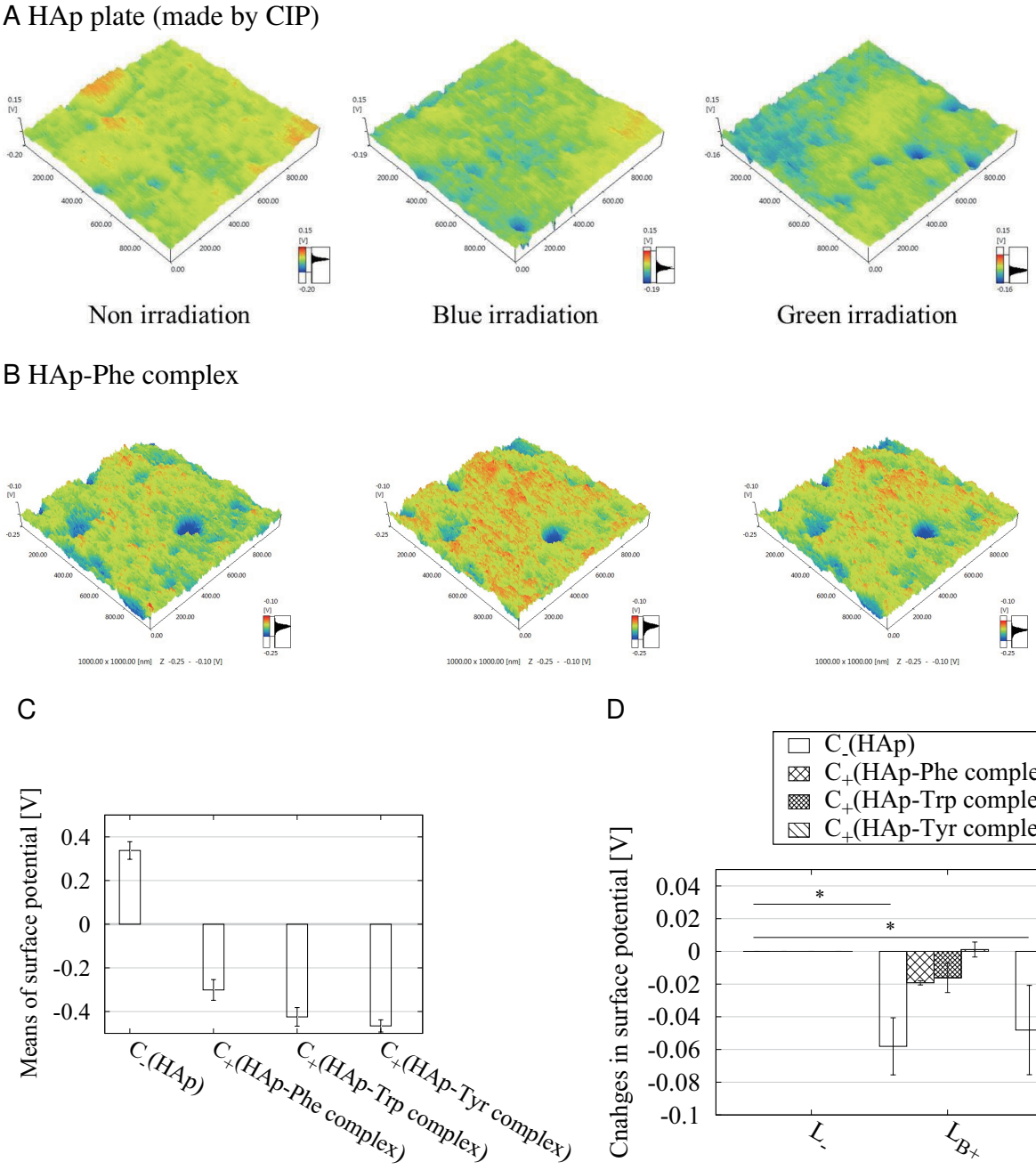

Fig. 3.6 The preserving effect of HAp–amino acid complex on the surface potential during irradiation with a LED. (A) Surface potential distributions of CIPed HAp. (B) Surface potential distributions of the CIPed HAp–Phe complex. (C) Surface potentials in the presence of different types of ligands. (D) Changes in surface potential during irradiation with LEDs. Types of LED irradiation L_{-}, L_{B+}, L_{G+} are no irradiation, blue LED irradiation, and green LED irradiation, respectively. Data are presented as the mean ± standard deviation of triplicate samples ($*p < 0.05$)

and KFM, and no significant changes in temperature were observed. Consequently, HAp–amino acid complexes maintained the cell adhesion performance of HAp during irradiation, which enhanced the antibacterial properties of gray titania induced by LED irradiation.

3.4 Discussions

In this study, a CIP method for fabricating fluorescent complexes between HAp and an amino acid was successfully developed. The fluorescent complexes of HAp with one of amino acids were insoluble *in vitro* even after a long incubation (Fig. 3.2). The HAp/ Phe complex after immersion showed red-shifted fluorescence, which exhibited the effect of CIP pressure on promoting molecular orientation of amino acid ligand and accompanying change in the fluorescent property. The red-shift fluorescence is attributed to an arrangement of Phe molecules onto the surface of HAp coating[97], and CIP process can exclusively promote such an arrangement. Furthermore, the HAp–amino acid complexes were nontoxic to mouse osteoblastlike cells (Fig. 3.3): a favorable feature for multifunctional coating layers. The HAp–amino acid complexes successfully enhanced light-induced antibacterial properties of gray titania under visible light (Fig. 3.4). Although the strong fluorescence of the HAp–Trp complex (Fig. 3.2E–H) significantly amplified the antibacterial effect of gray titania (Fig. 3.5B and E), such an enhancing effect was usually significant regardless of the type of ligand (Fig. 3.5). We also observed changes in the surface potential of HAp coatings, which is one of critical factors in the regulation of cell adhesion behavior. HAp–amino acid complexes increased absolute values of surface potential and preserved the potential even under light irradiation (Fig. 3.6).

The enhancement mechanism is illustrated in Fig. 3.7. Band gap energy of HAp (5.0 eV [98]) is too high to be excited by visible light, and HAp can absorb only thermal energy of light, which can promote recombination of polarized pairs on its surface (Fig. 3.7A). A relation between light intensity and amplitude of an electric field of light is determined by the following equations (3.1,3.2) of Beer's

law [99]:

$$E(t) = E_0 \cos(\omega t) \quad (3.1)$$

$$|E_0| = \sqrt{\frac{I_{LED}}{\varepsilon_0 nc}} \quad (3.2)$$

where ω is angular frequency of light, I_{LED} is irradiance of light [mW/cm^2], with permittivity of vacuum $\varepsilon_0 = 8.854\times10^{-12}$ F/m, refractive index n, and speed of light $c = 2.998\times10^8$ m/s. Reflectance of light is then calculated via the equation (3.3),

$$R_\perp = \frac{(1-n)^2 - k^2}{(1-n)^2 + k^2} \quad (3.3)$$

where k is the extinction coefficient. Dielectric loss by the electric field is then calculated using the equation (3.4) [100],

$$\Delta E_{ele} = \frac{1}{2}\varepsilon_0\varepsilon_1\omega|E_0|^2 \tan\delta \quad (3.4)$$

where $\varepsilon_1 = n^2 - k^2$, $\varepsilon_2 = 2nk$, and $\tan\delta = \frac{\varepsilon_2}{\varepsilon_1}$. If we consider recombination of polarized pairs by dielectric loss, then a reduction in electric potential can be calculated by means of the following equations (3.5,3.6):

$$(1 - R_{\perp})\Delta E_{ele} t_{ird} = \frac{1}{2} C(\Delta V)^2 \cdots (3.5)$$

$$C = \frac{\varepsilon_1 S}{d} \cdots (3.6)$$

where t_{ird} is irradiation time (s), S is examined sample area 1 (cm^2), and distance of recombination d is assumed to be 75 and 50 nm, respectively. $n = 1.65$ and $k = 0.000847$ were determined from experimental values by Bento *et. al.* [101]. The calculated result of equations (3.2, 3.5) is in good agreement with the observed change in surface potential (Figs. 3.6C and 3.7B). Though the values of surface potential were so sensitive on surface morphology and insulation conditions of the samples[102], the magnitude of the changes were not matched in different samples (Figs. 3.6C and 3.7B). Weakened surface potential could detach bacteria from the surface, thereby leading to deterioration of antibacterial effectiveness. On the other hand, the amino acid complex has lower band gap energy [103, 104] and can emit fluorescence (Fig. 3.7A). Consequently, fluorescence can preserve the surface potential of the amino acid complex and then bacteria can strongly adhere to its surface. Such bound bacteria are subjected to higher concentrations of radicals and are effectively killed (Fig. 3.7C). Our finding first and foremost points out the importance of electric properties of HAp as a dielectric for antibacterial action.

A conventional multifunctional coating involving antibacterial agents has difficulty in regulating its antibacterial performance owing to uncontrollable solubility. The use of UV light can regulate the antibacterial action by adjusting irradiance, but UV itself also affects the surrounding tissues. The newly developed coating composed of HAp–amino acid complexes with titania can be activated by visible light, which leads to be a new type of multifunctional coating controllable *in vivo*. The newly

developed coating made of HAp complexes with titania can be applied to enhance cell adhesion or detachment via appropriate selection of laser types and irradiance. Recently light-activated antibacterial effects of nanofiber or nanofibrous membranes, which were made of organic molecules based on benzophenones or polyphenols, were reported [82, 83, 84]. This study used inorganic material as photocatalyst. Combination of such organic photosensitizers with the proposed HAp complexes can provide different types of multifunctional coating.

The limitation is that the newly developed coating made of HAp complexes with titania was not optimized regarding its composition, and irradiation duration is still long when considering practical applications. Effects of irradiance and optimization of the mixing ratio of HAp with titania should be discussed further. The detailed observation of a mechanical interaction between the surface of HAp complexes and bacteria or mammalian cells can provide more quantitative data on interface mechanics, which should also be considered in further studies. Though radicals formed by light-irradiation to photocatalyst can commonly provide antibacterial effects on specific types of bacteria relating to dental or surgical implants[24, 10, 43, 44], further studies are also necessary to observe the variation in antibacterial property of proposed HAp–amino acid complex with gray titania coating. HAp–amino acid complex can be retained in liquid environments, however, durability of antibacterial effects should be discussed further.

3.5 Conclusion

The aim of this study is to develop HAp–Amino acid fluorescent complexes with gray titania photocatalyst coating focuses on biocompatibility and antibaterial propety by visible light irradiation

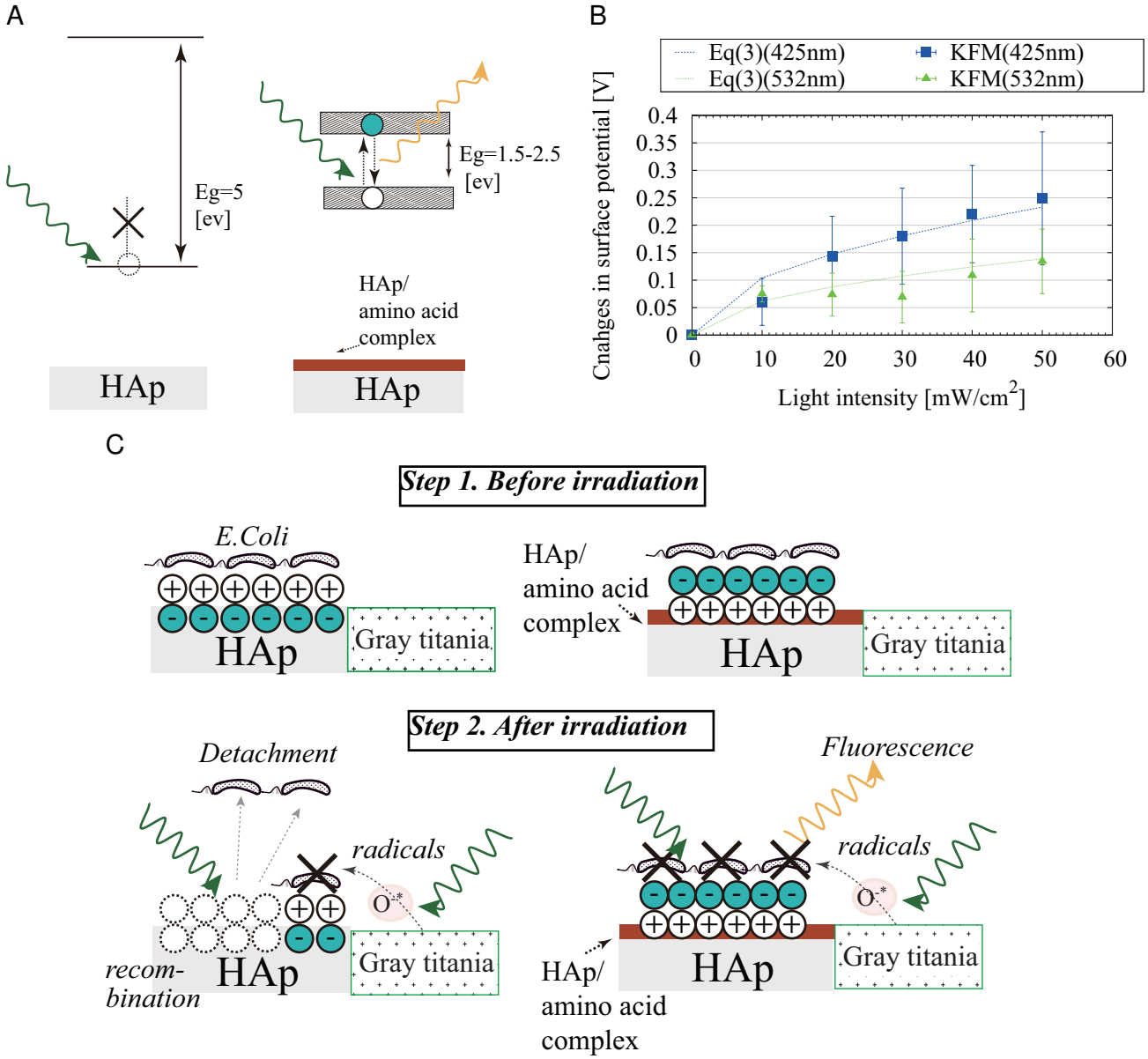

Fig. 3.7 Schematic illustration of the enhancing mechanism of the HAp–amino acid complex on antibacterial properties of titania via suppression of changes in surface potential. (A) A difference in optical band gap. (B) A calculated relation between light intensity and changes in voltage according to equations in the main text. (C) Different reactions during light irradiation; HAp manifested recombination of polarized pairs, and HAp complexes emitted fluorescence.

for dental implant. A CIP process successfully fabricated complexes of HAp with each of several amino acids as a fluorescent coating that is biocompatible and stable for use in human fluids *in vivo*. The HAp–amino acid complexes were retained in a liquid environment, and had no cytotoxicity to MC3T3-E1 osteoblast. Antibacterial testing against *E. coli* indicated a reduction in CFUs by an ex-

isting the HAp–amino acid complexes after visible-light irradiation. KFM measurement revealed that the surface potential of HAp–amino acid complex was maintained during light irradiation due to emission of fluorescence, which could suppress detachment of bacteria. Enhancement of antibacterial testing is from surface potential of HAp–Amino acid fluorescent complex coating keeps holding cell on to surface while applying light irradiation regardless to surface profile and wettability. The newly developed coating made of HAp complexes with titania can be applied to one of multifunctional coating.

Chapter 4 Conclusion

4.1 General conclusion

The aim of this study is to develop HAp-Amino acid fluorescent complexes with gray titania photocatalyst coating focuses on biocompatibility and antibaterial propety by visible light irradiation for dental implant. The results are concluded as following; CIP process successfully fabricated the HAp – amino acid fluorescent complexes and their fluorescence intensity was increase by increasing the pressure during fabrication. Though the thickness of amino acid layer was saturated in higher pressure cases, the concentration of amino acid proportionally increased by the higher pressure, which suggest the packed structure of ligands in the HAp- amino acid complexes. Polarized raman spectroscopy measurement clearly detected the normally arraigned ligands to the HAp laryer in highly pressurized conditions, which can provide highly packed ligand structure in HAp- amino acid complexes. Highly packed ligand structure in HAp- amino acid complexes could emit stronger fluorescence by increased density of the complexes. The newly found pressure dependency in optical property of HAp-amino acid complexes is beneficial to develop biocompatible fluorescent materials or enhancement agent of antibacterial coating layers.

1. CIP process success fabricated the complex of HAp with amino acid fluorescent coating which it is biocompatible and sustainable for using in human fluid body.

2. SBF immersion testing demonstrated non dissolving from fluorescent complex coating, the

remaining of fluorescnce was observed after immersion 2 months later.

3. Cytotoxicity revealed no significant reduction of MC3T3-E1 osteoblast cell proliferation and cell activity for all types of HAp-Amino acid fluorescent complex coatings. Biocompatibility is obtained because of cytotoxicity level reduces.

4. HAp-Amino acid fluorescent complex ligands enhances antibacterial property. Antibacterial testing against to E.Coli demonstrated redution of colony forming unit in existing complex ligands after visible light irradiation.

5. Enhancement of antibacterial testing is from surface potential of HAp-Amino acid fluorescent complex coating keeps holding cell on to surface while applying light irradiation regardless to surface profile and wettability.

6. Antibacterial property was enhanced by Amino acid complex of HAp coating preserve the surface potential which it allows cell adhere strongly on coating surface where it leads itself expose to higher concentration of oxygen radical.

4.2 Future work

In our result has been investigated and discussed about the antibacterial fluorescent complex of HAp – amino acid coating and its effective fabrication for dental implant. Though we success in fabrication of fluorescent complex of HAp – amino acid coating by cold isostatic pressing and its fluorescent properties were discussed to be depending on the pressurization, there is still remain of controlling stability of fluorescent complex during fabrication aiming to increase fluorescent complex

efficiency. Moreover, the visible light irradiation enhancing the antibacterial properties of fluorescent complex of HAp – amino acid with gray titania coating was discussed based on the surface potential and its surface property. The further investigation is suggested as following;

1. In order to adjust the controllable of mechanocromic forming of fluorescence, the molecule structure of fluorescent ligands should be investigated. The dependency of pressurization may be effected by poly – amino acid molecule structure.

2. The outer layer of non reacted fluorescent complex and its light absorption in solid structure effect on the lower quantum yield in fluorescent property. It is necessary to discuss how to prevent the existing unreacted outer layer of its fluorescent complex HAp – amino acid that possible to reduce the fluorescent intensity.

3. The immersion testing and its temperature effect should be investigated to further optimization for applicable and compatible.

4. The developed HAp – amino acid with gray titania coating can be activated by visible light irradiation enhancing antibacterial property is still not applicable. Because of its irradiation is too long to be applied practically.

5. Effects of power intensity should be considered relative to the composite ration of HAp and grey titania coating. These two factor should be optimized and discuss the antibacterial performance.

6. The interaction between cell adhesion and fluorescent complex HAp – amino acid should be provided more discussion about mechanical interfacial strength and its cyto – compatibility.

Acknowledgement

I would like to deeply thanks to my advisor, associate professor Yuichi Otsuka for giving me athe opportunity to learn and conduct the new development for materials science and assist the biomaterial medical technology. For all the lesson taught and for all the lesson left to learn and experience on my own, with my deepest thank for all giving opportunity and encouragement to keep going on no matter the opportunity seem so few but always pass through works.

I would like to deeply thank to associate professor Yukio Miyashita for always support and give me the critical comment both working and living during my pass years. With your advises always be my encouragement and conquer all the obstacle.

With all respect to their advises, I would like to thank to associate professor Kiyoshi Ohnuma and associate professor Motohiro Tagaya who always support my study and allow me to conduct the research in their laboratory.

I would like to thank entire staff members at machining center and analysis center who always enable the technique and experimentation.

I owe my gratitude to Professor Yoshiharu Mutoh for all the great opportunity ever since my first arriving to Japan. All the lesson working and living of Japanese, I really appreciate and I will keep in my to improve myself always.

It my pleasure to thank to Mr. Maeda's family who always give me an effort like family all entire

of my year living in Japan Finally, thank to my dearest Morakul family; Chaval Morakul, Benjamas Morakul and Sima Morakul who always support and hear every moment. To trust and give me the wing to fly to exploit my own experience and although how far or how long I am away, there will always be warm place to call home.

References

1) Ivan Martin, David Wendt, and Michael Heberer. The role of bioreactors in tissue engineering. *Trends in Biotechnology*, 22(2):80 – 86, 2004.

2) Fergal J. O'Brien. Biomaterials & scaffolds for tissue engineering. *Materials Today*, 14(3):88 – 95, 2011.

3) Mitsuo Niinomi. Mechanical properties of biomedical titanium alloys. *Materials Science and Engineering: A*, 243(1–2):231 – 236, 1998.

4) Limin Sun, Christopher C. Berndt, Karlis A. Gross, and Ahmet Kucuk. Material fundamentals and clinical performance of plasma-sprayed hydroxyapatite coatings: A review. *Journal of Biomedical Materials Research*, 58(5):570–592, 2001.

5) Lars Palm, Sven-Arne Jacobsson, and Ingemar Ivarsson. Hydroxyapatite coating improves 8- to 10-year performance of the link {RS} cementless femoral stem. *The Journal of Arthroplasty*, 17(2):172 – 175, 2002.

6) Olav Reikerås and Ragnhild B. Gunderson. Long-term results of ha coated threaded versus ha coated hemispheric press fit cups: 287 hips followed for 11 to 16 years. *Archives of Orthopaedic and Trauma Surgery*, 126:503 – 508, 2006.

7) Robert B. Heimann. Thermal spraying of biomaterials. *Surface and Coatings Technology*, 201(5):2012 – 2019, 2006.

8) B. R. Chrcanovic, T. Albrektsson, and A. Wennerberg. Reasons for failures of oral implants. *Journal of Oral Rehabilitation*, 41(6):443–476, 2014.

9) H.K. Gupta, A. Garg, and N.K. Bedi. Peri-implantitis: A risk factor in implant failure. *Journal of Clinical and Diagnostic Research*, 5(1):138–141, 2011.

10) Marc Quirynen, Marc De Soete, and Daniel Van Steenberghe. Infectious risks for oral implants: a review of the literature. *Clinical Oral Implants Research*, 13(1):1–19, 2002.

11) T. W. Bauer and J. Schils. The pathology of total joint arthroplasty ii. mechanisms of implant failure. *Skeletal radiology*, 28(9):483–497, 1999. Cited By (since 1996): 161.

12) D.R. Drake, J. Paul, and J.C. Keller. Primary bacterial colonization of implant surfaces. *International Journal of Oral and Maxillofacial Implants*, 14(2):226–232, 1999.

13) K. Subramani, R.E. Jung, A. Molenberg, and C.H.F. Hämmerle. Biofilm on dental implants: A review of the literature. *International Journal of Oral and Maxillofacial Implants*, 24(4):616–626, 2009.

14) K. Bruellhoff, J. Fiedler, M. Möller, J. Groll, and R.E. Brenner. Surface coating strategies to prevent biofilm formation on implant surfaces. *International Journal of Artificial Organs*, 33(9):646–653, 2010.

15) Jörg Fiedler, Jürgen Groll, Erika Engelhardt, Peter Gasteier, Claudia Dahmen, Horst Kessler, Martin Moeller, and Rolf E. Brenner. Nco–sp(eo–stat–po) surface coatings preserve biochemical properties of rgd peptides. *International Journal of Molecular Medicine and Advance Sciences*, 27(1):139 – 145, November 2010.

16) E.N. Hansen, B. Zmistowski, and J. Parvizi. Periprosthetic joint infection: What is on the horizon? *International Journal of Artificial Organs*, 35(10):935–950, 2012.

17) W. Chen, Y. Liu, H.S. Courtney, M. Bettenga, C.M. Agrawal, J.D. Bumgardner, and J.L. Ong. In vitro anti-bacterial and biological properties of magnetron co-sputtered silver-containing hydroxyapatite coating. *Biomaterials*, 27(32):5512–5517, 2006.

18) G.A. Fielding, M. Roy, A. Bandyopadhyay, and S. Bose. Antibacterial and biological characteristics of silver containing and strontium doped plasma sprayed hydroxyapatite coatings. *Acta Biomaterialia*, 8(8):3144–3152, 2012.

19) Paul DeVasConCellos, Susmita Bose, Haluk Beyenal, Amit Bandyopadhyay, and Lewis G. Zirkle. Antimicrobial particulate silver coatings on stainless steel implants for fracture management. *Materials Science and Engineering: C*, 32(5):1112 – 1120, 2012. Nanotechnology for Tissue Engineering and Regenerative Medicine.

20) Nathan A. Trujillo, Rachael A. Oldinski, Hongyan Ma, James D. Bryers, John D. Williams, and Ketul C. Popat. Antibacterial effects of silver-doped hydroxyapatite thin films sputter deposited on titanium. *Materials Science and Engineering: C*, 32(8):2135 – 2144, 2012.

21) P.N. Lim, E.Y. Teo, B. Ho, B.Y. Tay, and E.S. Thian. Effect of silver content on the antibacterial and bioactive properties of silver-substituted hydroxyapatite. *Journal of Biomedical Materials Research - Part A*, 101 A(9):2456–2464, 2013.

22) A.A. Yanovska, A.S. Stanislavov, L.B. Sukhodub, V.N. Kuznetsov, V.Yu. Illiashenko, S.N. Danilchenko, and L.F. Sukhodub. Silver-doped hydroxyapatite coatings formed on ti-6al-4v substrates and their characterization. *Materials Science and Engineering: C*, 36(Supplement C):215 – 220, 2014.

23) Bo Tian, Wei Chen, Degang Yu, Yong Lei, Qinfei Ke, Yaping Guo, and Zhenan Zhu. Fabrication of silver nanoparticle-doped hydroxyapatite coatings with oriented block arrays for enhancing bactericidal effect and osteoinductivity. *Journal of the Mechanical Behavior of Biomedical Materials*, 61(Supplement C):345 – 359, 2016.

24) Bart Gottenbos, Henny C van der Mei, Flip Klatter, Dirk W Grijpma, Jan Feijen, Paul Nieuwenhuis, and Henk J Busscher. Positively charged biomaterials exert antimicrobial effects on gram-negative bacilli in rats. *Biomaterials*, 24(16):2707 – 2710, 2003.

25) Christopher Walsh. Molecular mechanisms that confer antibacterial drug resistance. *Nature*, 406:775–781, August 2000.

26) P. N. Lim, L. Chang, B. Y. Tay, V. Guneta, C. Choong, B. Ho, and E. S. Thian. Proposed mechanism of antibacterial action of chemically modified apatite for reduced bone infection. *ACS Applied Materials & Interfaces*, 6(19):17082–17092, 2014.

27) L.G. Harris, S. Tosatti, M. Wieland, M. Textor, and R.G. Richards. Staphylococcus aureus adhesion to titanium oxide surfaces coated with non-functionalized and peptide-functionalized poly(l-lysine)-grafted- poly(ethylene glycol) copolymers. *Biomaterials*, 25(18):4135–4148, 2004.

28) Fan Zhang, Zhengbiao Zhang, Xiulin Zhu, En-Tang Kang, and Koon-Gee Neoh. Silk-functionalized titanium surfaces for enhancing osteoblast functions and reducing bacterial adhesion. *Biomaterials*, 29(36):4751 – 4759, 2008.

29) Fatima El Khadali, Ge´ rard He´ lary, Graciela Pavon-Djavid, , and Ve´ ronique Migonney. Modulating fibroblast cell proliferation with functionalized poly(methyl methacrylate) based copolymers: Chemical composition and monomer distribution effect. *Biomacromolecules*, 3(1):51 – 56, 2002.

30) Junjian Chen, Yuchen Zhu, Yancheng Song, Lin Wang, Jiezhao Zhan, Jingcai He, Jian Zheng, Chunting Zhong, Xuetao Shi, Sa Liu, Li Ren, and Yingjun Wang. Preparation of an antimicrobial surface by direct assembly of antimicrobial peptide with its surface binding activity. *J. Mater. Chem. B*, 5:2407–2415, 2017.

31) L. Rimondini, S. Farè, E. Brambilla, A. Felloni, C. Consonni, F. Brossa, and A. Carrassi. The effect of surface roughness on early in vivo plaque colonization on titanium. *Journal of Periodontology*, 68(6):556–562, 1997.

32) Sabrina D. Puckett, Erik Taylor, Theresa Raimondo, and Thomas J. Webster. The relationship between the nanostructure of titanium surfaces and bacterial attachment. *Biomaterials*,

31(4):706 – 713, 2010.

33) Joanna Podporska-Carroll, Eugen Panaitescu, Brid Quilty, Lili Wang, Latika Menon, and Suresh C. Pillai. Antimicrobial properties of highly efficient photocatalytic tio2 nanotubes. *Applied Catalysis B: Environmental*, 176–177:70 – 75, 2015.

34) Gal Eyal, Jörg Wiedenmann, Mila Grinblat, Cecilia D ' Angelo, Esti Kramarsky-Winter, Tali Treibitz, Or Ben-Zvi, Yonathan Shaked, Tyler B. Smith, Saki Harii, Vianney Denis, Tim Noyes, Raz Tamir, and Yossi Loya. Spectral diversity and regulation of coral fluorescence in a mesophotic reef habitat in the red sea. *PLOS ONE*, 10(6):1–19, 06 2015.

35) Takehiko Matsuya, Yuichi Otsuka, Motohiro Tagaya, Satoshi Motozuka, Kiyoshi Ohnuma, and Yoshiharu Mutoh. Formation of stacked luminescent complex of 8-hydroxyquinoline molecules on hydroxyapatite coating by using cold isostatic pressing. *Materials Science and Engineering: C*, 58:127 – 132, 2016.

36) K. Nagura, S. Saito, H. Yusa, H. Yamawaki, H. Fujihisa, H. Sato, Y. Shimoikeda, and S. Yamaguchi. Distinct responses to mechanical grinding and hydrostatic pressure in luminescent chromism of tetrathiazolylthiophene. *Journal of the American Chemical Society*, 135(28):10322–10325, 2013.

37) Takehiko Matsuya, Sarita Morakul, Yuichi Otsuka, Kiyoshi Ohnuma, Motohiro Tagaya, Satoshi Motozuka, Yukio Miyashita, and Yoshiharu Mutoh. Visible light-induced antibacterial effects of the luminescent complex of hydroxyapatite and 8-hydroxyquinoline with gray titania coating. *Applied Surface Science*, 448:529 – 538, 2018.

38) T. Shimazaki, H. Miyamoto, Y. Ando, I. Noda, Y. Yonekura, S. Kawano, M. Miyazaki, M. Mawatari, and T. Hotokebuchi. In vivo antibacterial and silver-releasing properties of novel thermal sprayed silver-containing hydroxyapatite coating. *Journal of Biomedical Materials Research - Part B Applied Biomaterials*, 92(2):386–389, 2010.

39) Dorota Bociaga, Piotr Komorowski, Damian Batory, Witold Szymanski, Anna Olejnik, Krzysztof Jastrzebski, and Witold Jakubowski. Silver-doped nanocomposite carbon coatings (ag-dlc) for biomedical applications – physiochemical and biological evaluation. *Applied Surface Science*, 355(Supplement C):388 – 397, 2015.

40) A. Cochis, B. Azzimonti, C. Della Valle, E. De Giglio, N. Bloise, L. Visai, S. Cometa, L. Rimondini, and R. Chiesa. The effect of silver or gallium doped titanium against the multidrug resistant acinetobacter baumannii. *Biomaterials*, 80(Supplement C):80 – 95, 2016.

41) Zhi-Chao Xiong, Zi-Yue Yang, Ying-Jie Zhu, Fei-Fei Chen, Yong-Gang Zhang, and Ri-Long Yang. Ultralong hydroxyapatite nanowires-based paper co-loaded with silver nanoparticles and antibiotic for long-term antibacterial benefit. *ACS Applied Materials & Interfaces*, 9(27):22212–22222, 2017.

42) J.J.T.M. Swartjes, P.K. Sharma, T.G. VanKooten, H.C. Van DerMei, M. Mahmoudi, H.J. Busscher, and E.T.J. Rochford. Current developments in antimicrobial surface coatings for biomedical applications. *Current Medicinal Chemistry*, 22(18):2116–2129, 2015.

43) Stuart B. Goodman, Zhenyu Yao, Michael Keeney, and Fan Yang. The future of biologic coatings for orthopaedic implants. *Biomaterials*, 34(13):3174 – 3183, 2013.

44) Jordan Raphel, Mark Holodniy, Stuart B. Goodman, and Sarah C. Heilshorn. Multifunctional coatings to simultaneously promote osseointegration and prevent infection of orthopaedic implants. *Biomaterials*, 84:301 – 314, 2016.

45) Sarita Morakul, Yuichi Otsuka, Kiyoshi Ohnuma, Motohiro Tagaya, Satoshi Motoduka, Yukio Miyashita, and Yoshiharu Mutoh. Antibacterial evaluation of fluorescent hap complex with photocatalyst coating by visible light irradiation. In *Proceedings of Asian-Pacific Conference on Fracture and Strength*, 2016.

46) Achariya Rakngarm Nimkerdphol, Yuichi Otsuka, and Yoshiharu Mutoh. Effect of dissolution – precipitation on the residual stress redistribution of plasma-sprayed hydroxyapatite coating on titanium substrate in simulated body fluid (sbf). *Journal of the Mechanical Behavior of Biomedical Materials*, 36(0):98 – 108, 2014.

47) Hailiang Zhao, Jiamin Chang, and Lin Du. Effect of hydrogen bonding on the spectroscopic properties of molecular complexes with aromatic rings as acceptors. *Computational and Theoretical Chemistry*, 1084:126 – 132, 2016.

48) Mustafa Karakaya, Yusuf Sert, Swamy Sreenivasa, Parameshwar Adimoole Suchetan, and Çağrı Çırak. Monomer spectroscopic analysis and dimer interaction energies on n-(4-methoxybenzoyl)-2-methylbenzenesulfonamide by experimental and theoretical approaches. *Spectrochimica Acta Part A: Molecular and Biomolecular Spectroscopy*, 142:169 – 177, 2015.

49) Nataliya S. Myshakina, Zeeshan Ahmed, and Sanford A. Asher. Dependence of amide vibrations on hydrogen bonding. *The Journal of Physical Chemistry B*, 112(38):11873–11877, 2008.

50) Urban J. Wünsch, Kathleen R. Murphy, and Colin A. Stedmon. Fluorescence quantum yields of natural organic matter and organic compounds: Implications for the fluorescence-based interpretation of organic matter composition. *Frontiers in Marine Science*, 2:98, 2015.

51) Vasil Pajcini, X. G. Chen, Richard W. Bormett, Steven J. Geib, Pusheng Li, Sanford A. Asher, and Edward G. Lidiak. Glycylglycine pi–pi and charge transfer transition moment orientations; nearresonance raman single crystal measurements. *Journal of the American Chemical Society*, 118(40):9716–9726, 1996.

52) Mukunda Madhab Borah and Th. Gomti Devi. The vibrational spectroscopic studies and molecular property analysis of l-phenylalanine using quantum chemical method. *Journal of Molecular Structure*, 1136:182 – 195, 2017.

53) Banyat Lekprasert, Vladimir Korolkov, Alexandra Falamas, Vasile Chis, Clive J. Roberts, Saul J. B. Tendler, and Ioan Notingher. Investigations of the supramolecular structure of individual diphenylalanine nano- and microtubes by polarized raman microspectroscopy. *Biomacromolecules*, 13(7):2181–2187, 2012.

54) M. Brinkmann, G. Gadret, M. Muccini, C. Taliani, N. Masciocchi, and A. Sironi. Correlation between molecular packing and optical properties in different crystalline polymorphs and amorphous thin films of mer-tris(8- hydroxyquinoline)aluminum(iii). *Journal of the American Chemical Society*, 122(21):5147–5157, 2000.

55) Ardizzoia G. Attilio, Brenna Stefano, Durini Sara, Therrien Bruno, and Veronelli Mattia. Synthesis, structure, and photophysical properties of blue- emitting zinc(ii) complexes with 3-

aryl- substituted 1- pyridylimidazo[1,5- a]pyridine ligands. *European Journal of Inorganic Chemistry*, 2014(26):4310–4319, 2014.

56) K. Pereira da Silva, M. Ptak, P.S. Pizani, J. Mendes Filho, F.E.A. Melo, and P.T.C. Freire. Raman spectroscopy of l-phenylalanine nitric acid submitted to high pressure. *Vibrational Spectroscopy*, 85(Supplement C):97 – 103, 2016.

57) M. Rakkum, M. Brandt, K. Bye, K. R. Hetland, S. Waage, and A. Reigstad. Polyethylene wear, osteolysis and acetabular loosening with an ha-coated hip prosthesis. a follow-up of 94 consecutive arthroplasties. *Journal of Bone and Joint Surgery - Series B*, 81(4):582–589, 1999.

58) Lingzhou Zhao, Paul K. Chu, Yumei Zhang, and Zhifen Wu. Antibacterial coatings on titanium implants. *Journal of Biomedical Materials Research Part B: Applied Biomaterials*, 91B(1):470–480, 2009.

59) M.N. Rahaman, B.S. Bal, and W. Huang. Review: Emerging developments in the use of bioactive glasses for treating infected prosthetic joints. *Materials Science and Engineering C*, 41:224–231, 2014.

60) Y.S. Zhao, C. Di, W. Yang, G. Yu, Y. Liu, and J. Yao. Photoluminescence and electroluminescence from tris(8- hydroxyquinoline)aluminum nanowires prepared by adsorbent-assisted physical vapor deposition. *Advanced Functional Materials*, 16(15):1985–1991, 2006.

61) Rui-Hua Dong, Yue-Xiao Jia, Chong-Chong Qin, Lu Zhan, Xu Yan, Lin Cui, Yu Zhou, Xingyu Jiang, and Yun-Ze Long. In situ deposition of a personalized nanofibrous dressing via a handy electrospinning device for skin wound care. *Nanoscale*, 8:3482–3488, 2016.

62) Shuai Jiang, Beatriz Chiyin Ma, Jonas Reinholz, Qifeng Li, Junwei Wang, Kai A. I. Zhang, Katharina Landfester, and Daniel Crespy. Efficient nanofibrous membranes for antibacterial wound dressing and uv protection. *ACS Applied Materials & Interfaces*, 8(44):29915–29922, 2016.

63) Viktor Stabnikov, Volodymyr Ivanov, and Jian Chu. Construction biotechnology: a new area of biotechnological research and applications. *World Journal of Microbiology and Biotechnology*, 31(9):1303–1314, Sep 2015.

64) Jin Di, Jennifer Price, Xiao Gu, Xiaoning Jiang, Yun Jing, and Zhen Gu. Drug delivery: Ultrasound-triggered regulation of blood glucose levels using injectable nano-network (adv. healthcare mater. 6/2014). *Advanced Healthcare Materials*, 3(6):789–789, 2014.

65) Erin Yiling Teo, Shin-Yeu Ong, Mark Seow Khoon Chong, Zhiyong Zhang, Jia Lu, Shabbir Moochhala, Bow Ho, and Swee-Hin Teoh. Polycaprolactone-based fused deposition modeled mesh for delivery of antibacterial agents to infected wounds. *Biomaterials*, 32(1):279 – 287, 2011.

66) Shuai Jiang, Li-Ping Lv, Katharina Landfester, and Daniel Crespy. Nanocontainers in and onto nanofibers. *Accounts of Chemical Research*, 49(5):816–823, 2016.

67) Yong Liu, Wanshun Ma, Wenwen Liu, Chao Li, Yaling Liu, Xingyu Jiang, and Zhiyong Tang. Silver(i)glutathione biocoordination polymer hydrogel: effective antibacterial activity and improved cytocompatibility. *Journal of Materials Chemistry*, 21:19214–19218, 2011.

68) Takafumi Shimazaki, Hiroshi Miyamoto, Yoshiki Ando, Iwao Noda, Yutaka Yonekura, Shunsuke Kawano, Masaki Miyazaki, Masaaki Mawatari, and Takao Hotokebuchi. In vivo antibacterial and silver-releasing properties of novel thermal sprayed silver-containing hydroxyapatite coating. *Journal of Biomedical Materials Research Part B: Applied Biomaterials*, 92B(2):386–389, 2010.

69) Poon Nian Lim, Erin Yiling Teo, Bow Ho, Bee Yen Tay, and Eng San Thian. Effect of silver content on the antibacterial and bioactive properties of silver-substituted hydroxyapatite. *Journal of Biomedical Materials Research Part A*, 101A(9):2456–2464, 2013.

70) K. Herkendell, V.R. Shukla, A.K. Patel, and K. Balani. Domination of volumetric toughening by silver nanoparticles over interfacial strengthening of carbon nanotubes in bactericidal hydroxyapatite biocomposite. *Materials Science and Engineering C*, 34(1):455–467, 2014.

71) M. P. Sullivan, K. J. McHale, J. Parvizi, and S. Mehta. Nanotechnology. *Bone & Joint Journal*, 96-B(5):569–573, 2014.

72) H. Melero, C. Madrid, J. Fernández, and J. M. Guilemany. Comparing two antibacterial treatments for bioceramic coatings at short culture times. *Journal of Thermal Spray Technology*, 23(4):684–691, Apr 2014.

73) Mehdi Kazemzadeh-Narbat, Benjamin F.L. Lai, Chuanfan Ding, Jayachandran N. Kizhakkedathu, Robert E.W. Hancock, and Rizhi Wang. Multilayered coating on titanium for controlled release of antimicrobial peptides for the prevention of implant-associated infections. *Biomaterials*, 34(24):5969 – 5977, 2013.

74) Z.-B. Huang, X. Shi, J. Mao, and S.-Q. Gong. Design of a hydroxyapatite-binding antimicrobial peptide with improved retention and antibacterial efficacy for oral pathogen control. *Scientific Reports*, 6, 2016.

75) Juan Shen, Bo Jin, Yong cheng Qi, Qi ying Jiang, and Xue feng Gao. Carboxylated chitosan/silver-hydroxyapatite hybrid microspheres with improved antibacterial activity and cytocompatibility. *Materials Science and Engineering: C*, 78(Supplement C):589 – 597, 2017.

76) Garima Bhardwaj, Hilal Yazici, and Thomas J. Webster. Reducing bacteria and macrophage density on nanophase hydroxyapatite coated onto titanium surfaces without releasing pharmaceutical agents. *Nanoscale*, 7:8416–8427, 2015.

77) X. Chatzistavrou, J.C. Fenno, D. Faulk, S. Badylak, T. Kasuga, A.R. Boccaccini, and P. Papagerakis. Fabrication and characterization of bioactive and antibacterial composites for dental applications. *Acta Biomaterialia*, 10(8):3723–3732, 2014.

78) Poon Nian Lim, Zuyong Wang, Lei Chang, Toshiisa Konishi, Cleo Choong, Bow Ho, and Eng San Thian. A multi-material coating containing chemically-modified apatites for combined enhanced bioactivity and reduced infection via a drop-on-demand micro-dispensing technique. *Journal of Materials Science: Materials in Medicine*, 28(1):3, 2016.

79) Mario Kurtjak, Marija Vukomanović, Lovro Kramer, and Danilo Suvorov. Biocompatible nanogallium/hydroxyapatite nanocomposite with antimicrobial activity. *Journal of Materials Science: Materials in Medicine*, 27(11):170, 2016.

80) Ken Welch, Yanling Cai, Håkan Engqvist, and Maria Strømme. Dental adhesives with bioactive and on-demand bactericidal properties. *Dental Materials*, 26(5):491 – 499, 2010.

81) I. Bajpai, K. Balani, and B. Basu. Synergistic effect of static magnetic field and ha-fe3o 4 magnetic composites on viability of s. aureus and e. coli bacteria. *Journal of Biomedical Materials Research - Part B Applied Biomaterials*, 102(3):524–532, 2014.

82) Shuai Jiang, Beatriz Chiyin Ma, Wei Huang, Anke Kaltbeitzel, Gönül Kizisavas, Daniel Crespy, Kai A. I. Zhang, and Katharina Landfester. Visible light active nanofibrous membrane for antibacterial wound dressing. *Nanoscale Horiz.*, 3:439–446, 2018.

83) Monika Arenbergerova, Petr Arenberger, Marek Bednar, Pavel Kubat, and Jiri Mosinger. Light-activated nanofibre textiles exert antibacterial effects in the setting of chronic wound healing. *Experimental Dermatology*, 21(8):619–624, 2012.

84) Yang Si, Zheng Zhang, Wanrong Wu, Qiuxia Fu, Kang Huang, Nitin Nitin, Bin Ding, and Gang Sun. Daylight-driven rechargeable antibacterial and antiviral nanofibrous membranes for bioprotective applications. *Science advances*, 4(3):eaar5931, 2018.

85) Oscar H. Willemsen, Margot M.E. Snel, Kees O. van der Werf, Bart G. de Grooth, Jan Greve, Peter Hinterdorfer, Hermann J. Gruber, Hansgeorg Schindler, Yvette van Kooyk, and Carl G. Figdor. Simultaneous height and adhesion imaging of antibody-antigen interactions by atomic force microscopy. *Biophysical Journal*, 75(5):2220 – 2228, 1998.

86) Yea-Ling Ong, Anneta Razatos, George Georgiou, and Mukul M. Sharma. Adhesion forces between e. coli bacteria and biomaterial surfaces. *Langmuir*, 15(8):2719–2725, 1999.

87) Claudio Canale, Alessia Petrelli, Marco Salerno, Alberto Diaspro, and Silvia Dante. A new quantitative experimental approach to investigate single cell adhesion on multifunctional substrates. *Biosensors and Bioelectronics*, 48(Supplement C):172 – 179, 2013.

88) Fahad Alam and Kantesh Balani. Adhesion force of staphylococcus aureus on various biomaterial surfaces. *Journal of the Mechanical Behavior of Biomedical Materials*, 65:872 – 880, 2017.

89) I. Lee, E. Chung, H. Kweon, S. Yiacoumi, and C. Tsouris. Scanning surface potential microscopy of spore adhesion on surfaces. *Colloids and Surfaces B: Biointerfaces*, 92:271 – 276, 2012.

90) Sho Sakata, Yuuki Inoue, and Kazuhiko Ishihara. Precise control of surface electrostatic forces on polymer brush layers with opposite charges for resistance to protein adsorption. *Biomaterials*, 105:102 – 108, 2016.

91) G. H. Enevoldsen, T. Glatzel, M. C. Christensen, J. V. Lauritsen, and F. Besenbacher. Atomic scale kelvin probe force microscopy studies of the surface potential variations on the tio_2(110) surface. *Phys. Rev. Lett.*, 100:236104, Jun 2008.

92) L. Gross, F. Mohn, P. Liljeroth, J. Repp, F.J. Giessibl, and G. Meyer. Measuring the charge state of an adatom with noncontact atomic force microscopy. *Science*, 324(5933):1428–1431, 2009.

93) Mohammad R. Elahifard, Sara Rahimnejad, Saeed Haghighi, and Mohammad R. Gholami. Apatite-coated ag/agbr/tio2 visible-light photocatalyst for destruction of bacteria. *Journal of the American Chemical Society*, 129(31):9552–9553, 2007.

94) D. Ke, A.A. Vu, A. Bandyopadhyay, and S. Bose. Compositionally graded doped hydroxyapatite coating on titanium using laser and plasma spray deposition for bone implants. *Acta Biomaterialia*, 84:414–423, 2019.

95) C. Fu, H. Bai, Q. Hu, T. Gao, and Y. Bai. Enhanced proliferation and osteogenic differentiation of mc3t3-e1 pre-osteoblasts on graphene oxide-impregnated plga-gelatin nanocomposite fibrous membranes. *RSC Advances*, 7(15):8886–8897, 2017.

96) M. Tagaya, S. Motozuka, T. Kobayashi, T. Ikoma, and J. Tanaka. Mechanochemical preparation of 8-hydroxyquinoline/hydroxyapatite hybrid nanocrystals and their photofunctional interfaces. *Industrial and Engineering Chemistry Research*, 51(34):11294–11300, 2012.

97) Sarita Morakul, Yuichi Otsuka, Andaradhi Nararya, Motohiro Tagaya, Satoshi Motozuka, Kiyoshi Ohnuma, Yukio Miyashita, and Yoshiharu Mutoh. Effects of compression on orientation of ligands in fluorescent complexes between hydroxyapatite with amino acids and their optical properties. *Journal of the Mechanical Behavior of Biomedical Materials*, 88:406 – 414, 2018.

98) V.S. Bystrov, C. Piccirillo, D.M. Tobaldi, P.M.L. Castro, J. Coutinho, S. Kopyl, and R.C. Pullar. Oxygen vacancies, the optical band gap (eg) and photocatalysis of hydroxyapatite: Comparing modelling with measured data. *Applied Catalysis B: Environmental*, 196:100 – 107, 2016.

99) Kazuhiro Ema. *Basic of photophysics*. Asakura Publishing Co. Ltd., 2001.

100) Chihiro Hamaguchi and Nobuya Mori. *Electronic Properties of solids*. Asakura Publishing Co. Ltd., 2014.

101) A.C. Bento, D.P. Almond, S.R. Brown, and I.G. Turner. Thermal and optical characterization of the calcium phosphate biomaterial hydroxyapatite. *Journal of Applied Physics*, 79(9):6848–6852, 1996.

102) Tomotarou Ezaki, Akihiro Matsutani, Kunio Nishioka, Dai Shoji, Mina Sato, Takayuki Okamoto, Toshihiro Isobe, Akira Nakajima, and Sachiko Matsushita. Surface potential on gold nanodisc arrays fabricated on silicon under light irradiation. *Surface Science*, 672-673:62 – 67, 2018.

103) P. S. Subramanian, E. Suresh, P. Dastidar, S. Waghmode, and D. Srinivas. Conformational isomerism and weak molecular and magnetic interactions in ternary copper(ii) complexes of [cu(aa)]clo4·nh2o, where aa = l-phenylalanine and l-histidine, l = 1,10-phenanthroline and 2,2-bipyridine, and n = 1 or 1.5:synthesis, single-crystal x-ray structures, and magnetic resonance investigations. *Inorganic Chemistry*, 40(17), 2001.

104) Mart-Mari Duvenhage, Martin Ntwaeaborwa, Hendrik G. Visser, Pieter J. Swarts, Jannie C. Swarts, and Hendrik C. Swart. Determination of the optical band gap of alq3 and its derivatives for the use in two-layer oleds. *Optical Materials*, 42:193 – 198, 2015.